Characterization of Dbf4 structure and function in *Saccharomyces cerevisiae* DNA replication and checkpoint responses.

by

Darryl Robert Jones

A thesis
presented to the University of Waterloo
in fulfillment of the
thesis requirement for the degree of
Doctor of Philosophy
in
Biology

Waterloo, Ontario, Canada, 2013

AUTHOR'S DECLARATION

I hereby declare that I am the sole author of this thesis. This is a true copy of the thesis, including any required final revisions, as accepted by my examiners.

I understand that my thesis may be made electronically available to the public.

Abstract

The Dbf4/Cdc7 kinase complex is required for the initiation of DNA replication and promotes this by acting upon members of the Mcm2-7 helicase. In addition to its role in replication, Dbf4/Cdc7 is a target of the S-phase checkpoint response through the Rad53 checkpoint kinase. In the budding yeast *Saccharomyces cerevisiae*, the regulatory subunit of this complex, Dbf4, is essential for kinase activity. Dbf4 is conserved throughout eukaryotes and contains three regions of discrete homology, termed the N, M, and C motifs, based on their location in the polypeptide chain.

Motif C shows the highest conservation of all the motifs of Dbf4 and contains a CCHH type zinc finger. Mutation of the conserved cysteine and histidine residues of this zinc finger impair interactions with origin DNA and the Mcm2-7 helicase subunit Mcm2, but do not disrupt associations with Cdc7, Orc2, or Rad53. Cells where the endogenous Dbf4 CCHH zinc finger has been mutated exhibit slowed growth, and are delayed in their entry to, and progression through S-phase. These cells also display sensitivity upon long-term exposure to the ribonucleotide reductase inhibitor hydroxyurea (HU) and the DNA alkylating agent methyl methanesulfonate (MMS).

The crystal structure of an amino-terminal region of Dbf4 containing motif N folds as a BRCA1-carboxy-terminal (BRCT) domain. This domain is required for the interaction with Rad53, but is not sufficient. A fragment of Dbf4 containing the BRCT domain and its fifteen preceding amino acids is sufficient to interact with Rad53 and folds as a modified BRCT domain containing an integral amino-terminal helical projection. Denoted the Helix-BRCT

(HBRCT) domain, mutations that destabilize it abrogate the interaction with Rad53, and result in sensitivity to genotoxic agents.

Dbf4 is recognized by the forkhead-associated FHA1 domain of Rad53, and the HBRCT domain of Dbf4 interacts directly with FHA1 *in vitro*. This interaction is phosphorylation independent and relies on a conserved lateral surface of FHA1, distinct from the phosphoepitope binding surface, which when mutated abrogates the interaction between Dbf4 and Rad53 and results in sensitivity to HU and MMS. The *in vitro* interaction between FHA1 and HBRCT does not require the ability of FHA1 to bind a phosphoepitope, while the *in vivo* interaction between full-length Rad53 and Dbf4 does. The FHA1 domain of Rad53 can simultaneously bind to a phosphopeptide and HBRCT, indicating that Rad53 recognition of Dbf4 may occur through a bipartite interaction using two surfaces of FHA1.

Acknowledgements

First I would like to thank my supervisor, Dr. Bernie Duncker, who opened his laboratory to me many years ago as an undergraduate student and provided me with my first taste of scientific research. Your guidance and supervision over the years has helped shape me into the scientist I am today. I am also greatly appreciative of the faculty and staff in the Department of Biology at the University of Waterloo for helping to making biology a home for my time here. I would particularly like to thank my committee members, Dr. David Rose and Dr. Susan Lolle, for their support over the years, and Dr. Brendan McConkey for his interest and enthusiasm in this project.

I would also like to thank our collaborators at McMaster University, especially Dr. Alba Guarné and Dr. Lindsay Matthews, with whom it has been a pleasure to work with. I have always enjoyed our semi-regular meetings that time and time again demonstrate that the excitement of science is truly contagious.

To my lab mates and friends (these are not mutually exclusive), thank you for sharing in this experience with me. Nobody understands the trials and tribulations of graduate studies better than other grad students. Lance, DR, Michelle, Hagen, Eve, and Aaron, you have all helped to make my time in the lab enjoyable. Ajai, your humour will always be appreciated and R.A. Broom, your culinary curiosities never forgotten. To those I have spent the most time with here; Matt, your expertise on how to expedite and improve work efficiency has been invaluable. Rohan, we have managed to communicate in a way that many (Laura/Michelle) would find unintelligible, yet always end up on the same page and I do

indeed see what you did there. My first floor friends, Wendy, Laura, Dinu, Nataliya, Navdeep, Lynsi, Neil, Liz, Carol, Erin, and Wilten, your company on late nights in the lab and excursions to grad house has always helped to make the evening a little more fun. There are many people in addition to those mentioned who have improved the quality of my time here and to each of them, thank you. Following sage advice, I must remember to always thank Atsushi. I also cannot forget to express my appreciation to everyone back home for the weekend escapes and to the guys for keeping me grounded and reminding me to have a life outside of the lab.

Finally, I would like to thank my parents, without them none of this would have been possible. You have always supported and encouraged me to pursue my interests, and for that I am truly grateful.

Table of Contents

List of Figures

List of Tables

List of Abbreviations & Acronyms

ACS: ARS consensus sequence

APC-C: Anaphase promoting complex-cyclosome

ARS: Autonomously replicating sequence

BRCT: BRCA1 carbox-terminus

Cdc: Cell division cycle

CDK: Cyclin dependent kinase

ChIP: Chromatin immunoprecipitation

CMG: Cdc45, Mcm2-7, GINS

Co-IP: Co-immunoprecipitation

DDK: Dbf4 dependent kinase

DNA: Deoxyribonucleic acid

dNTP: deoxynucleotide phosphate

DSB: Double strand break

DTT: Dithiothreitol

EDTA: Ethylenediaminetetraacetic acid

FHA: Forkhead homology associated

FACS: Fluorescence activated cell sorting

GINS: Go-Ichi-Ni-San

HA: Hemagglutinin

HU: Hydroxyurea

IPTG: Isopropyl β-D-1-thiogalactopyranoside

IR: Ionizing radiation

Kb: Kilobases

kD: Kilodalton

MCM: Minichromosome maintenance

MMS: Methyl methanesulfonate

MYC: Myelocytamatosis

NMR: Nuclear Magnetic Resonance

ONPG: 2-Nitrophenyl-β-D-galactopyranoside

ORC: Origin recognition complex

PCNA: Proliferating cell nuclear antigen

PCR: Polymerase chain reaction

PMSF: Phenylmethylsulphonyl fluoride

Pre-IC: Pre-initiation complex

Pre-LC: Pre-loading complex

Pre-RC: Pre-replicative complex

RNR: Ribonucleotide reductase

RPA: Replication protein A

SC: Synthetic complete

SDS: Sodium dodecyl sulfate

UV: Ultraviolet

WCE: Whole cell extract

YPD: Yeast extract, peptone, dextrose

Chapter 1
General Introduction & Project Goals

1.1 Yeast as a research model

Commonly known as baking or brewing yeast, the budding yeast, *Saccharomyces cerevisiae* is one of the most useful organisms in studying cellular and molecular biological processes in eukaryotes. Indeed much of what we know today about the molecular mechanisms that govern how eukaryotic cells function has been gleaned from work in *S. cerevisiae* and similar organisms (Botstein & Fink 1988; Fields & Johnston 2005; Botstein & Fink 2011). Insights into processes including DNA replication, gene regulation, protein secretion, cell signalling, and metabolism have all been gained, from work with *S. cerevisiae* (Fields & Johnston 2005; Dolinski & Botstein 2007; Botstein & Fink 2011). The ability of yeast to help elucidate underlying mechanisms in these processes resides in conservation of sequence and function. It is becoming increasingly clear that not only are genes conserved between species, the gene products function within the context of larger interaction networks, giving rise to conserved processes and pathways. Even in the case of a disease process that is restricted to metazoans, such as cancer, the underlying causative mechanisms that contribute to genomic instability, a hallmark of cancer, are conserved within yeast. This provides an opportunity to utilize yeast to provide insight into mechanisms of human disease.

1.1.1 Characteristics of yeast

The term yeast is a generic description used to describe a variety of single celled fungi, which can be classified into two phyla, Ascomycota and Basidiomyota. *S. cerevisiae*

fits into the former phylum based on its ability to form spores in a sac (ascus). Yeasts can commonly be found in a diverse array of environments ranging from soil, plant leaves, flowers, and fruit, to the skin and intestinal tracts of animals (Walker 1998; Landry et al. 2006). As chemoorganotrophs, yeast require an external carbon source to produce energy. This ability to metabolize sugars to alcohol and carbon dioxide has resulted in the domestication of *S. cerevisiae* for the production of wines, beer, and as a leavening agent in the baking of breads. In fact, molecular evidence from wine containers dating to one of the first Egyptian kings indicates that *S. cerevisiae* has been used for the fermentation of wine from at least 3150 B.C.E. and evidence for the production of fermented beverages in China dates to 7000 B.C.E. (Cavalieri et al. 2003; McGovern et al. 2004).

While the size of yeast cells can vary greatly between 2-50 μm in length to 1-10 μm in width, *S. cerevisiae* cells are ovoid in shape with typical dimensions ranging from 5-6 μm by 4-5 μm (Walker 1998; Herskowitz 1988). *S. cerevisiae* is viable in both a haploid and diploid state, where haploids tend to be smaller and more spherical compared to diploids. For both diploid and haploid cells, vegetative mitotic growth occurs through the process of budding in *S. cerevisiae*, where an emerging cell will bud from a mother cell eventually pinching off resulting in a new daughter cell.

Haploid cells exist as one of two mating types, a or α. Fusion of haploid cells of opposite mating types results in a diploid cell which may grow vegetatively or in times of nutrient starvation undergo meiosis to form a tetrad of haploid spores in an ascus (discussed in Neiman 2011). This fusion process relies on the fact that cells of each mating type secrete mating pheromones (α-factor by α-cells and a-factor by a-cells) which synchronize the cell

cycles of mating cell pairs. Exposure to mating pheromone from cells of the opposite mating type causes a cell to transiently arrest in late G1, just before the initiation of DNA synthesis, thus ensuring that mating cells will have only one copy of each chromosome, resulting in exactly two copies of each chromosome in the resulting diploid after fusion (discussed in Herskowitz 1988; Landry et al. 2006).

The physical anatomy of a yeast cell is much the same as any other eukaryotic cell, which is one of the main draws to using yeast as a model for eukaryotic cellular processes. A yeast cell consists of an outer cell wall and inner cellular membrane which contain a central vacuole that functions as the cellular lysosome. Within the confines of the cell membrane, the same organelles as would be seen in metazoan cells can be found, including a nucleus, ribosomes, Golgi apparatus, endoplasmic reticulum, and mitochondria (Barnett & Robinow 2002a; Barnett & Robinow 2002b; Walker 1998). Two important differences between yeast and metazoan cells involve the cell wall and the nucleus. Yeast maintain a 100-200 nm thick cell wall which is essential to protect cellular contents and to provide structural support for the cell. Metazoan cells undergo an open mitosis, the nucleus is dissolved to allow chromosome segregation, whereas in the case of *S. cerevisiae* the nuclear membrane is maintained and the nucleus migrates to the bud neck, pinching in half as the cell divides (Walker 1998).

1.1.2 Genetics of *S. cerevisiae*

The results from sequencing the first entire eukaryotic genome show that *S. cerevisiae* has a genome size of 12,068 kilobases, spanning 16 unique chromosomes which range in size from 230 kilobases to 1,532 kilobases (Goffeau et al. 1996). The genome of *S.*

cerevisiae contains 6,607 total open reading frames (ORFs) of which over 75% (5,065) of these have been experimentally verified to produce a gene product. Of the fewer than 25% of ORFs remaining approximately half (755) are classified as uncharacterized, sequences that likely encode an expressed protein but have yet to be verified, while the other half (787) are classified as dubious, meaning it is uncertain if they encode a gene product (SGD, 2013). Compared to metazoans, the genome of *S. cerevisiae* is relatively compact with genes representing over 70% of the total genome sequence (Sherman 2002). Interestingly, less than 250 genes in *S. cerevisiae* contain an intron and fewer than ten genes are known to have more than one intron (Ares et al. 1999). In addition to 16 chromosomes, most strains of *S. cerevisiae* also carry an extra chromosomal 2 micron plasmid which, despite its presence in most strains provides little to no obvious phenotype (Futcher 1988). The presence of a naturally occurring plasmid in eukaryotic cells is exceedingly rare, and the 2 micron plasmid has provided an excellent platform on which many recombinant yeast vectors have been based.

Descended from strains originally characterized by Carl Lindegren in the 1940s, the S288C and W303 strains of *S. cerevisiae* (the former is primarily used in this study) are two of the most prevalent for use in laboratory research (Mortimer & Johnston 1986; Ralser et al. 2012). Both strains capitalize on one of the largest advantages of *S. cerevisiae* as a model organism, its ability to readily undergo homologous recombination. This single attribute makes *S. cerevisiae* extremely amenable to genetic manipulation. Combined with an ability to efficiently be transformed with single stranded or circular DNA, this allows for quick single step modifications to the genome (Longtine et al. 1998). This straightforward

procedure allows for additions or deletions to be made with ease; proteins can be epitope tagged, gene promoters may be swapped, and mutant alleles of genes inserted with specificity into the genome, allowing investigation into gene function.

Nearly all lab strains contain mutations within biosynthetic pathways for amino or nucleic acids. These auxotrophic mutations are utilized as genetic markers. As a result, large collections of deletion mutants are available the world over. In addition to this, collections of temperature sensitive mutants also exist which have been amassed over generations of investigation into how the eukaryotic cell functions. These large collections of mutants can be used to capitalize on the power of yeast genetics.

Many human diseases can be attributed to genetic factors. It has been estimated that as many as 40% of genes involved in human genetic diseases are conserved in *S. cerevisiae* (Foury 1997; Kelly et al. 2001). In humans it is often unfeasible or unethical to conduct the experiments necessarily to completely discern the genetic contribution to disease aetiology. However in yeast these issues are not a concern. In a collaborative effort to identify gene function, the yeast genome deletion project successfully deleted 96% (5,916 genes) of annotated ORFs in *S. cerevisiae*, of which almost 19% (1,105) were found to be essential (Giaever et al. 2002; Winzeler et al. 1999). Taking advantage of the ability of yeast to grow as either haploid or diploid cells, a single copy of an essential gene may be deleted in a diploid host, while non-essential genes deleted in a haploid host allow for the consequences of loss of gene function to be assessed. Utilizing the different mating types of *S. cerevisiae*, it is possible to cross different genetic mutants with one another, allowing exploration into gene function by observing genetic interactions. This typically involves screening a known mutant

with other genetic mutants to observe suppression or enhancement of the original mutants phenotype (Hartman et al. 2001). This has been the basis for the development of several high throughput, parallel screening techniques to better understand genetic interaction networks, identify disease associated genes, and point to potential drug targets (Yan et al. 2008; Breslow et al. 2008; Giaever et al. 1999; Lum et al. 2004; Steinmetz et al. 2002; Yuen et al. 2007). All of these features combined in a host which is able to double in number every 90 minutes, and can be easily and inexpensively cultured, makes *S. cerevisiae* an excellent model to use for molecular based studies of the eukaryotic cell cycle.

1.2 The cell cycle

Cell cycle research has benefitted immensely from work with yeasts. In fact, two of the three winners of the 2001 Nobel Prize in Physiology or Medicine conducted their award winning research in yeast (*S. cerevisiae* and the fission yeast *S. pombe*). Awarding Leland Hartwell, Paul Nurse, and Timothy Hunt the Nobel Prize for their discoveries of key regulators of the cell cycle served to underscore the importance of understanding the mechanisms by which cell growth and division are regulated. The cell cycle represents a series of coordinated events, temporally separated, which must occur in order for a cell to grown and divide. The cycle can be divided into four parts, Gap1 (G1), Synthesis (S), Gap2 (G2), and Mitosis (M), all of which will be discussed below. The timing of these events depends on the actions of a cycling group of proteins, not so coincidently called the cyclins, which drive the activity of cyclin-dependent-kinases (CDKs) (Bertoli et al. 2013). The synthesis and degradation of cyclins modulates their temporal expression which mediates the transition between cell cycle stages. In *S. cerevisiae*, the primary CDK is Cdc28, the activity

of which is driven by its various cell cycle phase-specific binding partners (Bloom & Cross 2007). The morphology of *S. cerevisiae* changes as cells progress through the different stages of the cell cycle. This is a useful characteristic, making it possible to approximate the position of a cell in the cell cycle by its shape or bud morphology (**Figure 1.1**) (Hartwell 1974).

1.2.1 G1

The first of two gap phases and the longest stage of the cell cycle in *S. cerevisiae*, G1, is dedicated to cell growth and the accumulation of nutrients necessary to proceed through the cell cycle. During this period the cell has several options. It may proceed through the cell cycle to duplicate itself or in times of nutrient starvation, exit the cell cycle and enter into a quiescent G0 phase where it may remain or return to the cell cycle when nutrients are more abundant (Forsburg & Nurse 1991). An additional option exists depending on growth conditions and cell ploidy. During this time haploid cells may mate and diploid cells, if nutrient starved, may initiate a meiotic cycle to undergo sporulation (Herskowitz 1988; Forsburg & Nurse 1991). Cells that choose to proceed through the cell cycle must pass the START point. After this point cells are required to complete a full round of genome duplication and cell division before returning to a state where mating, meiosis, or exit from the cell cycle are possible. In order to pass START cells must have sufficient nutrients, and be in the absence of factors that promote meiosis or pheromone from cells of the opposite mating type (Hartwell 1974). Passing START for a cell coincides with the first emergence of a tiny bud that will go on to form the daughter cell. As cells reach sufficient size Cln3/Cdc28, activates the transcription factor SBF, which sets in motion events leading to the activation of

factors which prepare the cell for entry into the replicative phase of the cell cycle (discussed in Bertoli et al. 2013; Bloom & Cross 2007; Nasmyth 1996). Once replication competent origins fire the cell has moved on to the next stage of the cell cycle, synthesis.

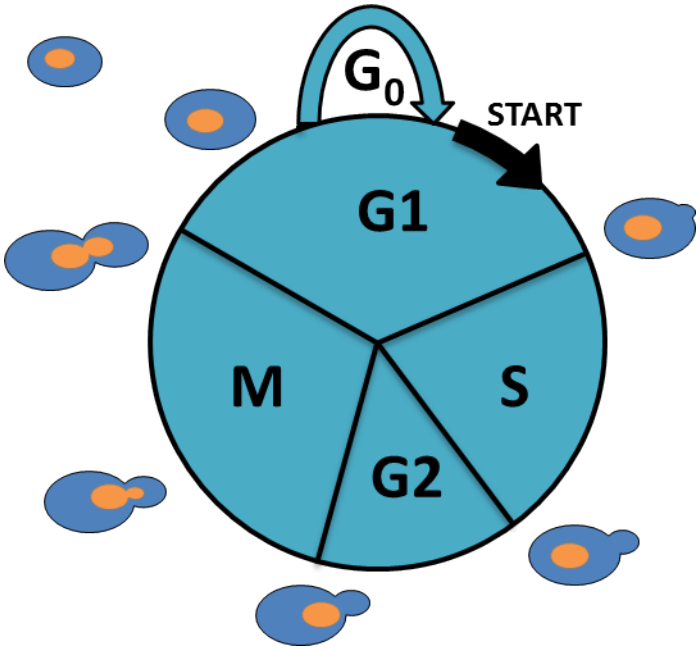

Figure 1.1: The *Saccharomyces cerevisiae* cell cycle.

Representation of the characteristic morphologies of a budding yeast cell as it progresses through the phases of the cell cycle. Once the cell has passed the START point it is irrevocably committed to cellular reproduction. Entry into or exit from G_0 must occur before START. (Adapted from Herskowitz 1988)

1.2.2 S-phase

The process of genome duplication begins as the replicative helicases processively unwind DNA in a bi-directional manner, moving away from origins of replication. The resulting single stranded DNA is acted upon by an assortment of factors ultimately resulting in the duplication of template by DNA polymerases (discussed in section 1.3). The

unwinding of DNA by helicase activity presents a topological issue. As DNA is unwound positive supercoiling is induced ahead of the moving replication machinery. This poses a problem as the buildup of torsional stress can impede the progress of the replication machinery and lead to unfavorable replication intermediates (discussed in Schvartzman et al. 2013). The enzyme topoisomerase, specifically Top2, is able to alleviate this stress. By relaxing positive supercoils ahead of the active helicase Top2 relieves the buildup of torsional tension.

Since replication is not initiated at the very end of chromosomes this results in two Y-shaped replication forks moving away from each other, creating a bubble of replicated DNA between them. *S. cerevisiae* contains 337 identified origins of replication spanning all 16 chromosomes (SGD, 2013). Every origin does not necessarily fire each time the genome is duplicated, as such some will remain dormant and be passively replicated through by replication forks originating from neighbouring origins that have been activated. These bubbles, or replicons, continue to expand until they merge with neighbouring replicons, resulting in the complete replication of the genome (Sclafani & Holzen 2007). The progression of cells through S-phase is promoted by CDK activity which during S-phase is primarily due to Cdc28 interaction with the B-type cyclins, Clb5 and Clb6 (Bloom & Cross 2007). During this time the tiny bud that first appeared as the cell passed START begins to grow, giving the cell the distinct appearance attributed to budding yeast.

1.2.3 G2

The second gap phase, G2, provides yet another opportunity for the cell to grow, ensuring sufficient cellular size before initiating cell division. At this point the cell and bud

both continue to increase in size and volume and the nucleus begins to migrate to the bud neck (Hartwell 1974). In *S. cerevisiae* G2 is rather brief, with cells seeming to transition from S-phase to mitosis relatively quickly (Nurse 1985). It is absolutely imperative that genome duplication is complete before chromosome segregation, failure to do so would be catastrophic for cell viability. G2 allows the cell to ensure replication is complete and provides a last chance to check the fidelity of replicated DNA, as any changes will become permanent in the daughter cell.

1.2.4 Mitosis

Nuclear and cellular division mark the final stage of the cell cycle. Mitosis can be broken down into four phases, prophase, metaphase, anaphase, and telophase, which are subsequently followed by cytokinesis, marking the complete division of mother and daughter cells. Here the mitotic B-type cyclins, Clb1-4, drive Cdc28 activity promoting nuclear division (discussed in Bloom & Cross 2007).

Prophase marks the beginning of mitosis as microtubules extending from opposite spindle poles attach to sister kinetochores. Both spindle poles are charged with recruiting a copy of each chromosome, one for the emerging daughter cell and one to remain in the mother cell. For equal segregation of chromosomes the bi-oriented attachment of sister kinetochores to spindle poles is essential as tension from each pole is required to align and separate chromosomes (reviewed in Tanaka 2008). Once chromosomes are aligned in metaphase, the anaphase promoting complex/cyclosome (APC/C) is activated which allows separation of sister chromatids to commence. The APC/C is an ubiquitin ligase that directs the degradation of proteins that inhibit the transition to anaphase. Securin, Pds1 in *S.*

cerevisiae, functions to ensure sister chromatids are secure by preventing the degradation of cohesin. This is accomplished by inhibiting separase, encoded by *ESP1* in yeast, which is responsible for the cleavage of the kleisin subunit of cohesin (discussed in Nasmyth 2005). Both securin and separase play a role in the regulation of mitotic exit in addition to initiation of anaphase (Tinker-Kulberg & Morgan 1999; Cohen-Fix & Koshland 1999). The cleavage of cohesin rings marks the entry to anaphase. Sister chromatids are now free to be pulled apart and travel to opposite spindle poles via their attached kinetochores. One of these spindle poles will then migrate to the daughter cell, while the other will remain in the mother (Zhang & Oliferenko 2013; Weiss 2012). As the end of mitosis nears in telophase, the spindle disassembles and the nuclear membrane constricts separating each complement of chromosomes, completing nuclear division (Winey & O'Toole 2001).

In preparation to exit mitosis CDK activity must return early G1 levels. This requires down regulation of the M-phase cyclins as they inhibit mitotic exit and cytokinesis (Bloom & Cross 2007). To ensure this occurs, the polo-like-kinase, Cdc5, helps to activate the mitotic exit network (MEN), a series of cascading events which results in the degradation of the M-phase cyclins and dephosphorylation of cytoplasmic CDK substrates, by the Cdc14 phosphatase (reviewed in Weiss 2012; Bosl & Li 2005). As the emerging daughter cell is ready to be released from the mother cell a contractile actomyosin ring forms around the bud neck. The next step in cytokinesis is the formation of a septum between mother and daughter. As the ring contracts and the septum is degraded, the two cells divide, leaving a concave chitinous bud scar on the mother and a reciprocal convex birth scar on the daughter (discussed in Weiss 2012; Barnett & Robinow 2002b; Hartwell 1974).

1.3 DNA replication

In eukaryotic cells the genome is spread over mutiple chromosomes, each of which is completely replicated from multiple origins of DNA replication. This feat requires careful organization as it is imperative that the entire genome be replicated once and only once per cell cycle. Failure to accurately and completely replicate the genome can be catastrophic for cell viability. Defects in the duplication of the genome are some of the major causes of genomic instability, a major contributing factor to cancer (reviewed in Abbas et al. 2013). This emphasizes the importance of understanding the cellular processes that govern the synthesis of new DNA.

Replication is an essential component of the cell cycle. The processes that allow genome duplication span both G1 and S-phases. Thus DNA replication can be broken down into several phases, the setup of replication competent origins, the initiation of DNA replication and the active process of elongation where the duplicated genome is completely synthesized.

1.3.1 Formation of replication competent origins

The initiation of DNA replication requires the formation of pre-replicative complexes (pre-RCs) at origins of replication (**Figure 1.2**). *S. cerevisiae* contains discrete origins of replication which span defined nucleotide sequences. These origins, termed Autonomously Replicating Sequences (ARSs), are distinguished by a specific 11 base pair ARS Consensus Sequence (ACS) (Brewer & Fangman 1987). In *S. cerevisiae* an origin spans 100-150 base pairs with a highly conserved core 17 base pair A element flanked by several B elements (Stillman 2005; Sclafani & Holzen 2007; S. P. Bell & Dutta 2002).

The setup of replication competent origins actually precedes S-phase and occurs in late M and early G1 phase when CDK activity is low. The genome must be duplicated once and only once per cell cycle. Cellular mechanisms have evolved to achieve this imperative by limiting the time in which replication competent origins can be assembled to one phase of the cell cycle. Cdc28 activity, driven by the cyclins Clb5 and Clb6, is required for the initiation of replication (Bloom & Cross 2007). However if pre-RCs were to be assembled in a time of CDK activity precocious activation of origins would occur resulting in over replication of portions of the genome. The temporal separation of pre-RC assembly and activation provide a level of control to prevent precocious origin firing. This temporal separation is a result of CDK activity being inhibitory to pre-RC assembly (Dahmann et al. 1995; Detweiler & Li 1998). Thus pre-RC formation can only occur in late M-phase and early G1 and these replication competent origins must be sufficient in number to allow the cell to traverse S-phase.

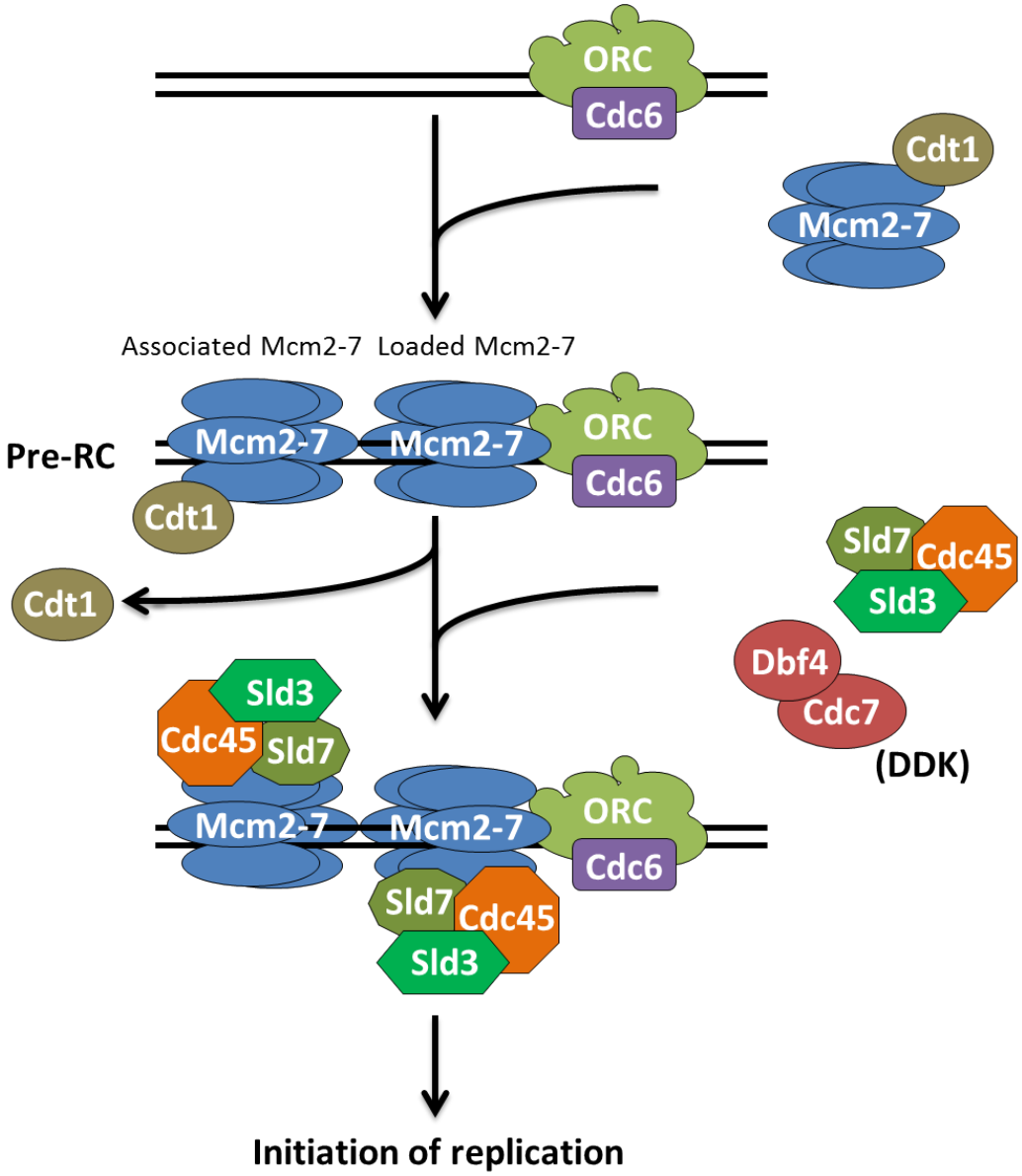

Figure 1.2: Assembly of pre-RCs at origins during G1.

Origins of replication are bound by ORC which recruits Cdc6. Heptamers of Mcm2-7 and Cdt1 then loosely associate with origins. Upon ATP hydrolysis requiring ORC,Cdc6, and Cdt1, the Mcm2-7 complex is loaded on DNA and Cdt1 is displaced. Formation of the pre-RC is complete once a double hexamers of Mcm2-7 are loaded. The activity of DDK is then required for the association of the complex of Sld3, Sld7, and Cdc45. (Adapted from Labib 2010)

The first step in pre-RC assembly is the binding of origins by the origin recognition complex (ORC) (Bell & Stillman 1992). This hexameric complex acts as the scaffold to which the rest of the factors required for pre-RC formation can be recruited. ORC specifically binds the A and B1 origin elements (Rao & Stillman 1995). Marked by ORC, Cdc6 then Cdt1 with the replicative helicase, Mcm2-7, are now able to sequentially associate with origins (Aparicio et al. 1997; Speck et al. 2005; Chen et al. 2007; Chen & Bell 2011) (**Figure 1.2**). This association of the Mcm2-7 complex with origins is dependent on a conserved C-terminal domain of Mcm3 (Frigola et al. 2013). At this stage the Mcm2-7 complex is loosely associated with origins and has yet to be loaded around DNA. The loading reaction requires a coordinated series of ATP hydrolysis reactions requiring ORC and Cdc6, which are stimulated by the C-terminal domain of Mcm3, and Cdt1 (Tanaka et al. 1997; Bowers et al. 2004; Randell et al. 2006; Kawasaki et al. 2006; Frigola et al. 2013). This reaction results in a set of head-to-head double hexamers of Mcm2-7 being loaded onto DNA (Remus et al. 2009; Evrin et al. 2009). The presence of double hexamers on DNA appears to be the result of sequential loading (Frigola et al. 2013; Fernández-Cid et al. 2013). Reconstitution of this loading reaction with purified proteins indicates that the first Mcm2-7 hexamer is quickly (taking only seconds) loaded via hydrolysis, while the second hexamer appears to be loaded relatively slowly (taking several minutes) (Fernández-Cid et al. 2013; Riera et al. 2013). Once the Mcm2-7 helicase complex is loaded, Cdc6 and Cdt1 are thought to be dispensable. Both are removed in a CDK dependent manner, where Cdc6 is targeted for degradation and Cdt1 for nuclear export (Drury et al. 2000; Tanaka & Diffley 2002). The stably loaded Mcm2-7 helicase complex is now ready for activation by CDK and another

important kinase complex, Dbf4 Dependent Kinase (DDK). The activation of CDK and DDK signals the transition from G1 to S-phase.

1.3.2 Initiation of DNA replication

For DNA synthesis, the timing of individual origin activation can vary. This allows origins to be classified early, mid, or late origins, based on when they fire (reviewed in Aparicio 2013). As cells transition into S-phase, Sld3, Sld7, and Cdc45 associate with early firing origins in a DDK dependant manner, not requiring CDK activity (Heller et al. 2011; Tanaka & Araki 2011). These early origins are then joined by several factors in what has been termed a pre-loading complex (pre-LC) (**Figure 1.3**). Identified by immunoprecipitation of cross-linked cell extracts, the pre-LC is composed of Polε, GINS (Go Ichi Ni San), Sld2, and Dpb11, requiring only CDK activity for formation (Muramatsu et al. 2010). The merger of the pre-RC and pre-LC is dependent on the scaffold protein Dpb11 and CDK activity. Dpb11 is a BRCT (BRCA1 C-Terminal) domain containing protein with two amino-terminal and two carboxyl-terminal repeats, tandem repeats of this domain are known as phosphopeptide binding modules (Araki 2010; Glover et al. 2004). Sld2 and Sld3 have been shown to be the minimal set of S-Phase CDK targets required for DNA replication, and are bound by the C-terminal and N-terminal BRCT repeats of Dpb11 respectively (Zegerman & Diffley 2007; Tanaka et al. 2007; Tak et al. 2006). Thus Dpb11 serves as a bridge between the pre-RC and pre-LC, forming what has been referred to as the pre-initiation complex (pre-IC) (Diffley & Labib 2002; Diffley 2010). The formation of the pre-IC unites Cdc45-Mcm2-7-GINS (CMG) which together constitute the active replicative helicase. Sld2, Sld3, Sld7, and Dpb11 then dissociate from the pre-IC, resulting in the formation of the active replisome

which will travel with replication forks (Gambus et al. 2006; Moyer et al. 2006; Labib & Gambus 2007; Gambus et al. 2009; Labib 2010).

It is not entirely clear when and where Mcm10 associates with origins or the exact molecular mechanisms of how it acts (discussed in Thu & Bielinsky 2013). What is clear is that Mcm10 is essential for DNA replication and appears to play an important role in DNA unwinding required for the firing of origins (Solomon et al. 1992; van Deursen et al. 2012; Kanke et al. 2012; Watase et al. 2012; Merchant et al. 1997; Homesley et al. 2000). Additionally Mcm10 is required for the recruitment of primase and the lagging strand DNA polymerase, although whether it is a stable component of the replisome remains to be elucidated (van Deursen et al. 2012; Kanke et al. 2012; Ricke & Bielinsky 2004; Heller et al. 2011).

It is interesting to note that many of the factors discussed above that are required for the initiation of DNA synthesis are in limited supply. Overexpression of Cdc45, Dpb11, Sld2, Sld3, Sld7, and DDK have been shown to advance the timing of origin firing, where late firing origins will fire earlier in S-phase (Mantiero et al. 2011; Tanaka et al. 2011). As Dpb11, the Sld proteins, and DDK do not travel with the replisome after early origins have fired it is likely these factors are recycled to initiate late firing origins (Gambus et al. 2006; Gambus et al. 2009; Mantiero et al. 2011). Knowing that Cdc45 and Sld3 association with the pre-RC corresponds to the timing with which these origins fire and suggests a mechanism whereby DDK dependent recruitment of Cdc45 and Sld3 regulates the temporal pattern of origin activation (Aparicio et al. 1999; Kamimura et al. 2001; Heller et al. 2011; Tanaka et al. 2011).

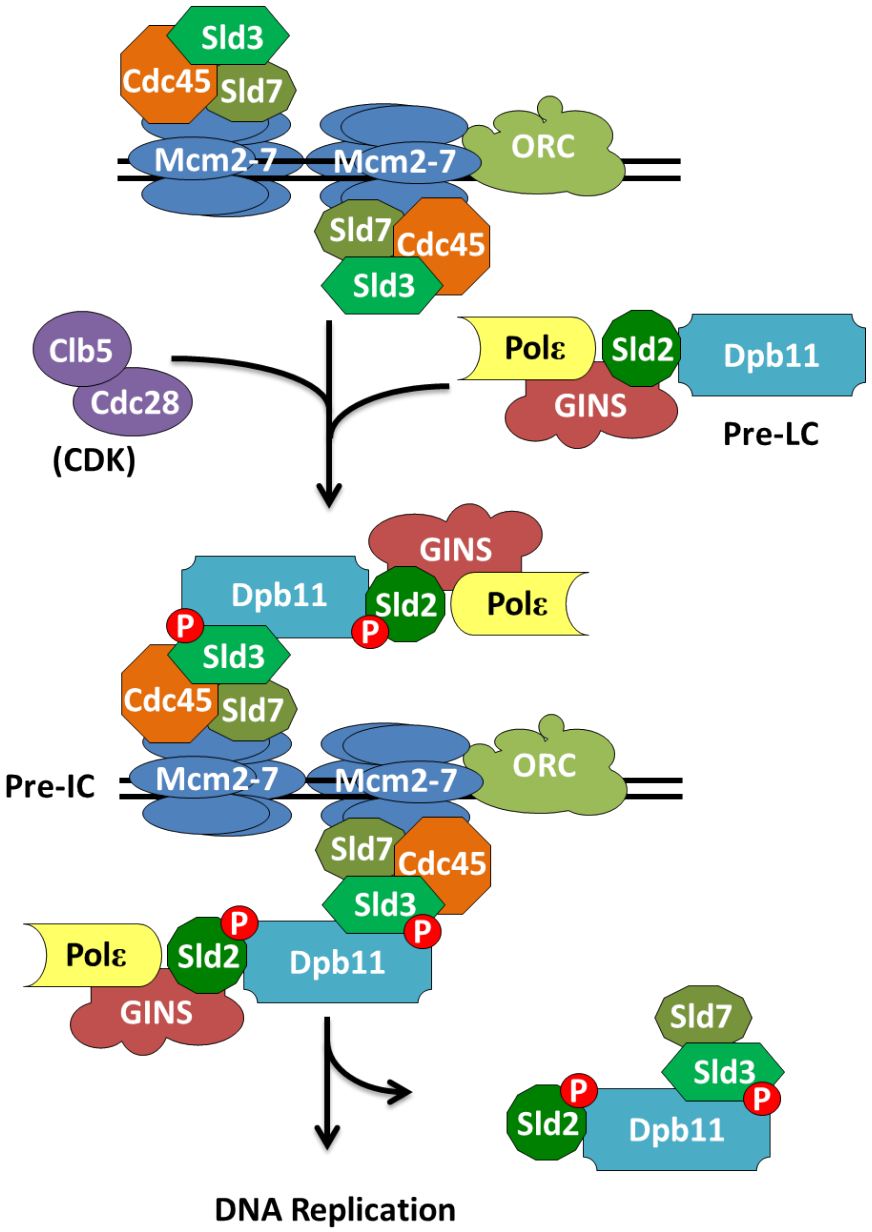

Figure 1.3: The initiation of DNA replication.

Upon the DDK dependent association of Sld3, Sld7, and Cdc45 with origins, CDK is required for pre-IC formation. CDK dependent phosphorylation of Sld2 and Sld3(depicted as red circles) allows the pre-LC to join the pre-RC to form the pre-IC, mediated by Dpb11. Disassociation of Sld2, Sld3, Sld7, and Dpb11 from the pre-IC results in active CMG helicase allowing bi-directional DNA replication to proceed. (Adapted from Labib 2010)

1.3.3 Elongation and DNA synthesis

As the template strands of DNA are separated, single stranded DNA is exposed in the 5' to 3' as well as 3' to 5' direction. The eukaryotic single strand binding protein, Replication Protein A (RPA), binds to these stands preventing them from re-annealing with one another. DNA polymerase is only able to synthesise DNA in the 5' to 3' direction, thus two different systems for synthesis of each strand are needed (**Figure 1.4**). The leading strand can be synthesized in a continuous fashion while the lagging strand must be synthesized semi-discontinuously by the joining of Okazaki fragments. *S. cerevisiae* utilizes three different polymerases (Polα, Polδ, and Polε) during times of unperturbed replication (Burgers 2009).

On the leading strand, template is read in the 3' to 5' direction allowing 5' to 3' synthesis to occur in long continuous stretches, this activity is carried out by the processive enzyme Polε. The association of Polε with origins is interdependent with CMG formation (Takayama et al. 2003; Zou & Stillman 2000). Loaded by Replication Factor C (RFC), the sliding clamp Proliferating Cell Nuclear Antigen (PCNA), encoded by the *POL30* gene, has been shown to assist processivity of Polε, helping tether it to DNA (Dua et al. 2002; Burgers 1991; Hamatake et al. 1990). On the lagging strand Okazaki fragment synthesis is required, where shorter fragments of DNA are synthesized and joined. Polymerases on both the leading and lagging strand require a primer to initiate synthesis of nascent DNA. The Polα-primase complex acts on both these strands, producing a short 8-12 nucleotide RNA primer which it then extends approximately 20 nucleotides which is eventually continued by the lagging strand polymerase (Garg & Burgers 2005). The association of the Polα-primase complex with DNA and its ability to initiate primer synthesis is dependent on Mcm10 and

Cdc45 (Ricke & Bielinsky 2004; Zou & Stillman 2000; Melendy & Stillman 1993; Collins & Kelly 1991). One primer should theoretically be sufficient for synthesis on the leading strand extending from a single origin of replication. However Okazaki fragments are 100-200 nucleotides long, with each one requiring its own primer, this means on the lagging strand approximately 100,000 primers are needed to complete replication of the genome (Garg & Burgers 2005). After the synthesis of each primer and its extension the switch from Polα to the primary lagging strand polymerase, Polδ, must occur. This is dependent on the action of the clamp loader RFC in complex with PCNA (Garg & Burgers 2005; Moldovan et al. 2007). Similar to Polε, PCNA stimulates Polδ activity (Burgers 1998).

The maturation and processing of Okazaki fragments relies on the activity of a flap endonuclease, Rad27, and the Cdc9 DNA ligase. Two pathways exist for maturation, the long and short flap pathways, where the latter is predominant in conditions of unperturbed replication (Burgers 2009). In the short flap pathway Polδ bumps into the 5' end of the downstream Okazaki fragment displacing 1-2 nucleotides of the RNA primer which are subsequently removed by Rad27. This process is iteratively repeated in a process known as nick translation until the RNA primer is completely removed, leaving a DNA-DNA junction that can be ligated by Cdc9 (Garg & Burgers 2005). Long flaps may be generated as a result of processive displacement of the downstream Okazaki fragment by Polδ. Once a flap is long enough to form secondary structure or bind proteins, such as RPA, Rad27 is unable to mediate its removal and requires the help of the nuclease/helicase Dna2 to trim the long flap to a size manageable by Rad27 (Ayyagari et al. 2003). Thus, the coordinate action of Polδ, Rad27, and Cdc9 is required to ensure efficient maturation of Okazaki fragments.

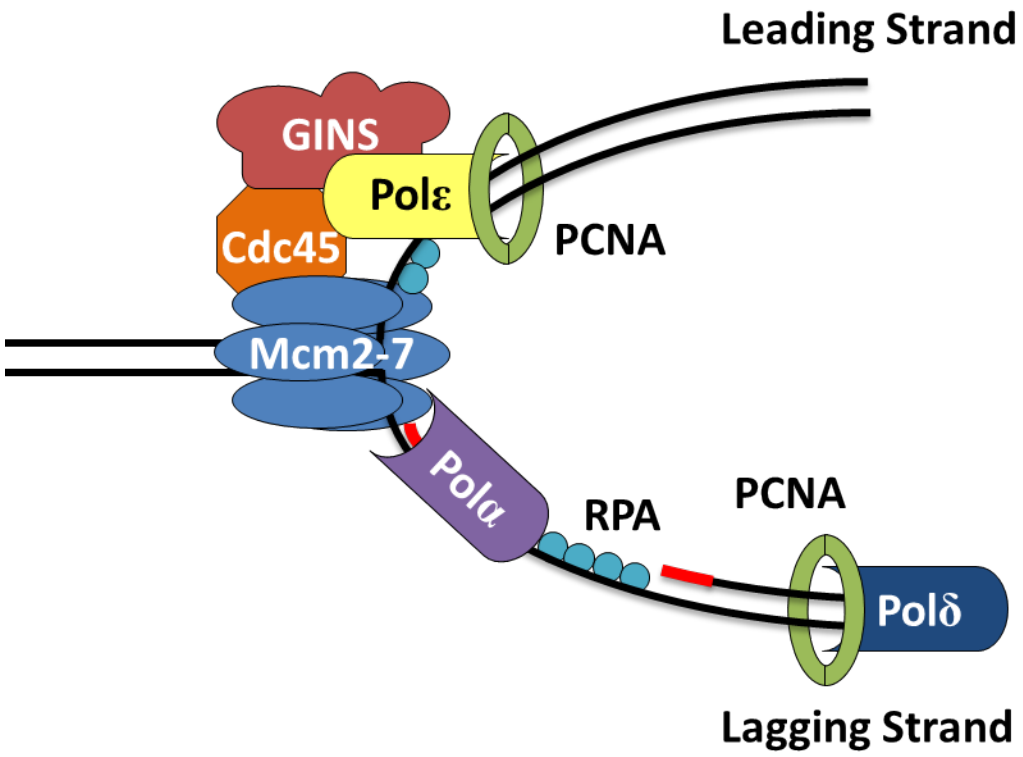

Figure 1.4: The eukaryotic DNA replication fork.

Replication proceeds bi-directionally from origins of replication following the replication fork. The CMG complex unwinds the DNA duplex and ssDNA is coated by RPA. Polα-primase produces the RNA primer (red strand), which is required for both leading and lagging strand synthesis. Polε is the processive leading strand polymerase while Polδ synthesizes Okazaki fragments on the lagging strand. Both Polε and Polδ are aided in processivity by the ring clamp PCNA. (Adapted from Burgers 2009)

1.4 The DNA damage & replication checkpoints

Checkpoints represent a collection of surveillance mechanisms that are integral to the maintenance of genome fidelity. In response to DNA damage or other stimuli the checkpoint provides a mechanism to arrest cell cycle progression and trigger repair. The factors involved in checkpoint signalling are very well conserved from single celled eukaryotes to mammals where their inactivation or mutation often results in a predisposition to cancer (discussed in

Aguilera & Gómez-González 2008; Negrini et al. 2010; Abbas et al. 2013). Thus the checkpoint response prevents the accumulation and transmission of heritable abnormalities by providing an opportunity to repair defects before cell division.

The checkpoint response typically functions through an integrative signalling network of proteins each with specialized functions. Broadly the proteins involved in checkpoint signalling can be stratified into three main classes, namely sensors, transducers, and effectors, based on how they perpetuate the checkpoint signal (**Figure 1.5**). At the heart of the checkpoint signaling response are the PI3K (phosphoinositide 3-kinase) like kinases, Mec1 and Tel1 (homologues of mammalian ATR and ATM). These kinases integrate signals from a variety of sources to initiate a signal cascade that through the mediators Rad9 and Mrc1 will activate the effector kinases Chk1 and Rad53 (Chk2 in mammals) (reviewed in Carr 2002; Nyberg et al. 2002).

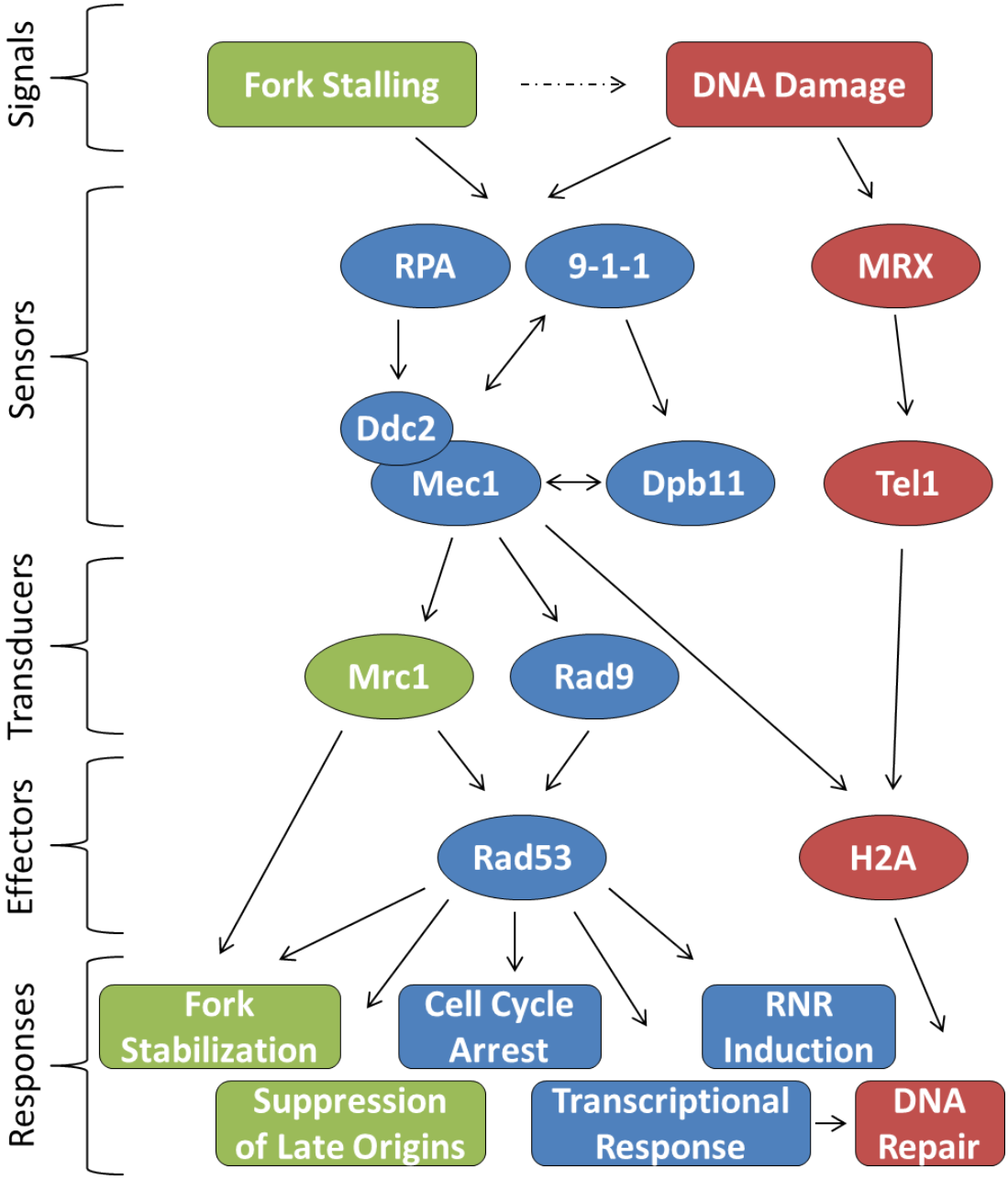

Figure 1.5: The replication and DNA damage checkpoint in *S. cerevisiae*.

The checkpoint is perpetuated as a signal that is detected by sensors and mediated by transducers to effectors which can elicit a variety of responses. The signal pathways specific to replication stress are shown in green while the cascade for DNA damage is shown in red. The central signaling pathway common to stresses is shown in blue. (Adapted from Schleker et al. 2009)

1.4.1 Signals for checkpoint activation

The signals that alert the sensors Mec1 and Tel1 vary depending on the type of DNA damage or lesion that is present. Tel1 is primarily activated in response to double stranded DNA breaks (DSBs), while Mec1 responds to the accumulation of ssDNA, which results from stalled replication forks and the repair of a variety of DNA damage including single stranded DNA (ssDNA) breaks , DSBs, bulky adducts, and ionizing radiation (reviewed in Cimprich & Cortez 2008; Sancar et al. 2004).

1.4.1.1 Stalled replication forks

During S-phase checkpoint activation occurs in response to replication fork stalling. Fork progress can be halted by impeding either the replicative helicase or DNA polymerases (Zegerman & Diffley 2009). Helicase stalling is typically the result of bulky DNA lesions, protein cross-linking, or inter-strand cross-links, while polymerase stalling may be caused by dNTP depletion, DNA alkylation, or exposure to pharmacological polymerase inhibitors (discussed in Labib & Hodgson 2007; Zegerman & Diffley 2009; Lambert & Carr 2013). Uncoupling the helicase from the replisome results in large stretches of ssDNA (Sogo et al. 2002). The accumulation of ssDNA recruits RPA, which in complex is required to bind Ddc2, an activating co-factor for Mec1 (discussed in Cortez 2005; Friedel et al. 2009; Zou & Elledge 2003). In addition to RPA, it appears the presence of a primer-template junction is also required for complete checkpoint activation (Byun et al. 2005; MacDougall et al. 2007). This is consistent with the observation that replication fork formation is required for checkpoint activation during S-phase as replication forks are a ready source of primed ssDNA (Tercero et al. 2003).

Mec1/Ddc2 activation also requires interaction with the 9-1-1 (mammalian Rad9-Rad1-Hus1, Rad17-Ddc1-Mec3 in *S. cerevisiae*) checkpoint clamp (Majka, Binz, et al. 2006; Navadgi-Patil & Burgers 2009). The 9-1-1 complex is recruited to DNA damage by ssDNA and is loaded by the alternate clamp loader Rad24-RFC (Navadgi-Patil & Burgers 2011; Harrison & Haber 2006). In addition to its role in DNA replication, Dpb11 is also required for checkpoint signalling and activation of Mec1/Ddc2 (Mordes et al. 2008; Navadgi-Patil & Burgers 2008). The 9-1-1 complex can activate Mec1/Ddc2 via two mechanisms. The Ddc1 subunit of the clamp directly binds to and robustly activates Mec1/Ddc2, while also recruiting Dpb11 (Majka, Niedziela-Majka, et al. 2006; Navadgi-Patil & Burgers 2009).

Activation of the effector kinase Rad53 by Mec1 in response to stalled replication forks is dependent upon the signal transducer Mrc1 (Alcasabas et al. 2001; Osborn & Elledge 2003). As a component of the replisome, Mrc1 is required for the normal progression of replication forks (Osborn & Elledge 2003). In the absence of Mrc1 replication forks progress slowly and do not collapse when the checkpoint is invoked, however when checkpoint conditions are lifted these forks are unable to restart (Szyjka et al. 2005; Tourrière et al. 2005; Hodgson et al. 2007). Since replication forks do not collapse in Mrc1 null cells, phosphorylation of Rad53 dependent on Mrc1 is dispensable for fork integrity (Tourrière et al. 2005). Mrc1 is partially redundant to the other checkpoint transducer, Rad9, in that they both mediate the checkpoint signal between sensor and effectors (Alcasabas et al. 2001). Rad9 and Mrc1 null cells show the same phenotype as Rad53 null cells with respect to fork collapse (Lee et al. 2004). While Mrc1 activity is important for propagation of the checkpoint

response and resumption of stalled forks it appears dispensable for the most important function of the replication checkpoint, fork stabilization (Tercero et al. 2003).

1.4.1.2 DNA damage

Interestingly, the accumulation of ssDNA and recruitment of RPA appears to be a common event signaling DNA damage. Most lesions are processed in a similar manner undergoing resection that produces ssDNA bound by RPA (discussed in Huertas 2010; Mimitou & Symington 2009; Majka, Binz, et al. 2006). Similar to fork stalling, Mec1 is then activated by Ddc2 bound by RPA and ssDNA, which is subsequently activated by the 9-1-1 complex and Dpb11 (Zou & Elledge 2003; Majka, Niedziela-Majka, et al. 2006; Mordes et al. 2008). However in response to DNA damage, the checkpoint signal is mediated by the transducer Rad9 not Mrc1 (Harrison & Haber 2006; Sancar et al. 2004; Carr 2002). Interestingly, while Dpb11 contributes to Mec1/Ddc2 activation, it also required for efficient Rad9 phosphorylation (Pfander & Diffley 2011; Puddu et al. 2008). Rad9 is a scaffold protein that is essential to perpetuate the checkpoint signal in response to DNA damage (Weinert & Hartwell 1988; Branzei & Foiani 2009). Mec1 dependent phosphorylation of Rad9 recruits Rad53 (Schwartz et al. 2002; Sweeney et al. 2005). Rad9 then facilitates recognition and activation of Rad53 by Mec1 and acts as a scaffold for Rad53 mediated autotransactivation (Sweeney et al. 2005; Gilbert et al. 2001; Ma et al. 2006).

DSB formation is directly detected by the MRX (Mre11-Rad50-Xrs2) complex where it can activate either of the checkpoint sensors Mec1 or Tel1 (Williams et al. 2010; Rupnik et al. 2010). The Mec1 mediated response relies on ssDNA formation by nuclease activity as discussed above (Mimitou & Symington 2009; Huertas 2010). The checkpoint sensor Tel1

functions in parallel with Mec1, also resulting in effector kinase activation, and requires MRX for activation, although the exact molecular mechanisms as to how this occurs are still unclear (reviewed in Gobbini et al. 2013).

1.4.2 The response to checkpoint activation

In *S. cerevisiae* the primary effector of the checkpoint response is Rad53. This effector kinase is composed of a central kinase domain flanked by two FHA domains. While Chk1 is present in yeast, its role in checkpoint signaling appears to be restricted to mitosis where it prevents degradation of securin (Pds1) (Sanchez et al. 1999). These checkpoint effector kinases act upon a variety of targets to complete the checkpoint response.

1.4.2.1 Ribonucleotide reductase (RNR) regulation

The RNR genes function to produce dNTPs required for replication and repair. Levels of dNTPs are cell cycle dependent with an increase in production during S-phase, the result of increased expression of RNR subunits and degradation of the RNR inhibitor Sml1(Chabes et al. 2003; Zhao et al. 2001; Elledge & Davis 1990). Checkpoint induction results in a six to eight fold increase in dNTP levels, which improves survival following DNA damage (Chabes et al. 2003). Up-regulation of RNR transcription by the Rad53 target Dun1 is the result of Sml1 degradation and inhibition of the RNR repressor Crt1 (Zhao & Rothstein 2002; Huang et al. 1998; Allen et al. 1994). Even in the absence of checkpoint induction Mec1 and Rad53 are essential for cell survival (Desany et al. 1998). Cells lacking Mec1 and Rad53 are only viable in unperturbed conditions if RNR expression is increased or Sml1 is deleted (Desany et al. 1998; Zhao et al. 1998; Zhao et al. 2001). However, even a modest two fold constitutive increase in dNTP levels results in increased rates of mutation (Chabes et al. 2003). Thus,

regulation that allows dNTP levels to fluctuate is important for replicative fidelity. While the essential role of Mec1 and Rad53 appears to be the regulation of dNTP levels, cells that lack either are still checkpoint defective and extremely sensitive to DNA damage (Desany et al. 1998).

1.4.2.2 Transcriptional activation

In response to DNA damage a myriad of transcriptional profiles change. Similar to the bacterial SOS response, eukaryotes execute a large program of change in response to DNA damage and other external stresses (reviewed in Fry et al. 2005; Jelinsky & Samson 1999). In response to both the DNA alkylating agent MMS (methyl methanesulfonate) and ionising radiation (IR), but not to other environmental stresses, a group of unique genes are markedly up-regulated in *S. cerevisiae*; of note are the kinase Dun1, RNR subunits Rnr2 and Rnr4, and contributors to homologous recombination Rad51 and Rad54 (Gasch et al. 2001). Other genes up-regulated were involved in glycosylation, mitochondrial function, and plasmid maintenance (Gasch et al. 2001). As discussed in the previous section, RNR regulation by Dun1 plays an important role in response to DNA damage (Huang et al. 1998; Zhou & Elledge 1993). In addition to increasing dNTP pools, Dun1 phosphorylation of Crt1 prevents Crt1 from repressing genes involved in the nucleotide excision repair (NER) and mismatch repair (MMR) DNA damage repair pathways (Huang et al. 1998; Gasch et al. 2001; de la Torre Ruiz & Lowndes 2000). In response to DSBs, a form of DNA damage frequently caused by ionizing radiation, homologous recombination is a particularly important repair mechanism (reviewed in Li & Heyer 2008; Wyman et al. 2004; Huertas 2010; Mimitou & Symington 2009). Thus in response to IR the up-regulation of genes

involved in homologous recombination would be expected. The transcriptional response to checkpoint invocation results in the activation of pathways that will allow DNA repair to occur.

1.4.2.3 Chromatin conformation

The importance of transcriptional regulation of genes in response to checkpoint activation has been discussed. Chromatin conformation not only plays an important role in gene transcription, but also in DNA repair and replication fork stability (reviewed in Schleker et al. 2009). In response to DSBs the histone H2A (H2AX in mammals) is phosphorylated at Ser129, in a Mec1/Tel1 dependent manner (Downs et al. 2004; Fillingham et al. 2006). As phosphorylated H2A (γH2A) flanks DSBs it provides an excellent marker for DNA breaks, serving to recruit DNA repair proteins (Downs et al. 2004). Acetylation of histone H4 is also important for DSB repair and to recruit chromatin remodelling complexes (Downs et al. 2004). Additionally, acetylation of histone H3 at lysine 56 (H3K56) has importance for cells enduring replicative stress as impediments to the acetylation of H3 results in cells sensitive to DNA damaging agents known to cause DSBs (Masumoto et al. 2005). H3K56 functions to create favorable chromatin conditions to facilitate DSB repair (Masumoto et al. 2005).

1.4.2.4 Cell cycle arrest

The most widely known of all check point responses, cell cycle arrest, functions to provide an opportunity for cells to undertake repair of DNA damage before progression to the next stage of the cell cycle. This arrest is particularly important in the case of DNA damage as improperly or unrepaired lesions have the potential to become permanent in future generations, and the accumulation of damage over generations would be disastrous.

The G1/S transition is blocked in response to DNA damage in a Mec1 dependent manner. Rad53 phosphorylates the Swi6 subunit of the SBF/MBF transcription factors, resulting in inhibition of Cln1 and Cln2 production (Sidorova & Breeden 1997). In the absence of Cln1 and Cln2, the positive feed-back loop that inactivates the Cdc28 inhibitor, Sic1, is not engaged and CDK is not activated to signal the transition to S-phase.

During mitosis, DNA damage inhibits the transition from metaphase to anaphase by preserving cohesin and preventing sister chromatid segregation. The checkpoint effectors Chk1 and Rad53, regulated by Mec1 and Rad9, engage separate mechanisms to prevent the APC/C mediated degradation of securin (Sanchez et al. 1999; Agarwal et al. 2003). Chk1 phosphorylates securin preventing its ubiquitination and targeting for destruction, while Rad53 inhibits the interaction between the Cdc20 activator of the APC/C and securin (Agarwal et al. 2003; Sanchez et al. 1999). Chk1 and Rad53 also play roles in preventing mitotic exit through inhibition of the Cdc14 phosphatase (Sanchez et al. 1999; Liang & Wang 2007).

1.4.2.5 Inhibition of late origin firing

In S-phase, origins of replication fire stochastically, with some firing earlier than others, while others rarely fire at all (Raghuraman et al. 2001). The block to late origin firing provides a mechanism to preserve the late-firing subset of origins in times of replication stress or DNA damage. As pre-RC formation can only occur in G1, there are a finite number of available origins for activation, which cannot be reloaded until the next cell cycle (Detweiler & Li 1998; Dahmann et al. 1995). During an unperturbed S-phase the odds of a particular origin firing may be low and it is often passively replicated, during a perturbed S-

phase such an origin may be key to completing genome replication in the event replication forks from early origins stall and irreparably collapse. In this situation the reserve late and dormant origins are the only hope to complete genome replication. Consistent with this model, an increase in the number of origins fired is observed in mammalian cells recovering from checkpoint arrest (Ockey & Saffhill 1976; Taylor 1977).

The suppression of origin firing absolutely requires the Mec1 dependent activation of Rad53 in response to DNA damage or fork stalling (Shirahige et al. 1998; Santocanale & Diffley 1998; Santocanale et al. 1999). As stalled replication forks can signal checkpoint activation, the block to origin activation primarily affects late and dormant origins as these constitute the bulk of unfired origins (Tercero et al. 2003). Origin activation requires both CDK and DDK activity, thus to block firing, the activity of these kinases on pre-RCs must be inhibited (Pasero et al. 1999). Rad53 acts to inhibit both kinase pathways, supressing origin firing (Lopez-Mosqueda et al. 2010; Zegerman & Diffley 2010). Rad53 directly phosphorylates Dbf4, the regulatory subunit of DDK, and the CDK target Sld3, which prevents interaction with the pre-LC, inhibiting helicase activation (Zegerman & Diffley 2010; Lopez-Mosqueda et al. 2010). As CDK activity at origins is inhibited through Rad53 phosphorylation of Sld3, the role of S-phase CDK in preventing new pre-RC formation is unhampered (Zegerman & Diffley 2010; Bloom & Cross 2007).

1.4.2.6 Replication fork stabilization

When replication forks encounter DNA damage, their progress is impeded leading to a drastic reduction in the rate of fork progression independent of Mec1 or Rad53 (Tercero & Diffley 2001). Depletion of Cdc7, the kinase subunit of DDK, during an S-phase arrest

prevents pre-RC activation leading to the formation of new replication forks; upon removal of the block cells are able to complete replication albeit at a reduced rate (Bousset & Diffley 1998). Since new origins could not be activated it stands to reason that replication must have been completed by previously stalled forks. The checkpoint kinases Mec1 and Rad53 are essential for completion of replication following a replication arrest as cells without either kinase are unable to complete synthesis (Desany et al. 1998; Tercero & Diffley 2001; Paciotti et al. 2001). Work with the separation of function mutant *mec1-100*, which is defective for inhibition of late origin firing but not for replication fork stabilization, does not display the marked sensitivity to MMS and IR seen in cells lacking Mec1 (Paciotti et al. 2001; Tercero et al. 2003). This demonstrates that the maintenance of stalled replication forks is the most important function of the checkpoint response during S-phase (Tercero et al. 2003).

Failure to stabilize stalled forks results in forks that are no longer able to resume synthesis after the replication block is removed. This irreversible collapse of forks is characterized by the dissociation of replication factors, such as DNA polymerase and RPA, from the fork (Tercero et al. 2003; Katou et al. 2003; Cobb et al. 2003; Lucca et al. 2004). The irreversibility of fork collapse likely stems from the loss of proteins that cannot be reloaded be at the fork, such as Mcm2-7 (Tercero et al. 2003; Labib et al. 2000).

Interestingly, a member of the replisome, Tof1, is required for fork pausing at programmed sites in the genome and for the stable association of replisome components in a S-phase arrest (Gambus et al. 2006; Katou et al. 2003; Hodgson et al. 2007). However, the mechanisms between programmed fork pausing and fork stalling appear to differ as

programmed pausing does not require the Mec1 and Rad53 checkpoint kinases (discussed in Lambert & Carr 2013; Lambert et al. 2007; Calzada et al. 2005).

Rad53 functions at sites of stalling to prevent the formation of precarious DNA structures such as reversed forks and the accumulation of ssDNA (Lopes et al. 2001; Sogo et al. 2002; Feng et al. 2006). The Exo1 nuclease is recruited to sites of stalled replication and under checkpoint conditions contributes to fork collapse in the absence of Rad53 (Cotta-Ramusino et al. 2005; Segurado & Diffley 2008). Curiously, deletion of Exo1 in cells lacking Rad53 completely suppresses the sensitivity phenotype to several DNA damaging agents (Segurado & Diffley 2008). While the mechanism for this suppression is not known it does indicate that the primary role of Rad53 in response to DNA damage is the stabilization of stalled forks.

1.5 The Dbf4/Cdc7 kinase complex (DDK)

Composed of the serine-threonine kinase Cdc7 and its regulatory subunit Dbf4, the conserved Dbf4 dependent kinase complex (DDK) is essential for mitotic cell growth (Culotti & Hartwell 1971; Chapman & Johnston 1989; Jackson et al. 1993). The catalytic subunit of the kinase complex, Cdc7, is stable and present at constant levels throughout the cell cycle, while levels of the activating subunit Dbf4 vary (Cheng et al. 1999). DDK activity fluctuates in a cell cycle dependent manner in connection with Dbf4 levels, which are high from late G1 through to late M-phase where it is degraded in an APC/C dependent manner (Cheng et al. 1999; Weinreich & Stillman 1999).

1.5.1 The three conserved motifs of Dbf4

Sequence alignment between Dbf4 orthologues in yeast and metazoans has identified three regions of discrete homology, despite little overall sequence similarity. These conserved regions have been named motif N, motif M, and motif C based on their location within the Dbf4 polypeptide (**Figure 1.6**) (Masai & Arai 2000). Each of these motifs have demonstrated importance in mediating intermolecular interactions vital to maintaining the distinct roles of DDK in replication and the checkpoint response.

1.5.1.1 Motif N

Dispensable for cellular proliferation in *S. cerevisiae* and the fission yeast, *Schizosaccharomyces pombe*, motif N is essential for viability in mouse embryonic stem cells (Ogino et al. 2001; Fung et al. 2002; Varrin et al. 2005; Gabrielse et al. 2006; Yamashita et al. 2005). Interestingly, the loss of viability seen in mouse embryonic stem cells lacking motif N occurs despite an intact ability to activate Cdc7 *in vivo* and *in vitro*, suggesting that interactions with other protein factors mediated by this region are crucial for proper Dbf4 function (Yamashita et al. 2005). In both yeasts, cells lacking motif N are sensitive to DNA damaging agents, and in budding yeast these cells also display slowed growth (Takeda et al. 1999; Fung et al. 2002; Varrin et al. 2005; Gabrielse et al. 2006)

The amino-terminus of Dbf4 interacts with the checkpoint kinase Rad53 and Orc6, of the Origin Recognition Complex, and this interaction requires motif N (Duncker et al. 1999; Varrin et al. 2005). An amino-terminal deletion of Dbf4 that interrupts the interaction with Rad53 compromises the block to late origin firing in a *sld3-38A* background (Chen et al. 2013). A portion of the amino-terminus of Dbf4, including motif N shows some primary

sequence similarity to a BRCT domain however, prior to this study no conclusive evidence has been provided to prove the true identity of the region (Masai & Arai, 2000).

1.5.1.2 Motif M

For both spDbf4 and scDbf4, motif M is essential for viability (Ogino et al. 2001; Fung et al. 2002; Varrin et al. 2005). In budding yeast, two-hybrid analysis has found that when motif M alone is deleted the interaction with Cdc7 is largely preserved however, the Mcm2 interaction is drastically reduced (Varrin et al. 2005).Interestingly, a temperature sensitive point mutation within motif M, P277L, imparts resistance to genotoxic stress at semi-permissive growth temperatures, where presumably a reduction in interaction with Mcm2 at this temperature facilitates Rad53 mediated removal of Dbf4 from chromatin under checkpoint conditions (Varrin et al. 2005).

1.5.1.3 Motif C

Of the three conserved regions, motif C is the most similar between species and is predicted to constitute a CCHH type zinc finger (Masai & Arai 2000). Although traditionally thought of as being involved in interactions with nucleic acid, there are now numerous examples of zinc fingers mediating protein-protein interactions (reviewed in Brayer & Segal 2008). Prior to this study little was known about how motif C modulates DDK activity in *S.cerevisiae.*

Truncation of spDbf4 (Dfp1) resulting in the removal of motif C yields cells specifically sensitive to MMS and results in severe meiotic defects (Fung et al. 2002; Dolan et al. 2010; Le et al. 2013). Expression of human Dbf4 in COS-7 cells has demonstrated that motif C is required for *in vitro* huCdc7 activation and *in vivo* phosphorylation of Mcm2 (Sato

et al. 2003). In the same study it was determined that motifs M, C and the intervening sequence constituted the minimal region of Dbf4 required for Cdc7 activation, agreeing with studies from budding yeast showing that regions encompassing motif M and most of motif C mediate the interaction with Cdc7 (Sato et al. 2003; Hardy & Pautz 1996). In mouse embryonic stem cells, both motif M and C are sufficient for Dbf4 activation of Cdc7 but not for cellular proliferation (Yamashita et al. 2005).

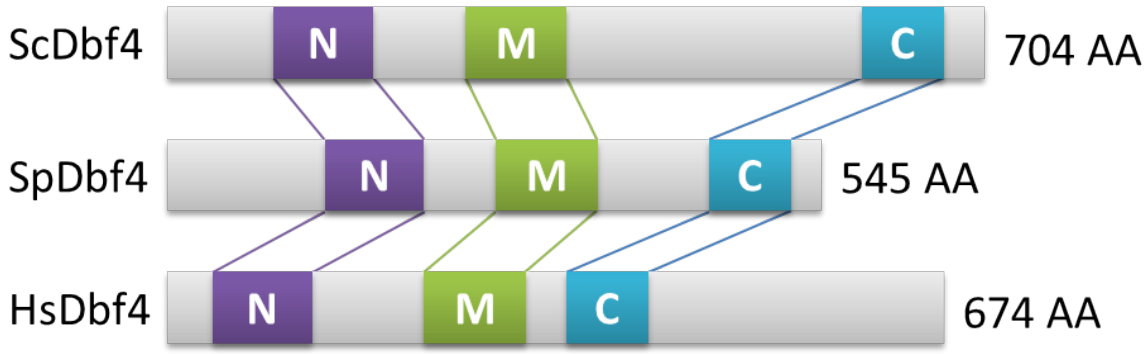

Figure 1.6: Conserved motifs of Dbf4.

Schematic representation of Dbf4 from *S. cerevisiae*, *S. pombe*, and *H. sapiens* depicting the conserved motifs N, M, and C. Length of each protein is indicated as well as relative position of the motifs for each species. (Adapted from Masai & Arai 2000)

1.5.2 DDK is required for helicase activation

The primary target of DDK activity appears to be the activation of the replicative helicase. Mcm2, Mcm3, Mcm4, Mcm6, and Mcm7 have all been shown as *in vitro* substrates for DDK activity (Lei et al. 1997; Weinreich & Stillman 1999). Additionally, the replisome components Cdc45,and Polα are also targets of phosphorylation by Dbf4/Cdc7 (Nougarède et al. 2000; Weinreich & Stillman 1999). DDK activity is required *in vitro* for recruitment of the helicase activating proteins Sld3 and Cdc45 to the pre-RC (Heller et al. 2011; Tanaka &

Araki 2010), ultimately resulting in the formation of chromatin bound CMG complex, which evidence from a variety of organisms indicates forms the active helicase complex (Gambus et al. 2006; Moyer et al. 2006; Aparicio et al. 2009). Using *in vitro* pre-RC assembly assays, it has been found that DDK preferentially phosphorylates pre-RC incorporated Mcm2-7, and that in this context DDK activity is yet still greater for DNA bound, licensed, Mcm2-7 complex (Francis et al. 2009). Interestingly, it appears that certain sites within Mcm2 are phosphorylated with different affinity depending on chromatin association (Montagnoli et al. 2006).

The essential role of Dbf4/Cdc7 is the modification of members of the replicative helicase. Proof of this stems from the ability to bypass the essential need for DDK by mutating components of the Mcm2-7 complex (Hardy et al. 1997; Sheu & Stillman 2010). The first mutation to bypass DDK requirement was found in Mcm5, ironically the only component of the Mcm2-7 complex not phosphorylated by DDK. The *mcm5-bob1* allele, which is a single point mutation P83L, is thought to induce a conformational change in the Mcm2-7 complex, mimicking the effect of DDK phosphorylation (Hardy et al. 1997; Fletcher et al. 2003). Similarly, deletion of an amino terminal serine/threonine rich domain (NSD) of Mcm4 alleviates the essential requirement for DDK (Sheu & Stillman 2010). It is important to note that although these mutations allow mitotic growth in the absence of Dbf4/Cdc7 these cells are by no means healthy, exhibiting slowed growth, sensitization to DNA damaging agents and failure to activate the intra-S-phase checkpoint (Weinreich & Stillman 1999; Sheu & Stillman 2010). The slowed growth and DNA damage phenotypes

seen in DDK null mutants suggests the likelihood that other interactions, while not essential, are important for vegetative growth in both perturbed and unperturbed environments.

1.5.3 Activity outside of the initiation of replication

Knowing DDK is regulated in a cell cycle dependent manner, it is not hard to imagine that Dbf4/Cdc7 would be a candidate to regulate targets beyond the initiation of replication, and indeed DDK activity has been found to play a role in the events of mitosis and meiosis. The initiation of meiotic recombination and separation of homologous chromosomes during meiosis I have both been implicated as cell cycle events where the activity of DDK is important (Matos et al. 2008; Wan et al. 2008; Sasanuma et al. 2008). Dbf4/Cdc7 promotes the initiation of meiotic recombination via interaction with the meiosis specific DSB protein Mer2, the phosphorylation of which is necessary for the association of DSB machinery with chromatin during meiosis (Wan et al. 2008; Sasanuma et al. 2008). DDK also promotes the recruitment of the monopolin complex to kinetochores of sister chromatids during meiosis I (Matos et al. 2008). This recruitment is essential for monopolar spindle pole attachment, which ensures that sister chromatids remain together and only homologous chromosomes are separated in meiosis I. In a *mcm5-bob1* background lacking Cdc7, chromosome segregation fails during meiosis I due to failure to preserve mono-oriented sister chromatids, resulting in only two diploid spores (Matos et al. 2008). Additionally, the activity of DDK is required to cleave the Req8 kleisin subunit of cohesin during meiosis I (Katis et al. 2010). The final step in meiotic recombination is the resolution of chiasmata by cleavage of cohesin along chromosome arms, thus initiation and exit from meiotic recombination both require Dbf4/Cdc7 activity.

The activity of Dbf4/Cdc7 (as previously discussed) is essential for the initiation of replication, the result of which is individual replicons proceeding from origin DNA. This requires constant changes in chromatin conformation as the replication machinery interacts with template DNA. Dynamic changes in chromatin are governed by post-translational modification of histones, which play a role in transcription regulation, mitosis, cell death, DNA damage repair, replication, and recombination (discussed in Ito 2007).

Histone H3 has been implicated as yet another target of Dbf4/Cdc7 in budding yeast (Baker et al. 2010). Serine 45 of histone H3 is phosphorylated by DDK, and mutations that prevent Ser45 phosphorylation result in growth defects and sensitivity to DNA damaging agents (Baker et al. 2010). Interestingly, a phosphomimetic mutation of Ser45 resulted in loss of viability, possibly causing a disruption in interaction between H3 and DNA (Baker et al. 2010). Consistent with this thought, the equivalent residue, Thr 45, in Xenopus has been shown to affect interactions with DNA (Ferreira et al. 2007). This indicates a mechanism where DDK activity can disrupt H3 association with DNA, resulting in changes in chromatin conformation.

The interaction between Dbf4 and Cdc5 appears important for mitotic cell division. A physical interaction between these two appears to be mediated by amino acids 78-96 of Dbf4 in *S. cerevisiae* (Hardy & Pautz 1996; Miller et al. 2009; Chen & Weinreich 2010). DDK can phosphorylate the Cdc5 polo-box-domain (PBD), and phosphorylation of Ser 84 abolishes the interaction between the two (Miller et al. 2009; Chen & Weinreich 2010). Conversely, mutations in Dbf4 that retard the interaction with the PBD suppress a temperature sensitive mutation in Cdc5 (Chen & Weinreich 2010). Dbf4 inhibits Cdc5 mediated activation of the

mitotic exit network (MEN), and it appears that this inhibition is caused by direct interaction between Dbf4/Cdc7 and Cdc5 (Miller et al. 2009; Chen & Weinreich 2010)

1.6 Project goals

Dbf4 motif C is the most conserved of three regions of homology between species (Masai & Arai 2000). Despite this it had been the most poorly understood Dbf4 motif in *S. cerevisiae*. My first research objective was to characterize the role the motif C of Dbf4 plays in DNA replication and the checkpoint response. Toward this aim a mutational study was undertaken to investigate the role conserved residues predicted to constitute a zinc finger have on the function of Dbf4. Of key interest was the protein-protein and protein-DNA interactions mediated by this motif, and the implications these interactions have on replication and the checkpoint response.

The role Dbf4 plays in the checkpoint response to regulate late origin firing has been identified (Zegerman & Diffley 2010; Lopez-Mosqueda et al. 2010). However how Dbf4 interacts with Rad53 had not been defined. The amino-terminus of Dbf4 mediates this interaction and motif N is required, but prior to this study it was not clear what constituted the minimal region of Dbf4 sufficient to interact specifically with FHA1 of Rad53 (Duncker et al. 2002; Varrin et al. 2005). A region of Dbf4 predicted to form a BRCT domain overlaps with portions of Dbf4 identified in the interaction with Rad53. Thus, the second objective of this study was to identify the minimal discrete unit of Dbf4 that interacts with Rad53 and determine if this region constitutes a BRCT domain using a crystallographic approach. Additionally, as FHA domains are known to bind phosphorthreonines, an attempt to identify a phosphoepitope within the Rad53 interacting region of Dbf4 was made.

The third and final objective was to explore the possibility of a phosphorylation independent mode of interaction between Dbf4 and Rad53. Using a combination of bioinformatic, mutational, and NMR spectroscopy strategies unique features of FHA1 were investigated. Toward this aim an important question to be studied will be how FHA1 binds Dbf4.

Chapter 2

Materials & Methods

Portions of this chapter appear in the following journal articles and are reproduced with permission.

This research was originally published in Cell Cycle. Jones DR, Prasad AA, Chan PK, & Duncker BP. The Dbf4 motif C zinc finger promotes DNA replication and mediates resistance to genotoxic stress. *Cell Cycle* 2010; 9: 2018-26. © Jones *et al*; Landes Bioscience

This research was originally published in The Journal of Biological Chemistry. Matthews LA, Jones DR, Prasad AA, Duncker BP & Guarné A. Saccharomyces cerevisiae Dbf4 has unique fold necessary for interaction with Rad53 kinase. J. Biol. Chem. 2012; 287: 2378-87. © the American Society for Biochemistry and Molecular Biology.

This research was originally published in The Journal of Biological Chemistry. Matthews LA, Selvaratnam R*, Jones DR*, Akimoto M, McConkey BJ, Melacini G, Duncker BP & Guarné A. A novel, non-canonical FHA binding interface mediates the interaction between Rad53 and Dbf4. *J. Biol. Chem.* 2014; 289:2589-99. © the American Society for Biochemistry and Molecular Biology.

**these authors contributed equally to this work*

Sections 2.16 – 2.21 were contributed by L.A.M., R.S., M.A., G.M., and A.G.

Section 2.22 was contributed by B.J.M.

2.1 Yeast strains

Table 2.1: List of yeast strains used.

Strain	Genotype	Source
DY-1	*MAT***a**, *ade2-1, can1-100, trp1-1, his3-11, his3-15, ura3-1, leu2-3, leu2-112, pep4::LEU2*	(Duncker et al. 2002)
DY-2	*MAT***a**, *can1-11, ura3-52, dna52-1(dbf4)*	(Varrin et al. 2005)
DY-26	*MAT***a**, *his3Δ200, leu2Δ0, met15Δ0, trp1Δ63, ura3Δ0*	ATCC
DY-27	*MAT***a/α**, *his3Δ1/ his3Δ1, leu2Δ0/ leu2Δ0, ura3Δ0/ ura3Δ0, lys2Δ0, met15Δ0*	ATCC
DY-145	*MAT***a**, *ade2-1, can1-100, his3-11,15, leu2-3, trp1-1, ura3-1, SML1::HIS3 RAD5*	(Tam et al. 2008)
DY-146	*MAT***a**, *ade2-1, can1-100, his3-11,15, leu2-3, trp1-1, ura3-1, SML1::HIS3 RAD5, RAD53::rad53-R70A*	(Tam et al. 2008)
DY-147	*MAT***a**, *ade2-1, can1-100, his3-11,15, leu2-3, trp1-1, ura3-1, SML1::HIS3, RAD5, RAD53::URA3*	(Tam et al. 2008)
DY-159	*MAT***a**, *His3Δ0, leu2Δ0 .lys2Δ0, met15Δ0, ura3Δ0; dbf4Δ0*	This study
DY-165	*MAT***a**, *his3Δ200, leu2Δ0, met15Δ0, trp1Δ63, ura3Δ0, DBF4::dbf4-H680C*	This study
DY-166	*MAT***a**, *his3Δ200, leu2Δ0, met15Δ0, trp1Δ63, ura3Δ0, DBF4::dbf4-H680A*	This study
DY-167	*MAT***a**, *his3Δ200, leu2Δ0, met15Δ0, trp1Δ63, ura3Δ0, DBF4::dbf4-H674A-H680A*	This study
DY-168	*MAT***a**, *his3Δ200, leu2Δ0, met15Δ0, trp1Δ63, ura3Δ0, DBF4::dbf4-C661A C664A*	This study
DY-195	*MAT***α**, *his3Δ200, leu2Δ0, ura3Δ0, lys2Δ0*	This study
DY-259	*MAT***a** *his3Δ1, leu2Δ0, met15Δ0, ura3Δ0, RAD5::KanMX*	ATCC
DY-260	*MAT***a** *his3Δ1, leu2Δ0, met15Δ0, ura3Δ0, REV3::KanMX*	ATCC
DY-282	*MAT***α** *, his3Δ200, leu2Δ0, ura3Δ, DBF4::dbf4- H680C*	This study
DY-297	*MAT***a** *his3Δ1, leu2Δ0, met15Δ0, ura3Δ0, RAD30::KanMX*	ATCC
DY-319	*MAT***a**, *his3Δ1, leu2Δ0, met15Δ0, ura3Δ0, DFB4:: dbf4-H680C, REV3::KanMX*	This study
DY-324	*MAT***a**, *his3Δ1, leu2Δ0, ura3Δ0, DBF4:: dbf4-H680C, RAD30::KanMX*	This study
DY-331	*MAT***a**, *his3Δ1, leu2Δ0, ura3Δ0, DBF4:: dbf4-H680C, RAD5::KanMX*	This study

Dbf4 motif C mutant strains (DY-165, DY-166, DY-167, and DY-168) were generated in by replacing *DBF4* in the DY-26 parental strain via standard two-step gene replacement protocols using yeast integrating plasmid pRS406 derived vectors linearized with *BglII* (Burke et al. 2000). Genotype of the resulting strains was confirmed by sequencing (Robarts Research Institute, University of Western Ontario). The mating-type-α strain containing *dbf4-CCHC* (DY-282) was generated by mating DY-165 to DY-195. The resulting diploid was sporulated and spore genotypes were determined by arrest in the presence of (5 μg/mL) α-factor, sequencing of the genomic *DBF4* allele, and growth on synthetic complete medium lacking either histidine, uracil, tryptophan, methionine, leucine, or lysine. Double mutants

containing *dbf4-CCHC* and either *rad5Δ*, *rad30Δ*, or *rev3Δ* were constructed by mating DY-282 to DY-259, DY-297, or DY-260. The resulting diploids were sporulated and genotype was determined by α-factor arrest, sequencing of genomic *DBF*, PCR flanking deleted genomic loci, and growth on synthetic complete medium lacking histidine, uracil, tryptophan, methionine, leucine, or lysine.

2.2 Yeast mating and sporulation

Equal sized colonies from freshly streaked plates containing opposite mating type yeast cells were taken and mixed into ~5mm circles on a new YPD (Yeast extract, Peptone, Dextrose) plate and incubated at 30ºC for 3 hours. After incubation the mating mixture was streaked along the edge of a fresh YPD plate and for isolation using a MSM micromanipulator (Singer Instruments). Zygotes resulting from fusion of opposite mating type cells were identified by their distinctive tri-lobed appearance and isolated to an untouched section of the YPD plate. Plates were then grown for 2-3 days until colonies formed by the isolated zygote were detected. The resulting cells were analysed by FACS analysis (see below section for method) to identify the presence of 2C and 4C peaks, confirming cells were indeed diploid.

Diploid cells were grown to stationary phase, and 500 µl of the culture was washed with sterile ddH_2O (double distilled water) and the pellet was resuspended in 5 ml sporulation media (0.3% potassium acetate, 0.502% raffinose) in a 50 ml falcon tube. Cultures were incubated at 23ºC for 4-7 days or until ascospores were observed. Once ascospore formation was observed 500 µl of the sporulation culture was resuspended in zymolyase solution (0.5 mg/ml in 1M sorbitol) for 8-10 minutes at 30ºC. After incubation,

800 µl sterile ddH_2O was slowly added down the side of the tube, cells were allowed to rest for 5 minutes on ice, and 800 µl was removed from the top of the tube. From the remaining mixture 10 µl was spotted onto the edge of a fresh YPD plate which was then tilted to allow the spotted mixture to drip along the edge of the plate. Tetrads were then dissected with a MSM micromanipulator (Singer Instruments) and individual spores were genotyped as discussed above.

2.3 Genomic DNA isolation

Yeast cells were grown to stationary phase in 10 ml media, washed with 30 ml ddH_2O, and resuspended in 2 ml screw cap tubes with 200 µl yeast genomic prep mix (2% Triton X-100, 1% SDS, 100 mM NaCl, 10 mM Tris-Cl (pH 8), 1 mM EDTA). To this 0.3g of 0.5 mm glass beads and 200 µl phenol:chloroform:isoamylalcohol (25:24:1) were added. The mixture was then vortexed for 4 minutes after which 200 µl of TE was added and the mixture centrifuged at 13,200 rpm for 5 minutes. The supernatant was then transferred to a new tube and 1 ml of 100% ethanol was added. Tubes were inverted ten times and then centrifuged for 2 minutes at 13,200 rpm. The supernatant was discarded and the pellet was resuspended in 400 µl of TE. Following resuspension 10 µl of RNaseA (10 mg/ml; Sigma) was added and samples were incubated at 37ºC for 10 minutes. To this 10 µl of 4M ammonium acetate and 1 ml of 100% ethanol was added and mixed by inversion ten times. The mixture was centrifuged at 13,200 rpm for 2 minutes. The supernatant was discarded, the pellet was allowed to air dry for ten minutes and was then resuspended in 50 µl ddH_2O.

2.4 Plasmid construction

Unless otherwise indicated, DY-27 genomic DNA was used as template for PCR amplification of genes of interest and all point mutations and deletions of less than 45 base pairs were created using the QuikChange multi or QuikChange II XL site-directed mutagenesis kits (Stratagene). Mutations were generated following QuikChange kit protocols with the minor deviations. *DpnI* digestion times were increased to 1.5 hours, and reaction volumes used for transformation were increased to 5 µl. For the QuikChange II XL kit, 2.5 µl of QuikSolution was added to the initial reaction mixtures. All constructs were completely sequenced to ensure no second site mutations were present (Robarts Research Institute, University of Western Ontario).

The pCM190 motif C mutants pCM190-*dbf4CCHC* pCM190-*dbf4CCHA*, pCM190-*dbf4CCAA*, and pCM190-*dbf4AAHH* were generated by QuikChange using pCM190-*DBF4* as template. The triple and quadruple motif C mutants pCM190-*dbf4AAHA*, and pCM190-*dbf4AAAA* were generated by QuikChange using pCM190-*dbf4AAHH* as template. The yeast integrating vector pRS406 derived constructs pRS406-*dbf4CCHC* pRS406-*dbf4CCHA*, pRS406-*dbf4CCAA*, and pRS406-*dbf4AAHH* were generated by amplifying the motif C mutant alleles from the pCM190 series and cloning them into the *EcoRI* and *BamHI* sites of pRS406. Similarly, the pEG202 bait series of motif C mutants were made by PCR amplification of the pCM190 motif C mutant set using *EcoRI* and *NcoI* containing forward and reverse primers respectively resulting in pEG202-*dbf4CCHC* pEG202 -*dbf4CCHA*, pEG202-*dbf4CCAA*, pEG202-*dbf4AAHH*, pEG202-*dbf4AAHA*, and pEG202-*dbf4AAAA*. The prey pJG4-6-*CDC7*, was generated by amplifying the *CDC7* open reading frame from

genomic DNA with forward and reverse primers containing *EcoRI* and *BglII* sites respectively.

The bait pEG202-*DBF4* was generated by amplification of genomic *DBF4* from DY-26, and ligation of that fragment into the *EcoRI* and *NcoI* sites of pEG202. All pEG202 derivatives containing fragments of DBF4 were created using pRS315-*DBF4* (formerly pPD32) as template, and fragments were cloned into the *EcoRI* and *XhoI* sites of pEG202. The bait pEG202-*dbf4Δ66-119* was created by ligating two separate fragments into pEG202. The region corresponding to amino acids 1 to 65 of Dbf4 (Fragment 1) was amplified using an *EcoRI* containing forward primer and a reverse primer ending at an internal *BglII* site within *DBF4*. The region corresponding to amino acids 120 through till the end of Dbf4 (Fragment 2) was amplified by a forward primer containing an in frame *BglII* site and a reverse primer containing an *NcoI* site. Fragment 1 was digested with *EcoRI* and *BglII*, fragment 2 was digested with *BglII* and *NcoI*, and pEG202 was digested with *EcoRI* and *NcoI*. Both fragments and the vector were joined together in a single ligation. The pEG202 constructs containing fragments of Dbf4 with the amino acids 66-119 deleted were made using pEG202-*dbf4Δ66-119* as template. All Dbf4 amino terminal point mutations were made using QuikChange with pEG202-*DBF4* as template. To generate pRS315-*dbf4T171R*, pRS315-*dbf4W116DM120A*, and pRS315-*dbf4Δ135-179*, the Bsu36I fragment of pRS315-*DBF4* was replaced with the equivalent fragment from pEG202-*dbf4T171R*, pEG202-*dbf4W116DM120A*, and pEG202-*dbf4Δ135-179*.

The prey vectors pJG4-6-*RAD53* and pJG4-6-*rad53R70A* were made by cloning genomic sequence encoding Rad53 from DY-145 and DY-146 respectively into the *NcoI* and

EcoRI sites of pJG4-6. Point mutations within FHA1 were generated by QuikChange using pJG-Rad53 as template. Sequence encoding amino acids 1-165 of the resulting constructs was then sub-cloned into the *NcoI* and *EcoRI* sites of pJG4-6 to create FHA1 prey vectors. The *RAD53* open reading frame, along with 500bp each of flanking upstream and downstream sequence, was PCR amplified from genomic DNA and cloned into the *Xba*I and *Pst*I sites of the CEN vector pRS315 to create pRS315-*RAD53*. The *Sex*AI to *Bgl*II fragment of the pJG-FHA1 variants, pJG4-6-FHA1N112A/E129A, pJG4-6-FHA1N112A/E129A/V144N/F146A, and pJG4-6-FHA1V144N/F146A, were used to replace the equivalent fragments in pRS315-*RAD53* to generate pRS315-*rad53N112A/E129A*, pRS315-*rad53N112A/E129A/V144N/F146A*, and pRS315-*rad53V144N/F146A*, respectively.

Table 2.2: List of primers used.

Primer Name	Sequence (5'-3')	Primer Use
pJG-Seq For	tgcctcctaccttatgatgtgcc	Reverse primer to sequence pJG4-6 insert
pJG-Seq Rev	tggagacttgaccaaacctctggc	Forward primer to sequence pJG4-6 insert
pEG202 insert For	ccaattgtcgtagatcttcgtcagc	Reverse primer for sequencing pEG202 insert
pEG202 insert Rev	gcttggctgcaggtcgactcg	Forward primer for sequencing pEG202 insert
BamHI Dbf4 For	gcaatcgggatccatggtttctccaacgaaaatg	Cloning primer from start of DBF4 with BamHI site
Dbf4NcoRev	gactta ccatgg ctatatttgaaatctgagattttc	Cloning primer from end of DBF4 with NcoI site
Dbf4 AA65 For Eco	ctccaacagcagcagcattt	Cloning primer from AA65 of DBF4 with EcoRI site
Dbf4 AA120 Eco For	tatatatagaattcatgaaaagagattctcgcatttac	Cloning primer from AA120 of DBF4 with EcoRI site
Dbf4 AA135 For Eco	gagatgaatacatataataa	Cloning primer from AA135 of DBF4 with EcoRI site
Dbf4 120 NcoI For	tatatatccatgggcatgaaaagagattctcgcatttactttgac	Cloning primer from AA120 of DBF4 with NcoI site
Dbf4 AA109 Rev Xho STOP	tatatatctcgagctacaattccttaggcgtaaccc	Cloning primer from ending at AA109 of DBF4 with XhoI site
Dbf4 AA179 Rev Xho STOP	tatatatctcgagctaaacagaccttcttgtgataa	Cloning primer from ending at AA179 of DBF4 with XhoI site

Primer Name	Sequence (5'-3')	Primer Use
Dbf4 AA221 StopXhoRev	atatatatctcgagctacaaatgatccaaatcaacatcaagat	Cloning primer from ending at AA221 of DBF4 with XhoI site
Dbf4 AA250 StopXhoRev	atatatatctcgagctagtctctatccgttggtccatata	Cloning primer from ending at AA250 of DBF4 with XhoI site
Dbf4 296 StopRev XhoI	tatatatactcgagctagtaaggtagttcgtctaagtttg	Cloning primer from ending at AA296 of DBF4 with XhoI site
Dbf4 250 EcoRI Rev	atatatatgaattcctagtctctatccgttggtccatataattttt	Cloning primer from ending at AA250 of DBF4 with EcoRI site
Dbf4105EcoFor	tatatatagaattcacgcctaaggaattgctggaa	Cloning primer from AA105 of DBF4 with EcoRI site
Dbf494EcoFor	tatatatagaattcggtacgggtctgaaaaatgtcg	Cloning primer from AA94 of DBF4 with EcoRI site
Dbf4 SacI 65 REV	tatatatagagctcgaggcgctcaagag	Cloning primer from ending at AA65 of DBF4 with SacI site
Dbf4 SacI 120 For	tatatatagagctcatgaaaagagattctcgc	Cloning primer from AA120 of DBF4 with SacI site
Dbf4 476 FOR	gtgcgcaaataactcaatttttgac	Primer to sequence Dbf4 from indicated NT
Dbf4 527 REV	cttgtgataactattgtgacagtagtg	Primer to sequence Dbf4 from indicated NT
Dbf4 730 FOR	caatcttctacacaatgaaaaattat	Primer to sequence Dbf4 from indicated NT
Dbf4 975 FOR	gagatactcgagagacaaagcaaac	Primer to sequence Dbf4 from indicated NT
Dbf4 1020 REV	aagttgcagtgcatatttttgtttgc	Primer to sequence Dbf4 from indicated NT
Dbf4 1508 FOR	atgtggcaacctcttttggcaatgg	Primer to sequence Dbf4 from indicated NT
Dbf4 1510 REV	catcattagattgatgtgcaccact	Primer to sequence Dbf4 from indicated NT
Rad53 K22 NcoI For	tatatatacccatgggcaagttttctcaagaacag	Cloning primer from AA22 of Rad53, with NcoI site
Rad53 165 EcoRI Rev Stop	tatatatagaattcctaagatcttatgcgatcaacttt	Cloning primer from AA165 of Rad53, with EcoRi site
RAD53NCOFOR	ctgattgccatgggcatggaaaatattacacaaccc	Cloning primer from start of Rad53, with NcoI site
RAD53ECOREV	gacttagaattcttacgaaaattgcaaattctc	Cloning primer from end of Rad53, with EcoRi site
Rad53 494 For	aaagttgatcgcataagatc	Primers used to sequence Rad53 from indicated NT
Rad53 1120 For	cagaggtaaagatacatccg	Primers used to sequence Rad53 from indicated NT
Rad53 1675 For	ctagagaacaaaaacttttac	Primers used to sequence Rad53 from indicated NT
Rad53 510 Rev	caggagaagctattttagag	Primers used to sequence Rad53 from indicated NT
Rad53 1061 Rev	tgccaaagtgccacagaagg	Primers used to sequence Rad53 from indicated NT
Rad53 1621 Rev	cttttgggctgtgtatatcg	Primers used to sequence Rad53 from indicated NT

Primer Name	Sequence (5’-3’)	Primer Use
Rad53 2222 Rev	tgaagaagaagccgagggtt	Primers used to sequence Rad53 from indicated NT
QC Dbf4 H674A	cgaatctttagaacaagccatagtttctgagaaggc	QuikChange Primer to make indicated Dbf4 mutation
QC Dbf4 H674A H680A	ctttagaacaagccatagtttctgaagaaggctttgtctttcgctg	QuikChange Primer to make indicated Dbf4 mutation
QC Dbf4 H680C	cacatagtttctgagaagtgtttgtctttcgctg	QuikChange Primer to make indicated Dbf4 mutation
QC Dbf4 C661A C664A V2	cggtaaaaaattccggatacgctgaaaatgctcgtgtaaaatacgaatc	QuikChange Primer to make indicated Dbf4 mutation
Dbf4 QC T163A	cattgggtgcgcaaatagctcaatttttgacactac	QuikChange Primer to make indicated Dbf4 mutation
Dbf4 QC T171A	caatttttgacactactgtcgctatagttatcacaagaaggtc	QuikChange Primer to make indicated Dbf4 mutation
Dbf4 QC T157A	gaaaagagggtttcttgcattgggtgcgcaaatac	QuikChange Primer to make indicated Dbf4 mutation
Dbf4 QC T224A	ggatcatttgagcaaggctaaatctgcttctttagc	QuikChange Primer to make indicated Dbf4 mutation
Dbf4 QC T163R	cttacattgggtgcgcaaatacgtcaatttttgacactactgtc	QuikChange Primer to make indicated Dbf4 mutation
Dbf4 QC T171R	caatttttgacactactgtccgaatagttatcacaagaaggtc	QuikChange Primer to make indicated Dbf4 mutation
Dbf4 QC T157R	attgaaaagagggtttcttcgattgggtgcgcaaatacgtc	QuikChange Primer to make indicated Dbf4 mutation
Dbf4 QC T224R	gatttggatcatttgagcaagcgtaaatctgcttctttagctgcg	QuikChange Primer to make indicated Dbf4 mutation
Dbf4 QC T163A RevComp	gtagtgtcaaaaaattgagctatttgcgcacccaatg	QuikChange Primer to make indicated Dbf4 mutation
Dbf4 QC T171A RevComp	gaccttcttgtgataactatagcgacagtagtgtcaaaaaattg	QuikChange Primer to make indicated Dbf4 mutation
Dbf4 QC T163R RevComp	gacagtagtgtcaaaaaattgacgtatttgcgcacccaatgtaag	QuikChange Primer to make indicated Dbf4 mutation
Dbf4 QC T171R RevComp	gaccttcttgtgataactattcggacagtagtgtcaaaaaattg	QuikChange Primer to make indicated Dbf4 mutation
Dbf4T175A	gacactacgtcacaatagttatcgcaagaaggtctgttgagaac	QuikChange Primer to make indicated Dbf4 mutation
DBF4 GA159LL	gatttattgaaaagagggtttcttacattgcttctgcaaataactc	QuikChange Primer to make indicated Dbf4 mutation
DBF4 (T171AT175A)	gacactactgtcgcaatagttatcgcaagaaggtc	QuikChange Primer to make indicated Dbf4 mutation
Dbf4 W202E	ctacatgaaagttgagagttacgaaaaggctgccag	QuikChange Primer to make indicated Dbf4 mutation
Dbf4 T105A For	gtcgagccaagggttgcgcctaaggaattgctg	QuikChange Primer to make indicated Dbf4 mutation
Dbf4 T105A RevComp	cagcaattccttaggcgcaacccttggctcgac	QuikChange Primer to make indicated Dbf4 mutation
Dbf4 QC T171D	caatttttgacactactgtcgatatagttatcacaagaaggtc	QuikChange Primer to make indicated Dbf4 mutation
Dbf4 QC T171E	caatttttgacactactgtcgaaatagttatcacaagaaggtc	QuikChange Primer to make indicated Dbf4 mutation

Primer Name	Sequence (5'-3')	Primer Use
Dbf4 QC T171E RevComp	gaccttcttgtgataactatttcgacagtagtgtcaaaaaattg	QuikChange Primer to make indicated Dbf4 mutation
Dbf4 W116E QC For	ggaattgctggaatggcaaacaaatgagaaaaagataatgaaaagagattctcgc	QuikChange Primer to make indicated Dbf4 mutation
Dbf4 W116E QC RevComp	gcgagaatctcttttcattatctttttctcatttgtttgccattccagcaattcc	QuikChange Primer to make indicated Dbf4 mutation
Dbf4 M120A W116E For	gctggaatggcaaacaaatgagaaaaagatagcgaaaagagattctcgcatttac	QuikChange Primer to make indicated Dbf4 mutation
Dbf4 M120A W116E RC	gtaaatgcgagaatctcttttcgctatctttttctcatttgtttgccattccagc	QuikChange Primer to make indicated Dbf4 mutation
Rad53 N71A QC For	gaaagtttggacatttggtagagccccagcctgtgactatcatttagg	QuikChange Primer to make indicated Rad53 mutation
Rad53 N71A QC RevComp	cctaaatgatagtcacaggctggggctctaccaaatgtccaaactttc	QuikChange Primer to make indicated Rad53 mutation
Rad53 V144N F146A QC For	ggcgtggaatcagatattttatctctgaacattgccataaacgacaaatttaagcagtgcc	QuikChange Primer to make indicated Rad53 mutation
Rad53 V144N F146A QC RC	ggcactgcttaaatttgtcgtttatggcaatgttcagagataaaatatctgattccacgcc	QuikChange Primer to make indicated Rad53 mutation
Rad53 I37A T39A QC	cgaaaacattgtgtgcagggtcgcttgtgccacgggtcaaatttcccatc	QuikChange Primer to make indicated Rad53 mutation
Rad53 I37A T39A QC RC	gatgggaatttgacccgtggcacaagcgaccctgcacacaatgttttcg	QuikChange Primer to make indicated Rad53 mutation
Rad53 E129A QC	gttactgtctcaaggtgatgcaataaccgttggtgtaggc	QuikChange Primer to make indicated Rad53 mutation
Rad53 E129A QC RevComp	gcctacaccaacggttattgcatcaccttgagacagtaac	QuikChange Primer to make indicated Rad53 mutation
Rad53 N112A QC	ccactaatgggacctggttagctgggcaaaaagtcgagaag	QuikChange Primer to make indicated Rad53 mutation
Rad53 N112A QC RevComp	cttctcgacttttgcccagctaaccaggtcccattagtgg	QuikChange Primer to make indicated Rad53 mutation
Rad53QC V134DI140A F	gatgaaataaccgttggtgacggcgtggaatcagatgctttatctctggtcattttc	QuikChange Primer to make indicated Rad53 mutation
Rad53QC V134DI140A RC	gaaaatgaccagagataaagcatctgattccacgccgtcaccaacggttatttcatc	QuikChange Primer to make indicated Rad53 mutation

2.5 Synchronizing yeast cultures

Exponentially growing yeast cultures were synchronized in late G1 phase with synthetic yeast mating pheromone α-factor (New England Peptide). Cultures of mating-type-a cells were grown to a density of $5x10^6$ cells/ml, washed twice in sterile ddH_2O, and resuspended in fresh media containing α-factor (10 μg/ml). After 2.5-3 hours incubation at 30ºC, 10 μl culture aliquots were taken and analyzed by light microscopy for the presence of

schmooed cells to confirm arrest. To release cells from the arrest, cultures were spun down and washed with sterile ddH_2O twice, then resuspended in fresh medium containing 50 μg/ml Pronase E (Sigma).

2.6 FACS analysis

Aliquots of 1 ml were taken from experimental yeast cultures, immediately centrifuged at 13,200 rpm for 30 seconds, resuspended in 1 ml of cold 70% ethanol, and stored at 4ºC until processing. Half of each sample aliquot was spun down and washed with 1ml ddH_2O, centrifuged for 30 seconds at 13,200 rpm and resuspended in 500 μl RNaseA (200 μg/ml in 50 mM Tris-HCl, pH8) for 2-4 hours at 37ºC. After incubation cells were centrifuged for 30 seconds at 13,200 rpm and resuspended in 500 μl Proteinase K (2 mg/ml in 50 mM Tris-HCl, pH7.5) for 30-60 minutes at 50ºC. Cells were then spun down for 30 seconds at 13,200 rpm and resuspended in 100 μl FACS buffer (200mM Tris-HCl pH 7.5, 200mM NaCl, 78mM $MgCl_2$) then transferred into 5 ml Falcon tubes (BD Biosciences) containing 500 μl Sytox solution (50mM Tris-HCl pH 7.5, 1:5000 dilution Sytox Green [Molecular Probes]). Samples were then analyzed on a BD FACSVantage SE flow cytometry system.

2.7 Yeast whole cell extract preparation and western blotting

A 20 ml volume of yeast cultures (~$1x10^7$ cells/ml), was spun down in 50 ml tubes at 4000 rpm for 3 minutes at room temperature, and resuspended in 400 μl ice cold lysis buffer (10 mM Tris-HCl, pH 8; 140 mM NaCl; 1% Triton X-100; 1 mM EDTA, PMSF) supplemented with 10 μl/ml protease inhibitor cocktail (Fisher). The mixture was then transferred to 2 ml screw cap tubes containing 0.3g of 0.5 mm glass beads and stored on ice.

Samples were lysed at 4ºC with a mini-beadbeater-16 (Biospec), following 8 cycles of 1 minute length each. Each cycle consisted of 30 seconds of agitation followed by 30 seconds cooling on ice. Samples were then centrifuged at 4ºC for 30 seconds at 13,200 rpm, then the supernatant (whole cell extract) was transferred to 1.5 ml tubes on ice. Protein concentration was determined by Bradford assay using Bio-Rad protein assay (BioRad).

Whole cell extracts were mixed with one-half their volume of sample loading buffer (60% 4x buffer [15% SDS; 40% glycerol, 166 mM tris-base]; 0.26 M DTT; 7% bromophenol blue), and boiled for 10 minutes. Samples were then either run directly on SDS polyacrylamide gels or stored at -20ºC until electrophoresis. Prepared samples were run on 7.5% or 10% SDS polyacrylamide gels with a 5% stacking gel, with equal total amount of protein loaded in each lane as determined by Bradford assay. After electrophoresis, protein from the polyacrylamide gel was transferred to nitrocellulose via wet transfer. The gel and nitrocellulose were sandwiched by Whatman paper and sponges, then completely submerged in transfer buffer (200 mM glycine; 25 mM tris-base; 20% methanol; 0.05% SDS). The transfer process was carried out for 2-16 hours at 50-30 volts. After transfer, blots were stained with 0.1% Ponceau S and imaged. Blots were then destained in TEN+T (20 mM Tris-HCl; 1mM EDTA; 0.14 M NaCl; 0.05% Tween 20), and blocked for 1-16 hours in TEN+T with 5% skim milk powder. After blocking the membranes are rinsed 3 times with ddH_2O, and probed with primary antibody in TEN+T with 3% Bovine Serum Albumin (Sigma) for 1 hours with gentle shaking. Before addition of secondary antibody in TEN+T with 5% skim milk powder, membranes were washed with TEN+T for 10 minutes, three times. Secondary detection is performed in the dark and blots were covered. After incubation in secondary

antibody for 1 hour, blots were again washed three times in TEN+T for 10 minutes each, and finally stored in ddH_2O. Blots were imaged with either a Typhoon 9400 (GE Healthcare) or a Pharos FX Plus (BioRad).

Table 2.3: List of antibodies used for western blot detection.

Antibody	Source	Catalog #	Concentration	Dilution
AlexaFluor 488 donkey anti-goat	Invitrogen	A11055	2mg/ml	1:3000
AlexaFluor 488 goat anti-mouse	Invitrogen	A11001	2mg/ml	1:3000
AlexaFluor 647 goat anti-rabbit	Invitrogen	A21446	2mg/ml	1:3000
anti-MYC (mouse monoclonal)	Sigma	M5546	2mg/ml	1:5000
anti-HA (mouse monoclonal)	Sigma	H9658	2mg/ml	1:5000
anti-LexA (rabbit polyclonal)	Cedarlane	PA1-4966	2mg/ml	1:3000
anti-Rad53 (goat polyclonal)	Santa Cruz	SC6749	0.2mg/ml	1:500

2.8 Kinase assays

Yeast whole cell extracts were prepared as described above, and 2 μg of whole cell extract, 10 μg of purified recombinant budding yeast Mcm2 and 2.5 μCi γ^{32}P ATP (Perkin Elmer Life Sciences) were incubated in 20 μl kinase buffer (40 mM HEPES pH 7.5, 0.5 mM EDTA, 2 mM DTT, 10 mM magnesium acetate, 0.1 mM ATP, 80 mg/ml BSA, PhosSTOP phosphatase inhibitor cocktail [Roche]), at 30°C for 30 minutes. The reaction was stopped by addition of 10 μl sample loading buffer and samples size seperated on a 10% SDS polyacrylamide gel. The gel was air dried at 50ºC then exposed to x-ray film.

2.9 Co-immunoprecipitation

DY-1 cells were transformed with pJG4-6 or pCM190 derived expression vectors and grown to a density of $1x10^7$ cells/ml in synthetic complete medium lacking uracil and tryptophan as described previously (Varrin et al. 2005). Cultures were then centrifuged at 4000 rpm for 3 minutes, washed with sterile ddH_2O, then resuspended in 2% galactose 1% raffinose media lacking uracil and tryptophan, then grown for 6 hours at 30°C. All

subsequent steps were performed at 4°C. Whole cell extracts were then prepared as previously described with the exception that 450 µl IP lysis buffer was used (50 mM Hepes, pH 7.5; 140 mM NaCl; 1 mM Na-EDTA; 1% Triton X-100) supplemented with 10 µl/ml Halt Protease Inhibitor Cocktail (Thermo-Fisher). Whole cell extracts were diluted to the same concentration with IP lysis buffer, and 400 µl each extract was incubated overnight on a rotating wheel with 15 µl Protein A sepharose beads (Sigma) saturated with mouse monoclonal anti-Myc antibody (Sigma). After 16-18 hours, the supernatant was removed and saved. Sepharose beads were washed 3 times with 500 µl IP lysis buffer, and resuspended in a final volume of 35 µl IP lysis buffer.

2.10 Complementation

Dbf4 complementation was performed as described previously (Varrin et al. 2005). The DY-2 strain harbouring a temperature-sensitive allele of *dbf4* was transformed with pCM190 derived vectors expressing either wild-type or mutant Dbf4. Transformants were grown to a density of $1x10^7$ cells/ml, and a total of $5x10^6$ cells of each transformant were streaked in duplicate onto synthetic complete media lacking uracil. One plate was incubated at the permissive temperature 23°C, while the other was incubated at the non-permissive temperature 37°C. After three days growth, plates from each growth temperature were compared for growth.

The *rad53Δ* strain, DY-147, was transformed with pRS315 derived centromeric vectors expressing wild-type *RAD53* or the *rad53* mutant allele under its own promoter. The isogenic *RAD53* strain, DY-145, was used as a wild-type control and was transformed with

empty vector pRS315 (Sikorski & Hieter 1989). Spot plate genotoxic sensitivity assays were then conducted as described below on synthetic complete media lacking leucine.

2.11 Plasmid shuffle

Viability of the DY-159 yeast strain harbouring the *dbf4Δ* deletion is achieved by ectopic expression of Dbf4 from pCM190-Dbf4. Vectors derived from the centromeric vector pRS315, expressing wild-type or mutant Dbf4, were transformed into DY-167 and cells were selected on synthetic complete media lacking uracil and leucine. These cells were then streaked onto plates containing 5' fluoroorotic acid to counter select against the *URA3* marker in pCM190. The resulting cells were solely supported for growth by pRS315 based expression. Cell synchronization, FACS analysis, and genotoxin sensitivity assays were then performed with these transformants as described in this chapter.

2.12 Yeast two-hybrid assay

The liquid culture yeast two-hybrid assay was performed as described previously (Duncker et al. 2002). DY-1 cells were transformed with pEG202 derived bait, pJG4-6 derived prey, and the lacZ reporter pSH18-34. Transformants were grown in synthetic complete medium lacking uracil, histidine, and tryptophan to a density of $1x10^7$ cells/ml. Approximately $1x10^8$ total cells were harvested and washed once with sterile ddH_2O, resuspended in 20 ml of 2% galactose 1% raffinose medium lacking uracil, histidine, and tryptophan, and allowed to grow for 6 hours at 30°C. $5x10^6$ total cells were isolated for analysis and the remainder of cultures was processed for western blot analysis as previously described. Isolated cells were resuspended in 500 µl Z-buffer (60mM Na_2HPO_4, 40mM

NaH_2PO_4, 10mM KCl, 1mM $MgSO_4$, 0.5M β-mercaptoethanol). From a P200 pipette, 2 drops of chloroform and 1 drop of SDS were added to each sample, which were then vortexed for 10 seconds and then incubated at 28°C for 5 minutes. After incubation 100 µl of ONPG (ortho-Nitrophenyl-β-galactoside) was added simultaneously to each sample and the reaction was monitored until a pale yellow colour appears. At this point 250 µl of 1M sodium carbonate was added simultaneously to all tubes to stop the reaction. β-galactosidase activity was calculated seing the following formula: β-galactosidase activity = 1,000 x A_{420} / (t x V x A_{600}), where t = time of the reaction, V = volume of culture used in the assay (to obtain $5x10^6$ total cells), A_{420} = absorbance of the reaction, and A_{600} = absorbance of the cell culture used.

2.13 Yeast one-hybrid assay

Liquid culture one-hybrid analysis was performed as described for yeast two-hybrid assay above with the following deviations. DY-1 cells were transformed with the pLI-ARS1$^+$ reporter plasmid and pJG4-6 derived prey. Transformants were originally grown in synthetic complete medium lacking uracil and tryptophan, and later resuspended in 2% galactose 1% raffinose medium lacking uracil and tryptophan.

2.14 Short-term viability assay

Viability assays were performed as described previously (Varrin et al. 2005). Yeast strains were grown overnight in YPD (~$1x10^7$ cells/ml) then diluted to$1x10^6$ cells/ml. The diluted culture was divided into a series of 10 ml aliquots. Each aliquot was treated at one of the indicated concentrations of HU (50mM, 100mM, 150mM, 250mM), MMS (0.015%,0.02%, 0.025%, 0.03%), or left as an untreated control. After 4 hours incubation at

30°C, 50 µl of culture from each treatment was removed, diluted 200-fold, and plated in triplicate on YPD plates. After 2 days growth at 30°C, the number of colonies was counted and the percentage of viable colonies was determined relative to untreated cells.

2.15 Genotoxin sensitivity assay

Serial dilution genotoxin sensitivity assays were performed as described previously (Varrin et al. 2005). Yeast cultures were grown to stationary phase (~$1x10^8$ cells/ml), and 10-fold serial dilutions were made ranging from $1x10^7$ cells/ml to $1x10^4$ cells/ml. 5 µl of each diluted yeast culture was spotted onto media containing the indicated concentration of HU (50-300 mM), MMS (0.005-0.03%), or Phleomycin (5-20 µg/ml). Plates were incubated at 30°C for 3 days.

2.16 Recombinant protein purification and crystallization

A codon optimized version of the HBRCT domain of Dbf4 (amino acids 105-220) was synthesized by GeneArt® (Invitrogen) and subcloned into an expression vector including a $(His)_6$-SUMO tag. The HBRCT-W116D/M120A was also subcloned in the pSUMO vector. Plasmids encoding wild type and $(His)_6$-SUMO-tagged HBRCT variants were transformed in RosettaTM cells (Novagen). Cultures were grown to OD600 of 0.7, induced by addition 1 mM isopropyl β-D-1-thiogalactopyranoside (IPTG) and incubated overnight at 16°C with orbital agitation.

Two variants of the Rad53 FHA1 domain, including amino acids 14-164 and 4-165, were subcloned in pPROEX HTa vectors (Invitrogen). The two variants were produced in RosettaTM cells (Novagen). Protein expression was induced with 1 mM IPTG and the

cultures were subsequently incubated for 4 hours at 30°C with orbital agitation. Cell pellets were resuspended in 20 ml of buffer A (20 mM Tris pH 8.0, 500 mM NaCl, 1.4 mM β -mercaptoethanol, and 5% glycerol) supplemented with 15 mM imidazole and lysed by sonication. Lysates were cleared by centrifugation at 39,000 g and the supernatants were loaded onto HiTrap Ni-chelating HP columns (GE Healthcare). $(His)_6$-SUMO-HBRCT and $(His)_6$-FHA1 variants were eluted with linear gradients to 300 mM imidazole. Tags were removed with TEV protease and aliquots of the purified HBRCT and FHA1 were stored at -80°C in 20 mM Tris pH 8.0, 100 mM NaCl, 1 mM EDTA, 5 mM DTT, and 5% glycerol.

The His-tagged version of the BRCT domain of Dbf4 was obtained by transforming the pAG8206 plasmid encoding amino acid residues 120-250 from *S. cerevisiae* Dbf4 (NP_010337) in either BL21(DE3) or B834(DE3) cells carrying the pRARELysS plasmid. Sel-Met labeled protein was subsequently overproduced in minimal media supplemented with Sel-Met as described (Hendrickson et al. 1990). Protein over-production and purification for both native and Sel-Met labeled Dbf4 was performed as previously described (Matthews et al. 2009). The histidine-tag was removed with thrombin (Sigma) and the protein was further purified by ionic exchange in a MonoS (10/100) GL column (GE Healthcare). Purified tagged and untagged Dbf4 were concentrated to 5 mg/ml in 20 mM Tris pH 8.0, 1 mM DTT, 100 mM NaCl, and 5% glycerol (storage buffer). Longer fragments of Dbf4 (encoding amino acid residues 65-221 and 105-220, pAG8391 and pAG8209 respectively) were produced and purified similarly. Protein concentration was determined using the Beer-Lambert law with an extinction coefficient of 23,950 M^{-1} cm^{-1}.

Sel-Met crystals of a 6xHis tagged Dbf4 fragment encompassing the predicted BRCT domain (amino acid residues 120-250) were grown using the hanging-drop method in 0.1 M Tris pH 8.5, 0.05 M $MgCl_2$ and 29% PEG400 (v/v). Native crystals of the untagged BRCT domain were grown in 100 mM NaK phosphate buffer pH 7.1 and 22% MPD (v/v) and cryoprotected by increasing the MPD concentration to 40% (v/v). Crystals of the minimal domain of Dbf4 sufficient for the interaction with Rad53 (residues 65-221, Helix-BRCT) were grown in 1.9 M $(NH4)2SO4$, 0.014 M $MgSO_4$, 0.05 M $(CH_3)2AsO_2Na$ pH 6.5, and 0.03 mM CYMAL-7, improved by streak seeding and cryoprotected by addition of 20% glycerol to the mother liquor prior to data collection. All crystals were grown from crystallization drops set at 4˚C by mixing 1 µL of protein with 1 µL of reservoir solution (Matthews et al. 2009). Complete data sets of Sel-Met labeled tagged and untagged BRCT domain crystals were collected using the X29 beamline, while data for the crystals of the Helix-BRCT domain were collected using the X25 beamline, at the National Synchrotron Light Source (Brookhaven National Laboratory). All data sets were processed with HKL2000 (Otwinowski & Minor 1997).

2.17 Crystal structure determination and refinement

The structure of the His-tagged BRCT domain was determined by the single anomalous diffraction (SAD) method. Thirty of the forty selenium sites were found and refined using standard protocols in PHENIX (Adams et al. 2002). The initial model was refined by iterative cycles of manual model building in Coot (Emsley & Cowtan 2004) and refinement using PHENIX and imposing non-crystallographic symmetry constraints that related the ten molecules in the asymmetric unit pair wise. This protocol yielded a final

model that includes amino acid residues 122-224 and has 93.6% of the residues in the most favored region of the Ramachandran plot and none in the disallowed regions. One BRCT monomer from this structure was subsequently used as the search model to solve the structure of the untagged BRCT domain using molecular replacement with Phaser (McCoy et al. 2007). The structure of the untagged BRCT domain was refined using standard protocols in Coot and PHENIX and the final model includes amino acid residues 119-242 for one of the five monomers in the asymmetric unit and residues 122-220 for the other four, has 94.2% of the residues in the most favored region of the Ramachandran plot and none in the disallowed regions.

The structure of the sufficient domain (H-BRCT) was solved by molecular replacement using the BRCT domain as the search model. The final model includes amino acid residues 98-220 and has 94% residues in the most favored regions of the Ramachandran plot and none in the disallowed regions. The refinement statistics for the three structures are presented in Table 4.1. Figures depicting molecular structures were generated using PyMol (Schrödinger). Atomic coordinates and structure factors for the three structures have been deposited in the Protein Data Bank (accession codes 3OQ0, 3OQ4 and 3QBZ, respectively).

2.18 NMR Spectroscopy

All experiments were conducted using a 700 MHz AV Bruker NMR spectrometer with a TCI cryoprobe. HBRCT samples were uniformly labeled by expressing the domain (amino acid residues 105-220) in M9 media containing $^{15}NH_4Cl$ and ^{13}C-D-glucose (^{15N,13C}HBRCT) or $^{15}NH_4Cl$ alone (^{15N}HBRCT). Labeled HBRCT was purified and stored as described above. All experiments with labeled HBRCT were conducted at 306 K in 20 mM

TRIS pH 8.0, 100 mM NaCl, 5 mM DTT, 1 mM EDTA, and 5% glycerol. The FHA1 domain of Rad53 (amino acid residues 14-164) was similarly labeled to produce ^{13C,15N}FHA1 or ^{15N}FHA1. The protein was purified as described above and stored in 10 mM sodium phosphate buffer pH 6.5, 1 mM EDTA, and 5 mM DTT. All experiments with labeled FHA1 were conducted at 293 K as described previously (Yongkiettrakul et al. 2004). Experiments including both ^{15N}FHA1 and HBRCT (or BRCT) were also performed in 10 mM sodium phosphate buffer pH 6.5, 1 mM EDTA, and 5 mM DTT.

To assign resonances for ^{13C,15N}HBRCT (0.5 mM), triple resonance experiments (HNCA, HNCO, HNCOCA, and CBCA(CO)NH) were collected as described previously (Selvaratnam et al. 2012). The ^{13C,15N}FHA1 sample (0.3 mM) was first mixed with an equimolar amount of HBRCT prior to collecting HSQC, HNCO, HNCACB, and CBCA(CO)NH spectra. All data were processed with NMRPipe (Delaglio et al. 1995) and resonance assignment was carried out using SPARKY (http://www.cgl.ucsf.edu/home/sparky/).

$^{1}H^{15}N$ NOE experiments were conducted using a 0.1 mM sample of ^{15N}HBRCT prepared as described above. $^{1}H^{15}N$ NOE data were acquired using a 3 second recycle delay, with and without proton saturation in alternate scans (Farrow et al. 1994). The ^{15}N dimension was digitized with 256 complex points for a spectral width of 31.82 ppm and the ^{1}H dimension was digitized with 1024 complex points for a spectral width of 14.28 ppm. After 16 dummy scans, a total of 128 scans were accumulated for each data set, with and without proton saturation. The steady state NOE values were computed as the ratio of the intensities in saturated to unsaturated spectra. The error for the NOE values were gauged based on the

standard deviation between fit heights in replicate spectra. Selected cross peaks were not included in the relaxation analyses due to line broadening and/or overlap.

2.19 Peptide titration experiments

Lyophilized phosphorylated peptide derived from Cdc7 (pPEP: ^{480}DGES**pT**DEDDVVS^{491}) and a nonphosphorylated control (PEP: ^{480}DGESTDEDDVVS^{491}) were synthesized by Biomatik. The peptides were resuspended in 10 mM sodium phosphate buffer pH 6.5 and titrated into a sample containing 0.12 mM ^{15N}FHA1 with an equimolar amount of HBRCT. HSQC spectra were collected after each addition and the total volume of peptide added was < 20% of the sample volume.

2.20 Trypsin Proteolysis

In a total reaction volume of 11 µl, 9 µl of HBRCT (20 µM in storage buffer) were mixed with 1 µl of 50 mM $MgCl_2$ and 1 µl of trypsin (0.195-12.5 µg/ml) and incubated for 1 hour at room temperature. The reaction products were subsequently visualized useing 15% SDS-polyacrylamide gels.

2.21 Statistical Analysis

The intensity losses for peaks in the ^{15N}FHA1 HSQC spectrum after addition of HBRCT were analyzed based on a method published previously (Farrow et al. 1994). The peak fit height was measured with SPARKY using a Lorentzian fit to integrate the peaks. Overlapping peaks were rejected (E26, I32, T39, K57, K64, C74, L99, Q114, S120, and N158). The remaining values were normalized dividing by the intensity of the most intense

peak, which was the C-terminal residue Arg164, prior to being compared with a similarly analyzed data set from a sample lacking HBRCT. The peak height ratio was expressed as a percentage. The average peak height ratio was computed excluding Arg164 to avoid bias. In addition, Ile163 was also excluded as its value exceeded the average beyond four standard deviations. Perturbed residues were defined as having a peak height ratio below one standard deviation from the average.

2.22 Bioinformatics analysis

To identify patterns of amino acid conservation in the FHA1 and FHA2 domains of Rad53, representative protein sequences were retrieved using PSI-BLAST (Altschul et al. 1997) run with an E-value cutoff of E=1e-6. Full length Rad53 from *Saccharomyces cerevisiae* (Uniprot ID: P22216) was used to query the UniRef90 database using PSI-BLAST, and sequences containing both FHA1 and FHA2 domains were retained. A total of 28 sequences were identified (Uniprot IDs: P2216, G3AR58, G3BDW6, H8X5Q1, B9WDY3, C5MJH1, B5RTA3, G8YJ57, C4Y319, A5DJY0, F2QUG7, C4R6G9, K0KML2, J7SAK5, Q6CKF2, G8JNR2, Q75CE9, I2GYM1, C5DF05, Q6FK01, H2AZ96, A7TKN4, G8BVR8, G8ZMW0, C5DXS2, G0WBA8, G0VCB8, E7NNR4), with no further sequences meeting the criteria after three PSI-BLAST iterations. The multiple sequence alignment produced by PSI-BLAST was edited to contain only regions corresponding to the FHA1 and FH2 domains. The Consurf server (http://consurf.tau.ac.il) was used to visualize conserved surface residues (Ashkenazy et al. 2010). A single PDB file containing both FHA1 and FHA2 domains was created by combining PDB files 1G6G and 1J4K. The combined file was

used to map patterns of residue conservation onto the protein surfaces using the same conservation scale.

Chapter 3

The Dbf4 motif C zinc finger promotes DNA replication and mediates resistance to genotoxic stress

Portions of this chapter appear in the following journal article and are reproduced with permission.

This research was originally published in Cell Cycle. Jones DR, Prasad AA, Chan PK, & Duncker BP. The Dbf4 motif C zinc finger promotes DNA replication and mediates resistance to genotoxic stress. *Cell Cycle* 2010; 9: 2018–2026. © Jones *et al*; Landes Bioscience

Figure 3.1A was contributed by B.P.D.
Figure 3.2A and blots for Figure 3.1B were contributed by A.A.P.
Figure 3.2B,D,E were contributed by A.A.P and P.K.C.

3.1 Introduction

The Dbf4-dependent kinase (DDK) complex, Dbf4-Cdc7, plays an essential and conserved role in the initiation of eukaryotic DNA replication (reviewed in Sclafani & Holzen 2007). Several replication factors have been identified as DDK substrates, including DNA polymerase α, Cdc45, and multiple members of the Mcm2-7 helicase complex (reviewed in S. Bell & Dutta 2002; Weinreich & Stillman 1999; Nougarède et al. 2000). Of these, the most important physiological targets are likely to be Mcm2-7 subunits, since a P83L mutation in Mcm5 and deletion of an amino-terminal region of Mcm4 are able to bypass the requirement of DDK for cell cycle progression (Hardy et al. 1997; Hoang et al. 2007; Sheu & Stillman 2010). Moreover, data from several studies suggest that the association of DDK with origins of DNA replication is dependent on interactions with Mcm2-7 (Varrin et al. 2005; Sheu & Stillman 2006; Francis et al. 2009; Sheu & Stillman 2010).

When budding yeast cells are treated with the ribonucleotide reductase inhibitor hydroxyurea (HU), the depletion of cellular dNTP pools leads to replication fork stalling and triggers the intra-S phase checkpoint. Under these conditions, the Rad53 checkpoint kinase (ortholog of mammalian Chk2 kinase) is activated, Dbf4 is removed from chromatin in a Rad53-dependent manner, and the rate at which new initiation events occur at origins of DNA replication is greatly reduced (Weinreich & Stillman 1999; Pasero et al. 1999; Alvino et al. 2007). The inhibition of late origin firing may be important for keeping unfired origins in reserve during a prolonged checkpoint arrest or in mutant backgrounds where replication fork stability could be compromised. However, studies of both Mec1 and Mrc1 have shown

that certain mutant strains for these checkpoint proteins, in which suppression of late origin firing has been compromised, are nevertheless tolerant of genotoxic stress (Alcasabas et al. 2001; Tercero et al. 2003). It has been suggested that an additional checkpoint role for DDK may be the stabilization and/or restart of replication forks (Duncker & Brown 2003).

Sequence comparisons between Dbf4 orthologs from multiple species has revealed the presence of three relatively well conserved regions, termed motifs N, M and C in accordance to their position within the protein (Masai & Arai 2000). Motif N is dispensable for viability in both fission and budding yeast, and its deletion results in hypersensitivity to genotoxic agents (Varrin et al. 2005; Ogino et al. 2001; Fung et al. 2002; Gabrielse et al. 2006). Studies with the latter organism have determined that this region mediates interactions with both Rad53 and the Orc2 subunit of the origin recognition complex (ORC) (Varrin et al. 2005). In contrast, motif N was found to be essential in murine embryonic stem cells (Yamashita et al. 2005). Motif M is required for proliferation in all of the above cell types, and has been shown to mediate the interaction between Dbf4 and Mcm2-7 (Varrin et al. 2005; Francis et al. 2009; Ogino et al. 2001; Fung et al. 2002; Yamashita et al. 2005). Despite being the most highly conserved of these three Dbf4 regions, motif C is the least well understood. One study with the fission yeast *Schizosaccharomyces pombe* reported that it was essential for cell viability (Ogino et al. 2001). However, another investigation revealed that cells for which the region encoding this motif was removed from the single genomic copy of *dfp1* (*S. pombe* DBF4 orthologue) were viable, and sensitive to the DNA alkylating agent methyl methanesulfonate (MMS) but not to other genotoxic agents (Fung et al. 2002).

Here, we present a functional characterization of *Saccharomyces cerevisiae* Dbf4 motif C. We demonstrate that a Dbf4ΔC mutant is unable to support mitotic growth, and that removal of motif C likely causes a major conformational change, since interactions with all known ligands examined were disrupted. Reduced interactions with origins of DNA replication and Mcm2, and defects in S-phase progression resulted from mutating the conserved histidines and cysteines, comprising a motif C zinc finger, to alanines. Furthermore, motif C mutant strains were sensitive to prolonged exposure to HU and MMS, both of which provoke checkpoint responses. Thus, motif C represents a region of Dbf4 that is required for DNA replication, likely through an interaction with Mcm2-7, and plays an additional role in protection against genotoxic agents.

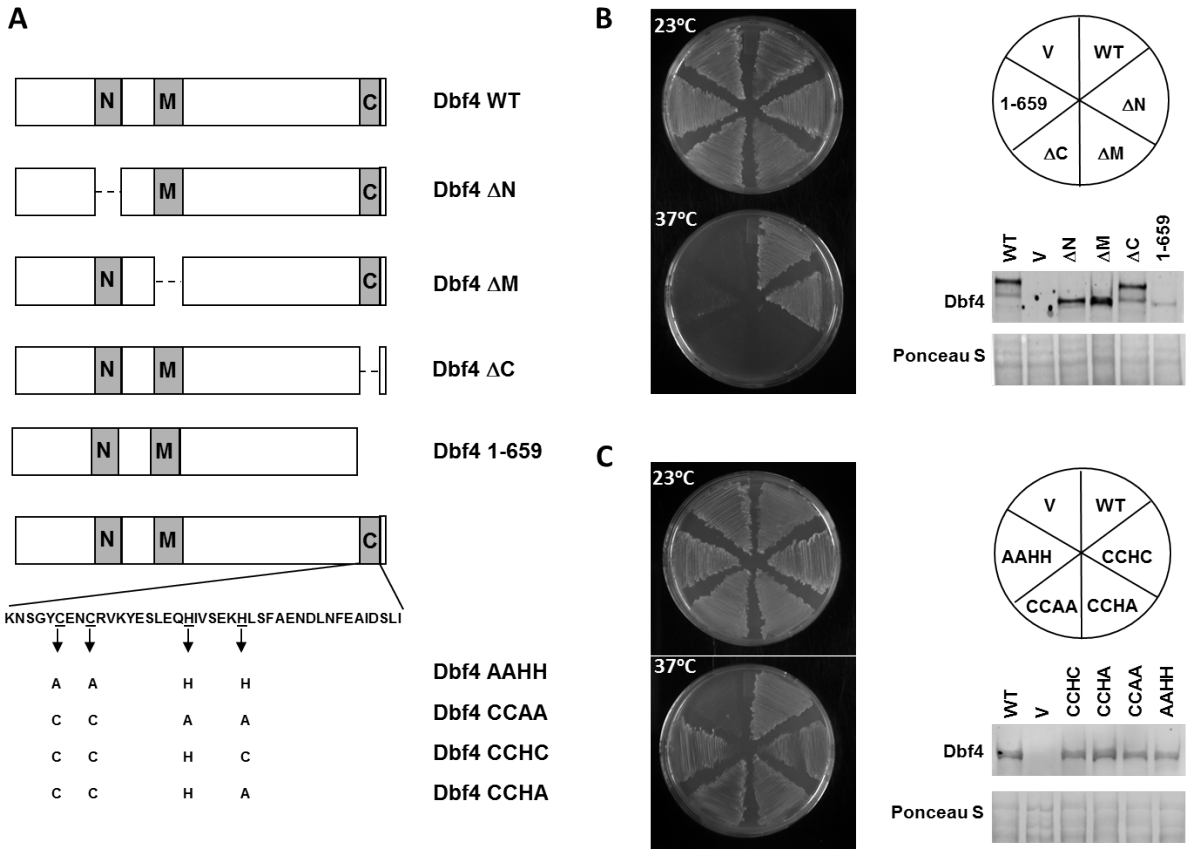

Figure 3.1: Dbf4 motif C mutants can support cell growth.

(A) Dbf4 expression cassettes (B) DY-2 cells (with the temperature-sensitive *DBF4* allele, *dna52-1*) were transformed with pCM190-Dbf4WT, -Dbf4ΔN, -Dbf4ΔM, -Dbf4ΔC, -Dbf41-659 or empty vector pCM190 (V), and a complementation assay was carried out as described in materials and methods. Western blot analysis to confirm plasmid based expression was conducted using a mouse monoclonal anti-Myc antibody (Sigma) and Alexa Fluor 488 goat anti-mouse IgG polyclonal secondary antibody (Invitrogen). (C) DY-2 cells were transformed with pCM190 -Dbf4WT, -Dbf4CCHC, -Dbf4CCHA, Dbf4CCAA, Dbf4AAHH, or empty vector pCM190 (V) and analyzed as in (B).

3.2 Results

3.2.1 Motif C mutants support essential Dbf4 function.

We previously investigated Dbf4 motifs N and M, and found that the former mediates DDK interactions with both Rad53 and Orc2, and is dispensable for growth, while the latter binds to Mcm2 and is required for viability (Varrin et al. 2005). In order to characterize the third and most highly conserved of these regions, we constructed a version of the DBF4 gene with a precise excision of motif C (Dbf4ΔC ; **Figure 3.1A**). Plasmid based expression of Dbf4ΔC did not complement growth of a strain with a temperature-sensitive (*ts*) *DBF4* allele at restrictive temperature (Fig. 1B). Given the previous findings that a *S. pombe* strain in which *dfp1* (*DBF4* ortholog) motif C had been removed was viable, and that a version of *S. cerevisiae* Dbf4 lacking amino acids 417–704 could complement a *DBF4-ts* sensitive strain, we decided to determine if additional motif C mutants could support cell growth (Fung et al. 2002; Dowell et al. 1994). Dbf4 1– 659 consisted of a complete truncation of the C-terminal 45 amino acids, including the entire C motif (Fig. 1A), and was also unable to complement the *DBF4-ts* strain at 37°C, however this mutant was less stable than the others tested as judged by western blot (**Figure 3.1B**).

Analysis of motif C has shown that it includes a sequence that appears to encode a CCHH-type zinc finger (Masai & Arai 2000). We next generated three *DBF4* alleles in which point mutations were made to change conserved cysteines (positions 661,664) and histidines (positions 674, 680) to alanines, *dbf4-AAHH*, *dbf4-CCAA* and *dbf4-CCHA* (**Figure 3.1A**). One further mutant, *dbf4-CCHC*, resulted from a mutation changing a histidine to a cysteine, thus more closely resembling a CCHC-type zinc finger in terms of the critical zinc

chelating residues. Each of these mutant forms of Dbf4 was able to support cell division at restrictive temperature when expressed from a plasmid in the *DBF4-ts* strain (**Figure 3.1C**).

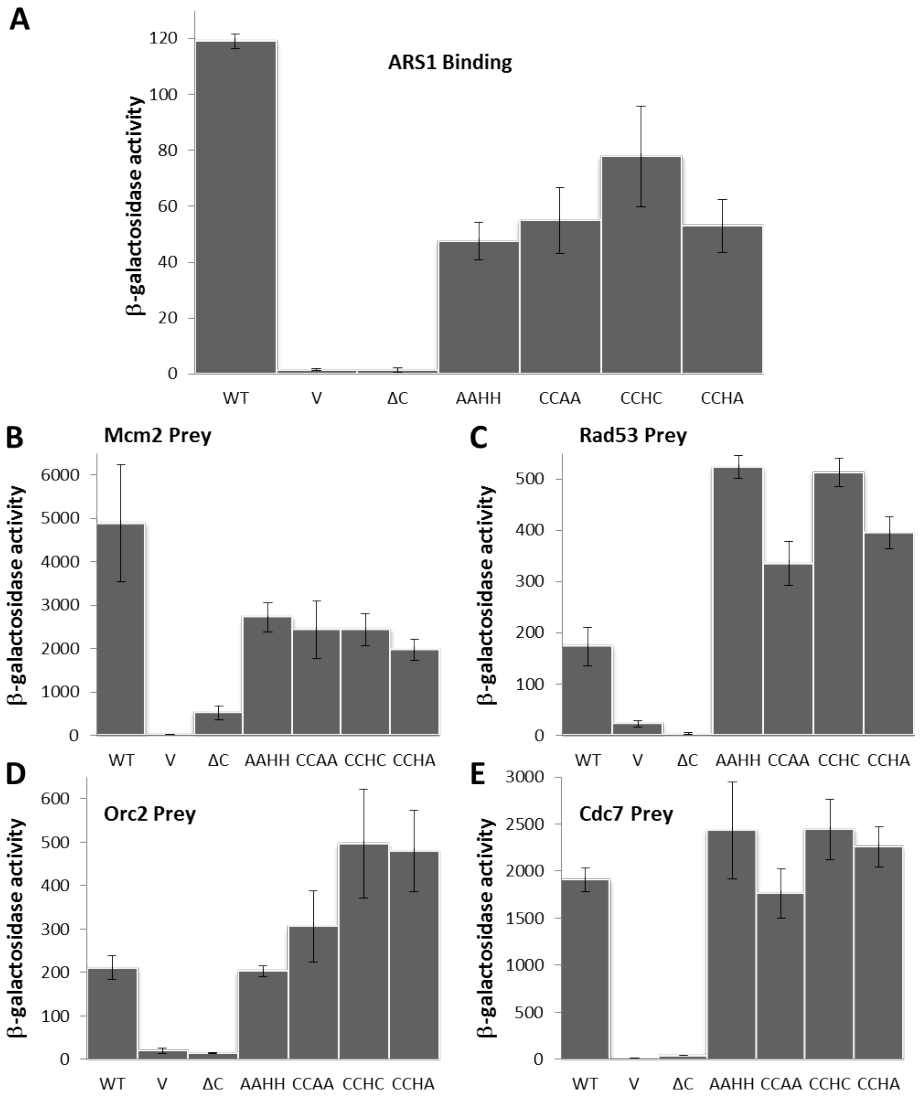

Figure 3.2: Dbf4 motif C mutants have weakened interactions with ARS1 and Mcm2, but not other replication factors.

(A) one-hybrid and (B-E) two-hybrid analyses were carried out as described in materials and methods. ß-galactosidase activity values represent the averages of three independent experiments, and the error bars indicate standard deviation.

3.2.2 Interaction with ARS1 and Mcm2 is impaired in Dbf4 motif C mutants.

To determine whether mutation of highly conserved motif C cysteines and histidines had an effect on the interaction of Dbf4 with replication origin DNA, one-hybrid analysis was carried out where expression of Dbf4 and its variants as fusion proteins with a transcriptional activation domain was used in conjunction with a reporter plasmid for which the ARS1 origin has been placed upstream of a ß-galactosidase gene (Dowell et al. 1994). For each of the motif C mutants, the interaction with ARS1 was reduced relative to that observed for wild-type Dbf4 (**Figure 3.2A**). This drop was not due to a change in the stability of Dbf4 as protein expression levels of the mutants are equivalent to that of wild-type Dbf4 (**Figure 3.1C**). Since a reduction in origin association could be mediated through other factors, and CCHH zinc fingers have been shown to mediate a wide variety of protein-protein interactions (reviewed in Brayer & Segal 2008) we assessed the ability of the motif C mutants to interact with a number of Dbf4 binding partners by two-hybrid analysis (**Figure 3.2B-E**). Association of the motif C mutants with Cdc7 was similar to that observed for wild-type Dbf4. When compared to wild-type Dbf4, the interactions with Orc2 and Rad53 were either comparable, or enhanced. In contrast, all four motif C mutants had reduced interaction with Mcm2. In all cases, the Dbf4ΔC mutant resulted in abrogated binding, consistent with large conformational changes to the protein as a consequence of removing the entire C motif, as has been previously found with removal of certain regions of Dbf4 motif N (Gabrielse et al. 2006). Since both the AAHH and CCAA mutants affected interactions with Mcm2, we were curious to see the effect of changing conserved cysteines and histidines to alanines

simultaneously. Both *dbf4-AAHA* and *dbf4-AAAA* mutants showed no greater reduction in Mcm2 association than the other motif C mutants (**Appendix A Figure 1**).

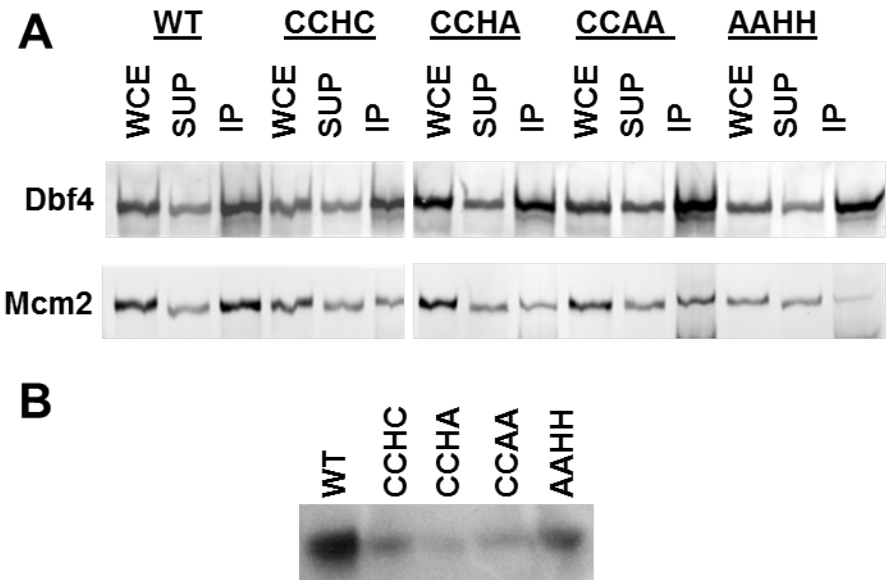

Figure 3.3: Mutation of Dbf4 motif C reduces the amount of co-immunoprecipitated Mcm2 and phosphorylation of Mcm2.

(A) Coimmunoprecipitation experiments were carried out as described in materials and methods, for DY-1 cells transformed with pJG-Mcm2 and either pCM190-Dbf4WT, pCM190-Dbf4CCHA, pCM190-Dbf4CCHA, pCM190-Dbf4CCAA or pCM190-Dbf4AAHH. An anti-Myc antibody (Sigma) was used to immunoprecipitate and detect Myc-tagged Dbf4, and an anti-HA antibody (Sigma) was used to detect HA-tagged Mcm2. Shown are immunoblots of the input whole cell extracts (12 µg each; WCE), supernatants (12 µg each; SUP) and immunoprecipitates (one third each of final bead suspensions; IP). (B) Kinase assays were carried out using recombinant purified Mcm2 and whole cell extract from the indicated strains as described in materials and methods.

3.2.3 Mutation to motif C impairs entry and progression through S-phase.

Given the reduction in Mcm2 interaction with the motif C mutations, we decided to explore this changed association further. We first confirmed the two-hybrid results by performing co-immunoprecipitation assays with whole cell extracts, in which

immunoprecipitated wild-type Dbf4 indeed pulled down more Mcm2 than any of the Dbf4 variants with mutations in motif C (**Figure 3.3A**). Given that DDK association with Mcm2-7 is required to promote S phase progression (Varrin et al. 2005; Sheu & Stillman 2006), and that Dbf4 interacts more strongly with Mcm2 than with other subunits of the helicase complex (Ramer et al. 2013), we hypothesized that a diminished Dbf4-Mcm2 interaction should lead to cell growth defects. To test this, we created a series of haploid yeast strains in which the wild type *DBF4* gene was replaced with sequence encoding the AAHH, CCAA, CCHA or CCHC mutants. We determined that all four motif C mutations resulted in reduced levels of Mcm2 phosphorylation (**Figure 3.3B**). Furthermore, cell counts of exponentially growing cultures indicated that all four mutant strains experienced impaired growth compared to an isogenic wild-type strain (**Figure 3.4A**). Since the Dbf4-Mcm2 interaction should promote DNA replication, we tested entry into and progression through S phase by first synchronizing cells in late G1 phase by addition of the mating pheromone α-factor, and then monitoring DNA content by FACS analysis following release of the cultures from the block. Whereas the wild-type strain had clearly entered S phase by 20 minutes after α-factor removal (as judged by DNA content between 1C and 2C), the earliest this was evident for any of the mutant strains was at 40 minutes, consistent with defects in origin firing (**Figure 3.4B**). Completion of S phase similarly lagged by at least 20 minutes in the mutant strains, with the wild-type showing a peak centred at 2C by 40 minutes, and the fastest of the mutants (*dbf4-AAHH* and *dbf4-CCHC*) showing equivalent profiles by 60 minutes.

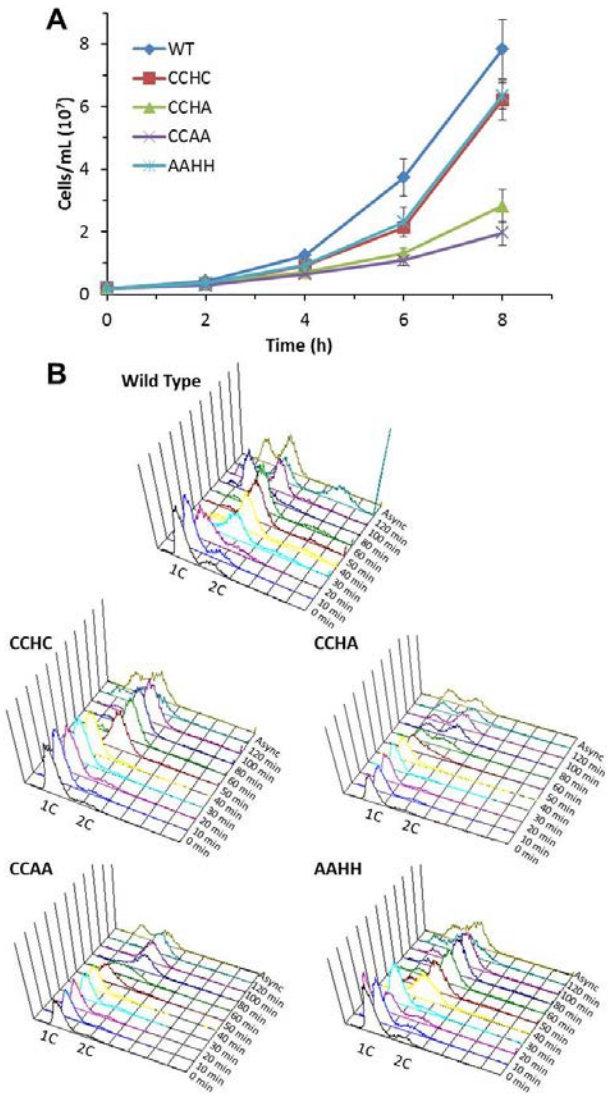

Figure 3.4: Mutation of Dbf4 motif C impairs entry and progression through S phase.

(A) Asynchronous wild-type and motif C mutant strain cultures were diluted to a starting concentration of 2 x 10^6 cells/ml and cell counts were taken every two hours. Each data point represents the average of three independent experiments. Error bars represent standard errors. (B) The same yeast strains as above were grown to a concentration of 5 x 10^6 cells/ ml, arrested in late G1 phase for 3 h with 5 µg/ml α-factor, washed once in sterile dH_2O, then resuspended in fresh medium without α-factor to release them from the block. Shown is FACS analysis of culture aliquots taken at the indicated time points following release from the a-factor block as well as from the original asynchronous cultures (Async). The positions of 1C and 2C DNA peaks are indicated.

3.2.4 Motif C mutants are sensitive to chronic but not acute exposure to HU or MMS.

Previously, we reported that a point mutation in Dbf4 motif M that weakens interaction with Mcm2 and compromises DNA replication actually has a protective effect when cells are exposed to genotoxic agents (Varrin et al. 2005). We reasoned that this might be due to a more efficient Rad53-mediated removal of Dbf4 from unfired origins as part of the checkpoint response. Thus, we might expect our Dbf4 motif C mutants to exhibit a similar phenotype, given that they indeed displayed an enhanced association with Rad53 (**Figure 3.2C**). On the other hand, if the interaction between motif C and Mcm2 is important for replication fork stabilization and/or restart, mutations to motif C that affect these potential roles could render cells more sensitive. To explore these alternative models, we first subjected the four mutant motif C strains to varying concentrations of HU and MMS for 4 h and then determined the effects of exposure to these compounds on cell viability (**Figure 3.5**). Relative to the isogenic wildtype strain, the motif C mutants showed similar rates of survival over the full range of HU concentrations tested (50 –250 mM), and trials with MMS exposure also revealed no major differences between mutant and wild-type strains. We next looked at long-term growth on HU and MMS media plates. Consistent with earlier observations (**Figure 3.4**), there was some impairment of growth for the motif C mutants, relative to isogenic wild-type cells on control plates without any HU or MMS supplement (**Figure 3.6**). This disadvantage was greatly enhanced as MMS and HU concentration was increased indicating that the motif C mutants were sensitive to prolonged exposure to genotoxic agents.

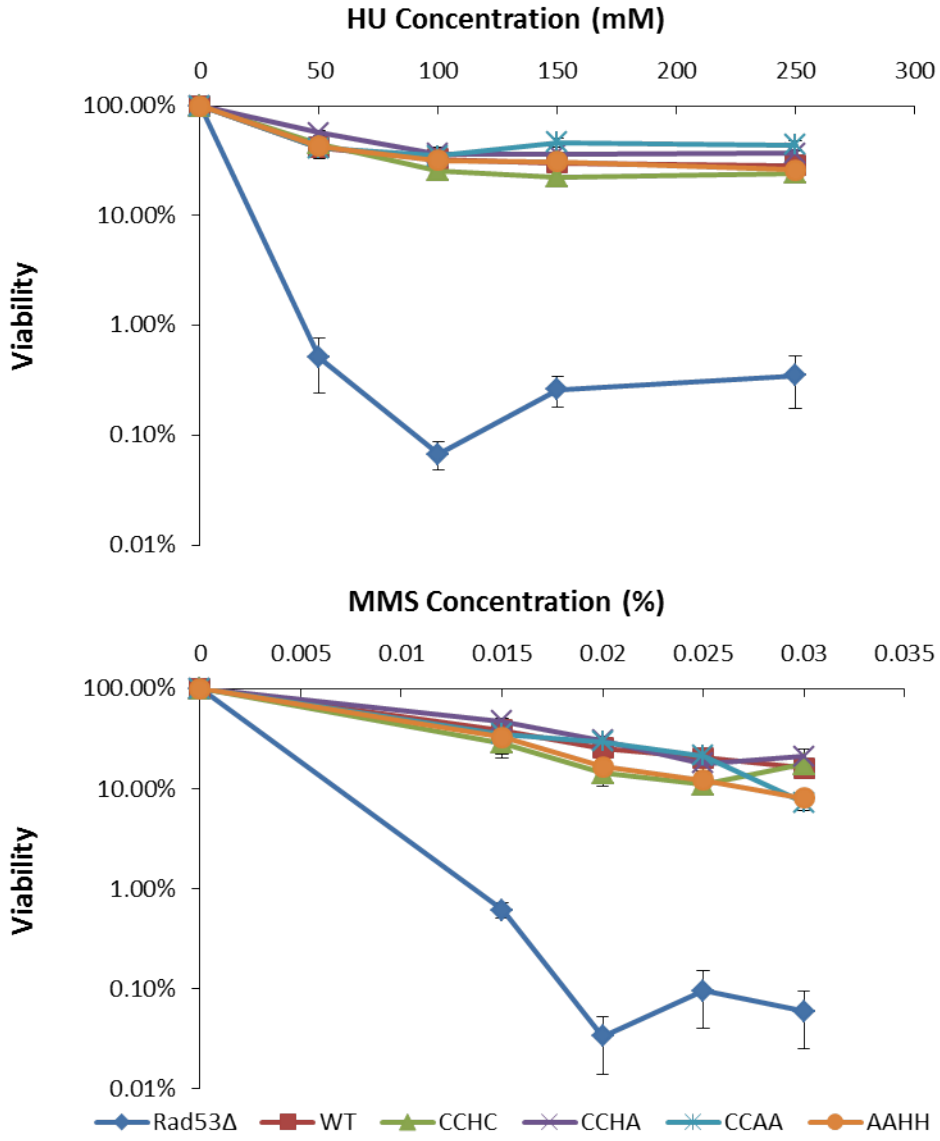

Figure 3.5: Motif C mutants are insensitive to short term exposure to either HU or MMS.

Wild type, ΔRad53 and motif C mutant strains were exposed to the indicated concentrations of HU or MMS for 4 h, plated in triplicate and incubated at 30°C for 2 days. Colonies were counted and the percentages were calculated relative to untreated cells. Each data point represents the average of three independent experiments. Error bars represent standard deviation.

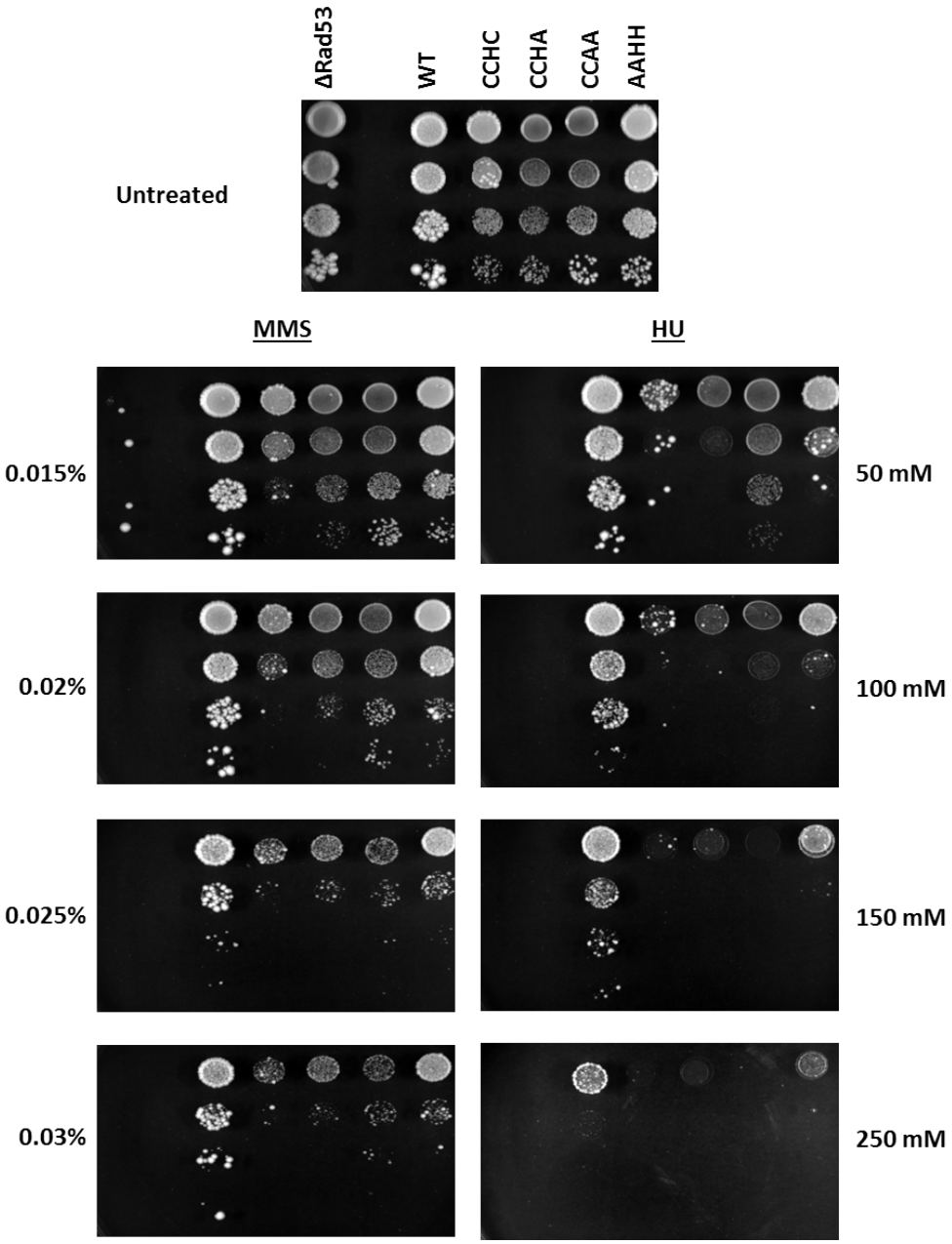

Figure 3.6: Motif C mutants are sensitive to long term exposure to either HU or MMS.

Wild-type, ΔRad53, and motif C mutant strains were spotted in 10-fold dilution series onto YPD plates containing the indicated concentrations of HU or MMS. Each plate was incubated at 30°C for three days.

3.3 Discussion

DDK has been shown to act locally at origins of DNA replication, and inactivation of either Dbf4 or Cdc7 in mid-S phase prevents initiation from occurring at unfired origins (reviewed in Pasero & Schwob 2000). The exact role that DDK carries out has not been precisely defined, although it almost certainly involves interaction with the Mcm2-7 helicase complex. Multiple Mcm2-7 subunits have been shown to be substrates for DDK phosphorylation *in vitro* (Weinreich & Stillman 1999; Francis et al. 2009; Lei et al. 1997; Kihara et al. 2000), and DDK-dependent phosphorylation has been shown for Mcm4 *in vivo* (Sheu & Stillman 2006; Masai et al. 2006). Moreover, a P83L mutation of Mcm5 is able to bypass the essential function of both Dbf4 and Cdc7 through a change of conformation that is thought to mimic the effect of Mcm2-7 phosphorylation by DDK (Hardy et al. 1997; Hoang et al. 2007). Similarly, deletion of an amino terminal domain of Mcm4 also relieves the requirement for DDK (Sheu & Stillman 2010). We have previously shown that deletion of Dbf4 motif M abrogates its interaction with Mcm2 and results in a loss of viability (Varrin et al. 2005), and have recently found that among Mcm2-7 subunits, Mcm2 interacts most strongly with Dbf4 (Ramer et al. 2013). Taken together, these data suggest that the Dbf4-Mcm2 interaction is important to efficiently target DDK to origins of DNA replication. Consistent with this model, our motif C mutants show both a loss of interaction with Mcm2 and defects in S-phase entry and progression. Interestingly, these mutants maintain a robust and, in some cases, enhanced association with Orc2. Orc2 has been shown to interact with Dbf4 through motif N (Varrin et al. 2005; Duncker et al. 2002). Furthermore, in an *orc2-1* back-ground (which completely destabilizes ORC at non-permissive temperature) the

punctate subnuclear foci observed for Dbf4 through immunofluorescence, thought to represent localization to replication centres, become diffuse (Pasero et al. 1999). Thus, it is likely that DDK is tethered to origins of DNA replication through multiple protein-protein interactions, with some being more crucial than others. The enhanced interaction with Orc2 we observed with the motif C mutants did not compensate for the reduction in Mcm2 association in terms of replication defects. However, it should be noted that the relative strength of interaction for Dbf4 with Mcm2 appears considerably stronger than with Orc2 (**see Figure 3.2 B,D**). Additionally, removal of Dbf4 motif N and consequent disruption of the interaction with Orc2 results in some growth defects, but cells maintain viability in contrast to the effects of deleting motif M (Varrin et al. 2005). It is also possible that the overall change in origin targeting may be less important than a reduction in phosphorylation of Mcm2 as a consequence of compromising its interaction with DDK. Mutation of a single conserved histidine (His680) to alanine within the CCHH-type zinc finger of motif C was sufficient to disrupt the Dbf4-Mcm2 interaction. Similar results were obtained when this residue was changed to cysteine, although the effects on S phase progression were less severe. Interestingly, a previous study has shown that a CCHC zinc finger in human histone acetylase HBO1 mediates its association with Mcm2 (Burke et al. 2001).

Multiple Mcm2-7 subunits have highly conserved zinc finger motifs (reviewed in Jenkinson & Chong 2003), and mutation of the CCCC-type Mcm4 zinc finger has been shown to destabilize subunit interactions (You et al. 2002). Taken together, these findings suggest that zinc fingers are important for mediating interactions between Mcm2-7 subunits and their ligands, and that specificity is imparted by the composition of the zinc binding

residues. Here we present evidence that the conserved cysteine and histidine residues within motif C comprise part of a functional domain that is required for timely replication and efficient response to genotoxic stress. The partial structure of the human ortholog of Dbf4 is now available, which encompasses motifs M and C. This structure shows unequivocally that motif C of Dbf4 constitutes a zinc finger and the conserved cysteine and histidine residues are responsible for chelation of zinc (Hughes et al. 2012). We observed no reduction in the interaction between Dbf4 and Cdc7 (**Figure 3.2E**) as a consequence of the zinc finger mutations, however it has been reported that Dbf4 motif C mutations in *S. cerevisiae* can lead to a reduction in DDK activity (Harkins et al. 2009). It is therefore possible that both a disruption of interaction with Mcm2 and reduced kinase activity contribute to motif C mutant phenotypes.

We found that a weakening of the interaction with Mcm2 through Dbf4 motif C mutations rendered cells more sensitive to continual exposure to the checkpoint inducing agents HU and MMS, but did not reduce viability compared to wild-type after short term incubation with these compounds. This argues that the effects we observed most likely had less to do with any influence on the timing of late origin firing, and more with a potential role for DDK in replication fork stabilization and/or restart during adaptation (Clémenson & Marsolier-Kergoat 2009). Such a function for DDK is supported by the finding that for *S. pombe* an *hsk1-ts* (*CDC7* ortholog) mutant is synthetically lethal with a null mutation for *rqh1*, which encodes a RecQ-type helicase, important for recovery from exposure to HU (Snaith et al. 2000). Furthermore, motif C mutants in this yeast have elevated levels of recombination and chromosome loss that are greatly enhanced with MMS treatment, which

could be due to an increase in fork collapse (Fung et al. 2002). Interestingly, we have found that overexpression of Mcm2, which might be expected to titrate some Dbf4 away from forks, further sensitizes motif C mutants to HU exposure (**Appendix A Figure 2**).

How might DDK function in the context of S phase checkpoint responses? Phosphorylation of Mcm2-7 may safeguard fork integrity or trigger replication restart by promoting association of Cdc45 with the rest of the replisome components, as it does during the initiation of DNA replication (Sheu & Stillman 2006; Masai et al. 2006). Consistent with our finding that motif C is responsible for mediating an interaction with Mcm2 of the Mcm2-7 helicase complex and that impairment of this interaction compromises a cells viability under genomic duress, two DDK phosphorylation sites important in mediating resistance to genotoxic stress have been found in Mcm2, S164 and S170 (Stead et al. 2011). Inability of Dbf4/Cdc7 to phosphorylate these residues results in sensitivity to the DNA alkylating agents MMS and the PI3K-like kinase inhibitor caffeine (Stead et al. 2011; Stead et al. 2012). Alternatively, interaction with Mcm2 may target DDK to phosphorylate either Cdc45 itself or DNA polymerase α, both of which are substrates of this kinase complex *in vitro* (Weinreich & Stillman 1999; Nougarède et al. 2000). The latter possibility is particularly intriguing since DDK has been shown to function in translesion synthesis (TLS), during which it is thought that normal replicative polymerases are substituted by ones capable of proceeding through the region of DNA damage (Pessoa-Brandão & Sclafani 2004). Similarly, we observe that Dbf4 motif C mutants are synergistic with mutations in the TLS pathway, resulting in increased sensitivity to MMS and phleomycin (**Appendix A Figure 3**). Recent work with human Dbf4 has shown that motif C mediates an interaction with the

amino-terminus of the ubiquitin ligase Rad18, important for translesion synthesis (Day et al. 2010; Yamada et al. 2013). DDK directly phosphorylates a cluster of serines in the C-terminus of Rad18 which is important for its interaction with the translesion polymerase η, and mutants of Rad18 unable to be phosphorylated by Dbf4/Cdc7 do not produce Polη foci after UV treatment, indicating Polη is not efficiently recruited to sites of DNA damage (Day et al. 2010). Under checkpoint conditions ATR (Mec1 ortholog) inactivates the APC/C preventing degradation of APC/C targets including Dbf4 (Yamada et al. 2013).Thus under checkpoint conditions Dbf4 is stabilized in an ATR dependent manner. Additionally, knockdown of DDK activity before exposure to HU results in an increase in DSB formation and increased H2AX phosphorylation (Lee et al. 2012), consistent with a role in preventing fork collapse. Rad53 has been implicated in both replication fork stabilization and restart, and it was suggested that it may carry out the latter role by stimulating Cdc7-Dbf4 activity at forks (Szyjka et al. 2008). The idea that DDK activity may be important for fork restart following a checkpoint response is further supported by the finding from a study with a Xenopus cell-free system that the block to DNA replication in an etoposide induced S-phase checkpoint was overcome by the addition of purified Dbf4/Cdc7 (Tsuji et al. 2008).

While the role of DDK in meiosis has been characterized, the contributions each of the conserved motifs has not been elucidated (Matos et al. 2008; Wan et al. 2008; Sasanuma et al. 2008; Katis et al. 2010). Work with the fission yeast *S. pombe* has recently shown that motif C likely also mediates important interactions in meiosis (Le et al. 2013). C-terminal truncation of Dfp1 (spDbf4), results in cells that are defective for a variety of meiotic events,

including delayed expression of meiotic genes, disrupted chromosome segregations, and reduced spore viability (Le et al. 2013).

Investigations with vertebrates have implicated DDK, Mcm2-7 and their interaction in cancer phenotypes (Shima et al. 2007; Montagnoli et al. 2008), and point to the need for a better understanding of how these factors associate with each other. Our characterization of conserved budding yeast Dbf4 motif C residues that mediate Mcm2 binding and phosphorylation, along with the consequences of mutating them, has shed important new light on this crucial interaction. It will now be of great interest to determine the extent to which these findings are paralleled for this well conserved motif in human cells.

Chapter 4

Saccharomyces cerevisiae Dbf4 has unique fold necessary for interaction with Rad53 kinase

Portions of this chapter appear in the following journal and are reproduced with permission.

This research was originally published in The Journal of Biological Chemistry. Matthews LA, Jones DR, Prasad AA, Duncker BP & Guarné A. Saccharomyces cerevisiae Dbf4 has unique fold necessary for interaction with Rad53 kinase. J. Biol. Chem. 2012; 287: 2378–87.

Table 4.1; Figure 4.1; 4.2 B,C; 4.3A; 4.4B; 4.5;A, 4.6; Appendix B Figure 1; 2; 4; 5 were contributed by L.A.M. and A.G.

Appendix B Figure 3 C, E was contributed by A.A.P.

Figure 4.4 was contributed by A.A.P and D.R.J

4.1 Introduction

Essential for mitotic growth, Dbf4 dependent kinase (DDK), Dbf4/Cdc7, is required for the initiation of DNA replication whereby it functions to activate the replicative helicase Mcm2-7, resulting in unwinding of duplex template to allow the replicative machinery access (Chapman & Johnston 1989; Jackson et al. 1993; Labib 2010). The kinase component of DDK, Cdc7, is present throughout the cell cycle, but is only activated by the binding of Dbf4, thus DDK is only active from late G1 through to late mitosis when Dbf4 synthesis is at its highest (Cheng et al. 1999; Ferreira et al. 2000). In addition to its requirement for the initiation of DNA replication DDK also plays a role in mitosis, meiosis, and the checkpoint response. In the intra-S-phase checkpoint Dbf4/Cdc7 is a target of the effector kinase Rad53 (mammalian Chk2), but also functions as an effector of the checkpoint response as DDK activity is also required for full activation of the checkpoint (Kihara et al. 2000; Ogi et al. 2008). As a checkpoint target in *Saccharomyces cerevisiae*, Dbf4 is phosphorylated and removed from chromatin in a Rad53 dependent manner and phosphorylation of DDK by Rad53 results in inhibition of Dbf4/Cdc7 kinase activity (Pasero et al. 1999; Kihara et al. 2000). The phosphorylation of Dbf4 is also critical for the block to late origin firing, preventing the activation of late firing origins during S-phase under times of replicative stress or DNA damage (Zegerman & Diffley 2010; Lopez-Mosqueda et al. 2010). It is also believed to have a role in the stabilization and possible restart of stalled replication forks, preventing their collapse and the accumulation of unstable DNA structures (Duncker & Brown 2003; Branzei & Foiani 2010).

In *S. cerevisiae* Rad53 is the primary effector kinase of the checkpoint response, and is activated by both Mec1 and Tel1 (ATR and ATM in mammals) dependant signaling pathways in response to DNA damage and replicative stress (reviewed in Clémenson & Marsolier-Kergoat 2009; Branzei & Foiani 2005; Carr 2002). Rad53 activation relies on the checkpoint mediators Mrc1 and Rad9, while Rad53 also autophosphorylates itself in *trans* to reach its fully activated hyperphosphorylated state (Pellicioli et al. 1999; Alcasabas et al. 2001; Harrison & Haber 2006). Interestingly, DDK is able to phosphorylate Rad53 and in cells lacking Dbf4 or Cdc7, Rad53 is hypophosphorylated and displays low autophosphorylation activity, and checkpoint specific transcription is not induced (Ogi et al. 2008). Thus, DDK is both an upstream regulator of the checkpoint kinase Rad53 and a downstream target during the replication checkpoint.

The Rad53 checkpoint kinase is composed of a central kinase domain flanked by two Fork-head associated (FHA) domains. Dbf4 interacts with Rad53 primarily through the amino-terminal FHA1 domain, but also weakly associates with the carboxy-terminal FHA2 domain of Rad53 (Duncker et al. 2002; Varrin et al. 2005). FHA domains are known to specifically bind phosphothreonine residues, and FHA1 of Rad53 specifically recognizes phosphothreonine residues found in unstructured loops (Durocher et al. 1999). Therefore, the interaction between Rad53 and most of its binding partners can be recreated using phosphothreonine containing peptides. We have previously identified that an FHA1 mutant unable to bind phosphopeptide is also compromised in its ability to bind Dbf4 (Duncker et al. 2002). This suggests that FHA1 binds a phosphoepitope within Dbf4. However, the phosphothreonine responsible for the interaction between Dbf4 and FHA1 has yet to be

identified. Interestingly, recent work has revealed additional phosphorylation-independent modes of interaction between FHA domains and their binding partners (Nott et al. 2009; Pike et al. 2004). One such mode of interaction still utilizes the phosphorylation recognition surface of the FHA domain (Nott et al. 2009). Thus, this indicates that the mode of recognition between Dbf4 and Rad53 has the potential to be independent of phosphoepitope recognition by FHA1.

Dbf4 is conserved from yeast to humans however, only three regions of high sequence conservation are present, these regions are termed motifs N, M, and C based on their location within the polypeptide chain (Masai & Arai 2000). Motif M and the zinc finger containing motif C (residues 260-309 and 656-697, respectively in *S. cerevisiae*) are necessary to maintain the interaction with Cdc7 and the replicative helicase component Mcm2 (Hardy & Pautz 1996; Varrin et al. 2005; Jones et al. 2010). In *S. cerevisiae* motif N of Dbf4 (residues 135-179) is required for recognition by Rad53 and to mediate interaction with origins of replication through the Orc2 subunit of the origin recognition complex (Duncker et al. 2002; Varrin et al. 2005; Dowell et al. 1994; Hardy & Pautz 1996). Deletions or point mutations within Dbf4 motif N result in increased sensitivity to genotoxic insults. These mutants are compromised in their ability to tolerate both replicative stress, the result of nucleotide depletion by the ribonucleotide reductase (RNR) inhibitor hydroxyurea (HU), and DNA damage caused by the DSB inducing drug bleomycin (Varrin et al. 2005; Gabrielse et al. 2006).

Primary sequence alignment has indicated that motif N may constitute part of a larger structural domain which bears resemblance to a BRCT domain (Masai & Arai 2000;

Gabrielse et al. 2006). However, it has yet to be determined exactly how this region folds. In support of the idea that motif N is part of a larger structurally conserved unit, motif N does not constitute an independent folding unit by itself however, the region of Dbf4 encompassing residues 120-250 can be over-produced on its own and it is well behaved in solution (Matthews et al. 2009). BRCT domains are commonly found in proteins that respond to DNA damage and many of them function as tandem repeats, which associate together using conserved hydrophobic residues to create an intervening hydrophobic pocket (Leung & Glover 2011; Mohammad & Yaffe 2009). These repeats act as a single unit to recognize binding partners by using both this pocket as well as a phosphoserine binding site contained within one of the BRCT domains (Williams et al. 2001). However, the mechanism by which single BRCT domains, such as the one presumably present in Dbf4, participate in protein-protein interactions is poorly understood.

In an effort to clarify whether Dbf4 has a *bona fide* BRCT domain and whether this domain mediates the interaction with Rad53, we have characterized the minimal region of Dbf4 necessary for the interaction with Rad53 and determined its crystal structure. We have found that the fragment of Dbf4 encompassing residues 105-221 is sufficient to mediate this interaction. The crystal structures of this sufficient domain of Dbf4, as well as, a shorter fragment encompassing residues 120-221 unveil a structural feature that is unique to Dbf4. Residues 120-221 fold as a *bona fide* BRCT domain, but residues 105-119 form an α-helix that is embedded in the core of the domain defining a novel structure that we name Helix-BRCT (H-BRCT). Using a combination of structure-guided site-directed mutagenesis and yeast two-hybrid analysis, we demonstrate that the presence of this N- terminal helix is

critical for both folding of the domain and the interaction with Rad53. Collectively, our work demonstrates that the structural integrity of the H-BRCT domain is essential for the ability of Dbf4 to interact with Rad53 and promote cell survival under genotoxic stress.

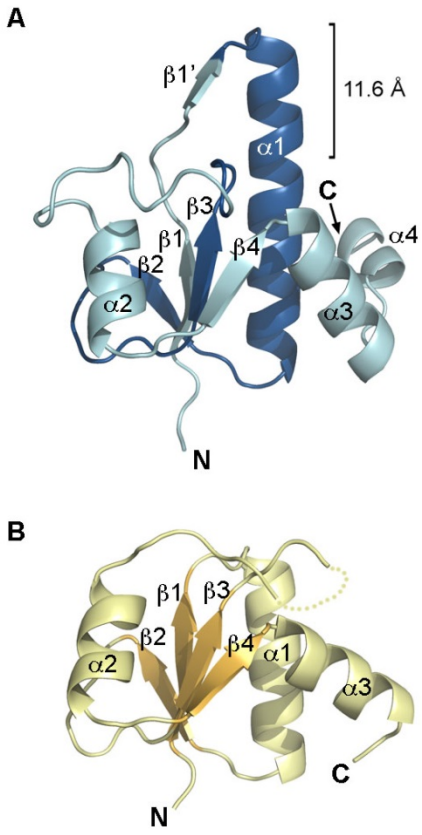

Figure 4.1: The fragment of Dbf4 including residues 120-250 folds as a BRCT domain.

(A) Ribbon diagram of the structure of Dbf4 (residues 120-250) colored in blue, with Motif N (residues 135-179) highlighted in a darker shade of blue. The N- and C-termini, as well as secondary structure elements are labeled. The section of helix α1 protruding from the BRCT core is indicated. (B) Ribbon diagram of the first BRCT from BRCA-1 (PDB ID: 1JNX, residues 1649-1737) shown as a pale yellow ribbon and in the same orientation as in (A). Secondary structure elements are shown in two shades of yellow and labeled, with the disordered β3-α2 loop depicted as a dotted line.

4.2 Results

4.2.1 Motif N of Dbf4 is part of a BRCT Domain

We have previously shown that motif N (residues 135 to 179) does not constitute an independent folding unit (Matthews et al. 2009). Conversely, the fragment of Dbf4 encompassing residues 120-250 includes the predicted BRCT domain and is well behaved in solution (Masai & Arai 2000; Matthews et al. 2009). The structure of this fragment of Dbf4, including a removable hexa-histidine tag at the N-terminus of the protein, was determined by single anomalous diffraction (SAD) using selenomethionine labeled crystals and 10 molecules were readily identified in the experimental electron density maps. About twenty residues at the C-terminus of each monomer (Ala230-Asp250) were disordered and could not be included in the final model. Residues Arg122 to Thr224 define a bona fide BRCT domain, consisting of a central four stranded parallel β-sheet surrounded by α-helices (**Figure 4.1**).

In comparison to the structures of other BRCT domains previously determined, this domain of Dbf4 has a significantly longer helix α1 that projects an additional β-strand (β1') out to the solvent (**Figure 4.1**). This additional strand interacts with the β2-strand of a neighboring molecule, defining a mixed β-sheet with four parallel strands (β4-β3-β1-β2) from one molecule and one anti-parallel (β1') strand from the adjacent one. As this intermolecular β1'-β2 interaction propagates through the crystal, it defines a right-handed helical filament (**Appendix B Figure 1A**). Formation of this filament was not due to the presence of the exogenous tag, as this supramolecular organization was also found in crystals grown after removal of the hexa-histidine tag (**Table 4.1 and Appendix B Figure 1B-C**). However, size exclusion chromatography and analytical ultra-centrifugation experiments

indicated that this fragment of Dbf4 exists predominantly as a monomer in solution (**Appendix B Figure 1D**). Therefore, while the protein-protein interactions seen in the crystals do not reflect the oligomeric state of Dbf4, they could indicate how Dbf4 interacts with other cellular partners.

Table 4.1: Data collection and refinement.

Dbf4 Fragment	Residues 120-250 (including His-tag)	Residues 120-250 (without His-tag)	Residues 65-220 (without His-tag)
Data Collection			
Space Group	$P2_1$	$P2_12_12$	$P6_422$
Unit Cell (Å)	a=90.2, b=79.4, c=127.4	a=83.7, b=99.7, c=127.0	a=b=83.7, c=103.7
	$\alpha=\gamma=90^o$, $\beta=110.7^o$	$\alpha=\beta=\gamma=90^o$	$\alpha=\beta=90^o$, $\gamma=120^o$
Matthews Coeff. ($Å^3Da^{-1}$)	2.44	3.44	2.78
Solvent content (%)	49.6	64.2	55.9
Wavelength (Å)	0.9796	1.081	1.1
Monomers in ASU	10	5	1
Resolution (Å)[a]	50-2.70 (2.75-2.70)	50-2.40 (2.44-2.40)	50-2.69 (2.74-2.69)
Completeness (%)[a]	99.3 (99.1)	99.8 (100)	99.7 (99.7)
Rmerge (%)[a]	0.10 (0.79)	0.192 (0.74)	0.06 (0.42)
$I/\sigma(I)$[a]	16.9 (2.8)	8.9 (2.6)	31.0 (3.5)
Redundancy[a]	7.0 (7.2)	6.2 (5.9)	6.9 (6.2)
Reflections (total)	323,273	262,516	43,786
Reflections (unique)	46,033	42,318	6,280
Refinement			
Resolution (Å)	35.5-2.7	46.4-2.4	38.8-2.69
Reflections (R_{work}/R_{free})	44,042/2,233	42,245/2,146	6,061/300
R_{work}/R_{free} (%)	20.5/24.4	20.3/22.9	22.4/27.3
Number of Atoms			
Protein	8,276	4,362	1,058
Solvent	99	230	10
Rms deviations			
Bonds (Å)	0.009	0.007	0.008
Angles (°)	1.161	0.959	1.034
Ramachandran Plot (%)			
Most Favored	93.6	94.2	94.0
Additionally allowed	6.2	5.8	6.0

[a] Data in the highest resolution shell is shown in parentheses.

4.2.2 The BRCT domain of Dbf4 is not sufficient to mediate the interaction with Rad53

Using yeast two-hybrid analysis, we have found that the fragment of Dbf4 encompassing residues 120-221 is not sufficient to sustain the interaction with Rad53 (**Figure 4.2A**). However, we have previously shown that a fragment of Dbf4 encompassing residues 1-296 binds Rad53 with similar affinity to wild-type Dbf4 (Duncker et al. 2002). Based on this, we generated several additional constructs, corresponding to larger fragments of Dbf4 which encompass the BRCT domain, and assessed their ability to interact with Rad53. Extending the C-terminal end to include residues 120-250 did not restore the interaction with Rad53. However, extending into the N-terminal region (65-220) did restore this interaction (**Figure 4.2A**). Fragments of Dbf4 that truncate portions of the BRCT domain despite starting at residue Leu65 (residues 65-179 and 65-109) did not support binding to Rad53 either, indicating that the BRCT domain is necessary for the interaction.

To test if the N-terminal extension (residues 65-119) was simply required as a spacer between the BRCT domain and the N-terminal LexA fusion tag we generated a fragment of Dbf4 encompassing residues 1-221 but lacking the intervening Gln66-Ile119 region. This internal deletion changed the sequence connecting the LexA tag to the BRCT domain while maintaining a similar spacing between the two proteins. Notably, this fragment of Dbf4 (1-221Δ66-119) did not support binding to Rad53 (**Figure 4.2A**), indicating that the integrity of the intervening region (residues 66-119) is also necessary for the Dbf4-Rad53 interaction. Collectively, this demonstrates that both the region encompassing residues Leu65 to Ile119 and the intact BRCT domain (Met120-Leu221) are necessary for the Dbf4- Rad53 interaction, while neither feature alone can support binding (**Figure 4.2A**). In turn, this

suggests that the fragment of Dbf4 encompassing residues Leu65-Leu221 may define a unique structure responsible for mediating the interaction with Rad53.

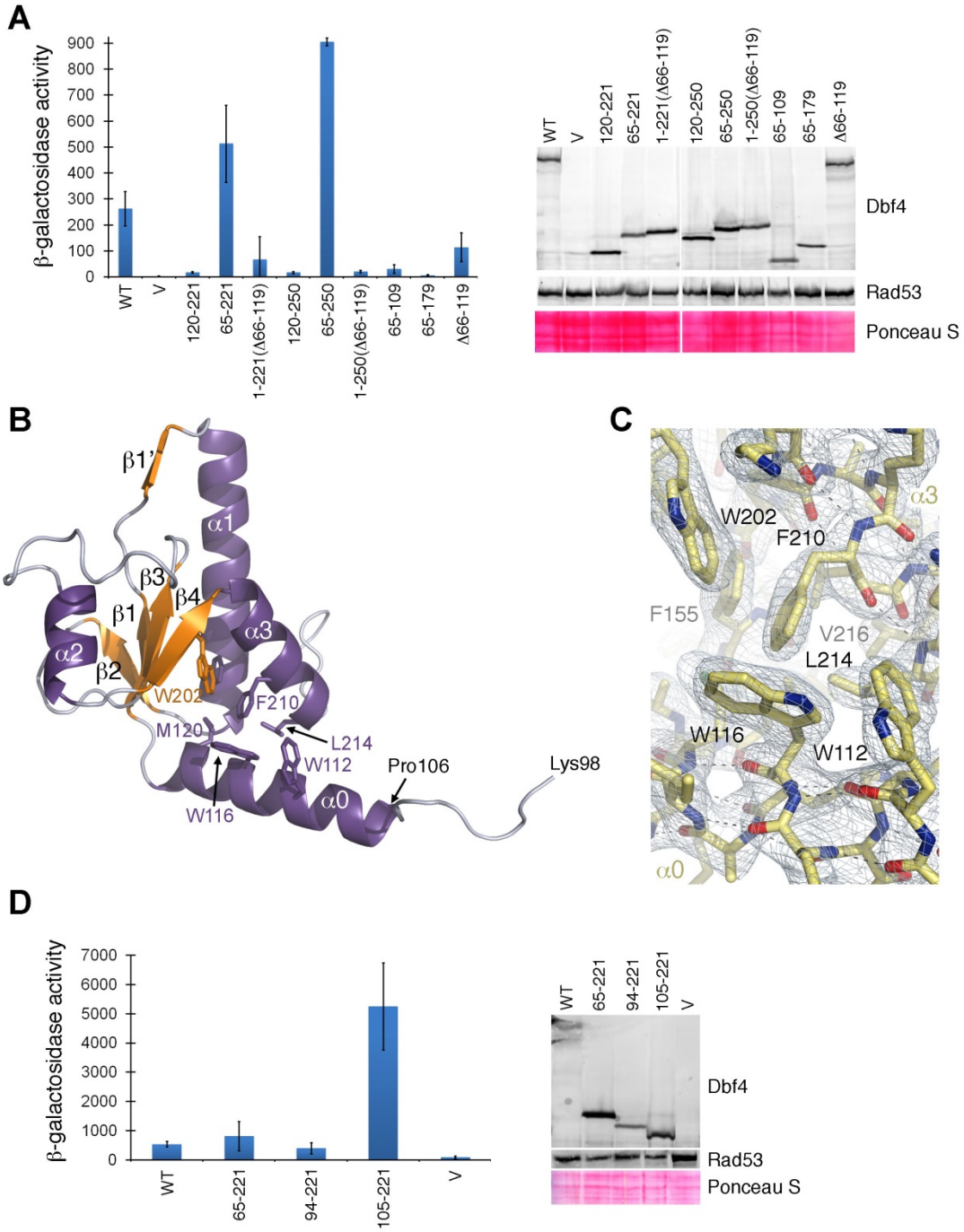

Figure 4.2: The fragment of Dbf4 including residues 105-221 is the minimal domain of Dbf4 that mediates the interaction with Rad53.

(A) Two-hybrid analysis using Rad53 as prey and either full-length Dbf4 (WT), empty vector (V), or regions of Dbf4 as indicated (numbering refers to amino acid positions within full-length Dbf4) as baits. The interaction is shown as β-galactosidase activity units, and in each case represents the average of three independent measurements. Error bars represent standard deviation. As a control, whole cell extracts were prepared from transformants following prey induction and analyzed by Western blot using rabbit anti-LexA antibody (Cedarlane Laboratories) to detect bait protein and a mouse monoclonal anti- HA antibody (Sigma) to detect prey protein, along with Alexa Fluor 647 goat anti-rabbit and 488 goat anti-mouse secondary antibodies (Invitrogen), respectively. Prior to detection, the membrane was stained with Ponceau S to assess relative protein loading. (B) Ribbon diagram of the H-BRCT domain of Dbf4 with α-helices shown in purple, β-strands in orange and loops in light blue. The N- and C-termini, as well as secondary structure elements are labeled. The additional N-terminal helix is labeled as α0 and the residues defining the hydrophobic core are shown as sticks and labeled. (C) Detail of the 2Fo-Fc electron density map around Trp116 contoured at 1σ. The H-BRCT model is shown as color-coded sticks with the residues latching the N-terminal helix (α0) to the hydrophobic core of the H-BRCT domain (β4, β1, α3) labeled. (D) Two-hybrid analysis using Rad53 as prey and either full-length Dbf4 (WT), or fragments of Dbf4 encompassing residues 65-221, 94-221 and 105-221 as baits.

4.2.3 Structure of the sufficient domain of Dbf4 for the interaction with Rad53

To elucidate whether this N-terminal extension (residues 65-119) altered the BRCT fold, we determined the crystal structure of the sufficient interaction region of Dbf4 (65-221). Crystals of this fragment diffracted X-rays to 2.6 Å resolution (**Table 4.1**), and contained only one molecule in the asymmetric unit, confirming that the filament seen in the previous structures was indeed a crystallographic artifact. Residues 98 to 221 were clearly defined in the electron density map, however the region encompassing residues 65-97 was not. We suspected that this fragment of Dbf4 was susceptible to degradation and, indeed mass spectrometry confirmed that the crystals contained a fragment of Dbf4 encompassing residues 84-221. As expected, residues 122-221 adopt the BRCT fold seen in the previous

structures of Dbf4 (**Figure 4.1 and Appendix B Figure 1**), while residues 107-121 form a well-defined amphipathic α-helix (α0) that is packed against the hydrophobic surface defined by the C-terminal end of α1, β1 and α3 (**Figure 4.2B**). Despite the low sequence conservation, the presence of a helix N-terminal to the BRCT domain is predicted in most Dbf4 homologues from lower eukaryotes (**Appendix B Figure 2**). The residues upstream of this helix (98-106) adopt an extended and relatively flexible conformation as judged by the quality of the electron density. To test whether helix α0 was the only relevant feature for binding Rad53 within the region encompassing residues 65-119, we repeated the yeast two-hybrid analysis with shorter fragments of Dbf4. Constructs consisting of residues 94 to 221 or just 105 to 221 were capable of binding Rad53 (**Figure 4.2D**; note the difference in scale compared to panel A). We therefore conclude that the region of Dbf4 encompassing residues 105 to 221 is the minimal structural unit of Dbf4 required for binding to Rad53. Interestingly, the fragment encompassing residues 105-221 interacts with Rad53 more efficiently than Dbf4 itself, suggesting that the full-length protein has additional mechanisms that down-regulate the interaction between the two proteins. This inhibitory effect may arise from other regions of the protein occluding the interaction interface or the competition between Rad53 and other cellular Dbf4-binding proteins. Consistent with the latter model it has been shown that Cdc5 interacts with Dbf4 through residues 83-93 and, hence, is conceivable that binding to endogenous Cdc5 restricts binding to Rad53 the *in vivo* two-hybrid assay (Chen & Weinreich 2010).

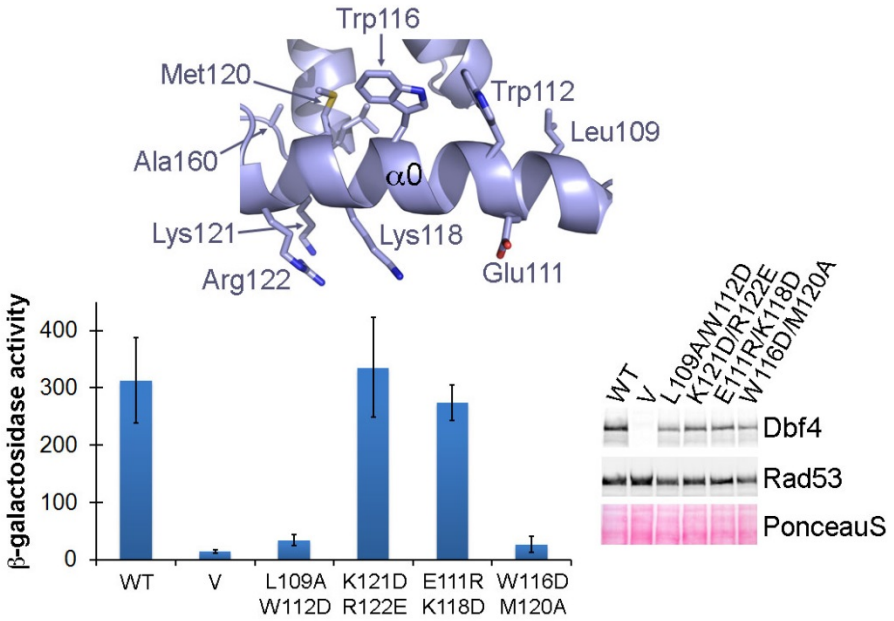

Figure 4.3: Mutation of the residues anchoring helix α0 to the core of the BRCT domain abolishes the interaction between Dbf4 and Rad53.

Two-hybrid analysis carried out using full-length Rad53 as prey and either wild-type *DBF4* (WT), empty vector (V), *dbf4-L109A-W112D* (L109A-W112D), *dbf4-K112D-R122E* (K112D-R122E), *dbf4-E111R-K118D* (E111R-K118D) or *dbf4-W116D-M120A* (W116D-M120A) as baits. Data is presented as in Figure 4.2A.

4.2.4 The H-BRCT fold is necessary for Dbf4-Rad53 interaction.

Arguably, helix α0 could be an independent motif adjacent to the BRCT domain whose relative orientation had been determined by crystal packing. However, the side chains of Trp116 and Met120, and to a lesser extent Trp112, have extensive van der Waals and aromatic interactions with the hydrophobic core defined by residues Phe155, Trp202, Phe210 and Leu214 (**Figure 4.2B-C**). Trp116 and Met120 are not strictly conserved in other Dbf4 homologues, but aromatic or bulky hydrophobic residues are found at these positions (**Appendix B Figure 2**), suggesting a common mechanism to occlude the hydrophobic surface defined by Phe155, Trp202, Phe210 and Leu214 and hence supporting the role of this

helix in maintaining the structural integrity of the domain. Mutation of Trp116 and Met120 abolishes the interaction between Dbf4 and Rad53 (**Figure 4.3**), indicating that the integrity of the hydrophobic core of the domain is critical for the interaction. These results confirm that the helix N-terminus to the BRCT domain is an inherent part of the domain of Dbf4 that we hereafter refer to as Helix-BRCT (H-BRCT). Recent work has shown that at least another BRCT domain also requires additional structural elements to perform its function (Kobayashi et al. 2010). However, the H-BRCT domain of Dbf4 constitutes the first example of a BRCT domain where this additional structural motif is an integral part of the folding unit.

Interestingly, the hydrophobic and polar faces of the α0 helix contribute differently to the interaction with Rad53. Mutation of Trp112 and Leu109, that contribute only minimally to the hydrophobic core the H-BRCT domain, also abrogate the Dbf4-Rad53 interaction. Conversely, mutation of the polar face of the helix (K121D/R122E or E111R/K118D) did not affect the interaction (**Figure 4.3**). Collectively, these results indicate that the concave surface defined by α0, β4 and α3 is important for the interaction with Rad53.

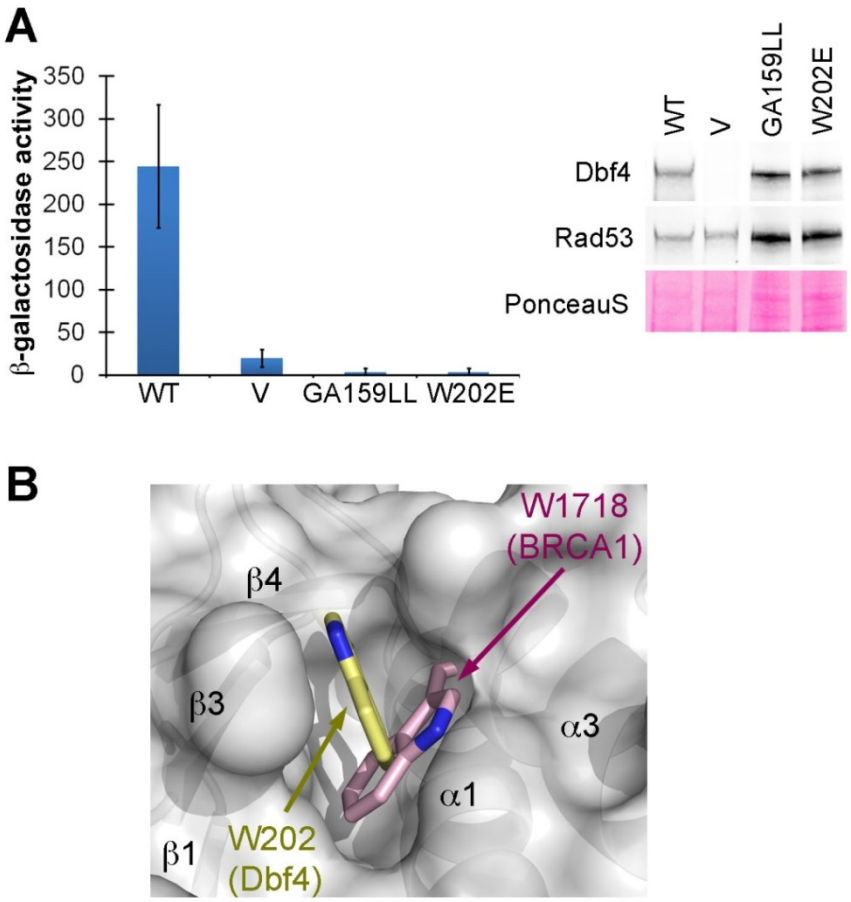

Figure 4.4: Dbf4 mutants that are sensitive to genotoxic agents fail to interact with Rad53.

(A) Two-hybrid analysis was carried out using Rad53 as prey and wild-type *DBF4* (WT), *dbf4- GA159LL* or *dbf4-W202E* as baits with data presented as in Figure 4.2A. (B) Superimposition of Trp1718 from BRCA-1 (pink color-coded sticks) onto the structure of Dbf4-N. Dbf4-N is shown as a semitransparent white surface with the secondary structure elements shown as a ribbon diagram. Trp202 from Dbf4 is shown as yellow color-coded sticks.

4.2.5 Point mutations that destabilize the H-BRCT fold disrupt the Dbf4-Rad53 interaction.

Internal deletions disrupting the H-BRCT fold disrupt the interaction with Rad53 (**Figure 4.2 and Appendix B Figure 3B,C**), demonstrating that the tertiary structure of the H-BRCT domain is important to maintain this interaction. Therefore, we subsequently

investigated whether previously described mutations impairing Dbf4 function could also have folding defects. Three highly conserved residues within the H-BRCT domain (Gly159, Ala160 and Trp202) are important for Dbf4 function. Mutation of any of these residues causes increased sensitivity to both the DSB inducer bleomycin and the fork stalling agent hydroxyurea (Gabrielse et al. 2006). We found that the *dbf4-W202E* and *dbf4- GA159LL* variants also lost their ability to interact with Rad53 (**Figure 4.4A**). The side chain of Trp202 lies at the hydrophobic pocket defined by the central β-sheet and the surrounding α0, α1 and α3 helices. While this residue is not conserved in other BRCT domains, a structurally equivalent tryptophan is found at the N-termini of helix α3 in most BRCT domains (**Figure 4.4B**), reinforcing the idea that a hydrophobic, bulky residue at this position is necessary to stabilize the hydrophobic core of the H-BRCT domain. Therefore, the defects associated with mutating Trp202 are likely due to the structural destabilization of the H-BRCT domain. The Gly159-Ala160 doublet is located in the short loop connecting α1 and β2 that is conspicuously exposed to solvent. This loop reverses the orientation of the polypeptide chain and hence, the substitution of these two small and flexible residues with bulky and hydrophobic amino acids likely reduces the plasticity of the α1-β2 loop, potentially destabilizing the central β-sheet (**Figure 4.1A**). Indeed, the phi/psi angles adopted by Gly159 to make this turn would not be favored for any residue other than glycine, in turn explaining the strict conservation of these two residues among BRCT domains. The H-BRCT-GA159LL variant was also insoluble when over-expressed in bacteria using identical conditions to those used to produce the H-BRCT domain (**Appendix B Figure 4**), reinforcing the idea that these

point mutations destabilize the H-BRCT fold. Together, these results strongly suggest that the integrity of the H-BRCT domain is critical for the interaction between Dbf4 and Rad53.

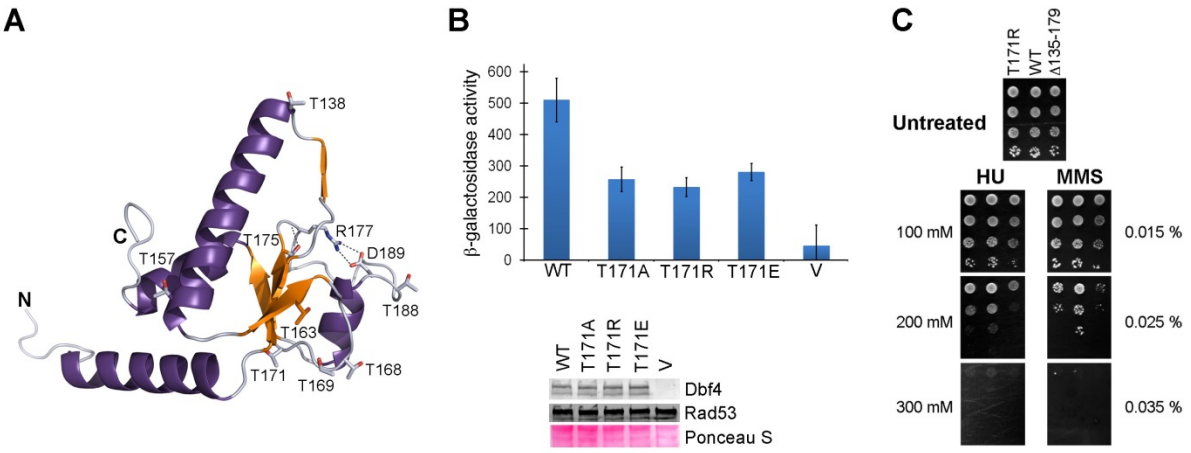

Figure 4.5: Role of Thr171 and Thr175 in mediating the Dbf4-Rad53 interaction.

(A) Ribbon diagram of the H-BRCT domain colored as in Figure 4.2B. The side-chains of the threonine residues found in the domain are shown as sticks. The hydrogen bond network restraining the β3-α2 loop is shown as black dashed lines. (B) Two-hybrid analysis carried out using full- length Rad53 as prey and either full-length Dbf4 or Dbf4 variants carrying point mutations at Thr171 as baits. Data is presented as in Figure 4.2A. (C) *DBF4Δ* cells transformed with *CEN* vectors (one copy per cell) expressing, either wild-type *DBF4* (WT), *dbf4-T171R* or *dbf4Δ135-179* (deletion of motif N) were spotted in 10-fold dilution series onto SC-Leu (synthetic complete medium, lacking leucine in order to select for plasmid maintenance) plates containing the indicated concentrations of HU or the alkylating agent methyl methanesulfonate (MMS). Each plate was incubated at 30ºC for three days.

4.2.6 Thr171 aids the interaction between Dbf4 and Rad53.

Arginine 70 within the FHA1 domain of Rad53 is important for the recognition of phosphothreonine (pThr) targets, and we have previously seen that mutation of Arg70 weakens the interaction with Dbf4 (Duncker et al. 2002). This observation is consistent with a model whereby Rad53 interacts with Dbf4 through FHA1 medicated recognition of phosphoepitope in Dbf4. We therefore scanned the sequences of the H-BRCT domains from

various Dbf4 homologues to identify threonines that could potentially mediate the interaction with Rad53. Only two threonine residues, Thr171 and Thr175, are conserved in the H-BRCT domain of Dbf4 (**Appendix B Figure 2**). Thr175 is buried in the hydrophobic core of the H-BRCT domain and is involved in a hydrogen-bond network that stabilizes the β3-α2 loop (**Figure 4.5A**). This loop is highly variable among BRCT domains, suggesting that Thr175 may have a conserved structural role in Dbf4 by stabilizing the β3-α2 loop (**Appendix B Figure 5**). Due to its location in the domain, we did not expect Thr175 to be the phosphorylated site recognized by Rad53. Accordingly, mutation of Thr175 to alanine did not affect the interaction between Dbf4 and Rad53 (**Appendix B Figure 3D**).

Conversely, Thr171 is relatively exposed **(Figure 4.5A)** and the equivalent serine in higher eukaryotes is part of a Chk1 kinase phosphorylation site (Kim et al. 2003). Mutation of Thr171 to either alanine or arginine significantly reduced binding to Rad53 (**Figure 4.5B**). Importantly, the *dbf4-T171R* variant also showed increased sensitivity to HU and MMS (**Figure 4.5C**), reinforcing the idea that this residue is important for the Rad53-dependent checkpoint response. However, the H-BRCT-T171A variant was also insoluble when overproduced in bacteria under identical conditions to those used to produce the H-BRCT domain (**Appendix B Figure 4**), suggesting that this mutation also destabilizes the H-BRCT fold. The side chain of Thr171 is hydrogen-bonded to the main chain of residue Arg125 and this interaction indirectly orients the α0 helix. Taking this into consideration it is likely that mutation of Thr171 destabilizes the H-BRCT fold and weakens the interaction between Dbf4 and Rad53.

We hypothesized that if Thr171 is the pThr recognized by Rad53, mutation of Thr171 to a phosphomimetic residue should maintain, or even strengthen, the interaction between the two proteins. However, the *dbf4-T171E* variant also showed reduced binding affinity for Rad53 (**Figure 4.5B**). This result reinforces the idea that Thr171 plays a structural role, rather than being the phosphoepitope recognized by Rad53, although we cannot exclude the possibility that the Thr171Glu mutation is not a sufficient substitute for a pThr. Indeed, in studies using pThr-containing peptides that recognize FHA1 domains in the absence of any structural context, aspartate does not efficiently mimic a phosphorylated threonine (Durocher et al. 1999).

We have demonstrated that the structural integrity of the H-BRCT domain of Dbf4 is important for its recognition by Rad53, and thus the structural context of the putative phosphoepitope must also be important. Furthering the idea that Thr171 plays a structural role in the stability of H-BRCT domain, double mutation of Thr171 and Thr175 to alanines completely disrupts the interaction between Dbf4 and Rad53 (**Appendix B Figure 3D**). Thus, these two destabilizing mutations synergistically act to undermine the structural integrity of the H-BRCT fold.

Within the H-BRCT of Dbf4 several other Thr residues have been proposed as damaged-induced phosphorylation sites (Zegerman & Diffley 2010; Lopez-Mosqueda et al. 2010; Duch et al. 2011). However, every non-conserved threonine residue within the H-BRCT domain with the exception of Thr163, can be replaced without negatively impacting the Dbf4-Rad53 interaction. Interestingly mutation of Thr163, which resides on the same surface of the H-BRCT domain as Thr171, reduces the affinity of Rad53 for Dbf4

(**Appendix B Figure 3A**). Thus the location of these residues may contribute to delineating the interaction interface between FHA1 of Rad53 and the H-BRCT of Dbf4 (**Figure 4.6**).

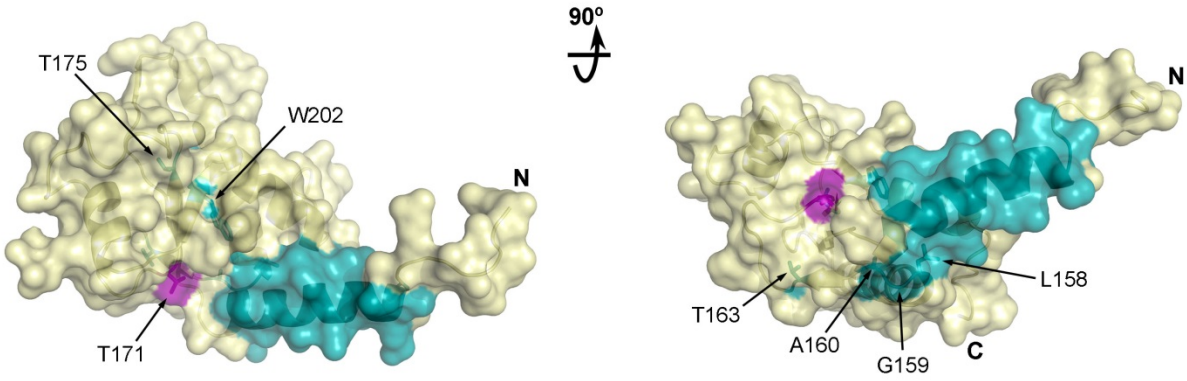

Figure 4.6: Putative Rad53-interaction interface of Dbf4.

Orthogonal views of the H-BRCT domain shown as a color-coded ribbon inside a semi-transparent surface. Residues that are important for the interaction with Rad53 are colored in cyan, except Thr171 that is shown in purple for clarity.

4.3 Discussion

Here we present the first ever structure for a portion of Dbf4. We have shown that the motif N of Dbf4 comprises part of a unique structure built upon a BRCT domain that includes an additional α-helix strictly required for the function this domain. We refer to this domain as H-BRCT (Helix-BRCT) to signify the location and the nature of the additional structural motif. The H-BRCT domain is necessary and sufficient to mediate the interaction between Dbf4 and Rad53. Interestingly, other proteins containing single BRCT domains also include additional structural elements surrounding the domain that aid their function, suggesting that the BRCT fold is a core that complex structures with different specificities can be built upon. Tandem BRCT repeats are known to function as a single unit, and could

be considered one of the types of structures that can be built upon a single BRCT core. Similarly, single BRCT domains should be viewed as part of larger functional units, akin to a tandem BRCT repeat where one BRCT domain has been replaced by either a different domain, such as the case of Nbs1 or Chs5 (Martín-García et al. 2011; Lloyd et al. 2009; Williams et al. 2009), or additional structural elements that complement the BRCT fold. These observations in combination with our results suggest that other single BRCT domains may also require additional structural motifs, thereby explaining why no common mechanism of interaction exists between single BRCT domains and their binding partners. In turn, this would also justify why BRCT domains, which are commonly found in DNA replication and repair proteins, do not show a high degree of sequence conservation (Williams et al. 2001). The most variable regions within the BRCT domain are the loops connecting β2-β3 and β3-α2, which may provide the means to establish specificity for different binding partners (**Appendix B Figure 5**). Here, we propose that additional secondary structural elements at either terminus of a BRCT domain can also increase target specificity and present the first example of a BRCT where the additional structural elements have become an integral part of the domain.

The role BRCT and FHA domains play in DNA repair and checkpoint signaling as well as their mechanisms of pThr recognition and have been studied extensively (Durocher et al. 2000; Glover et al. 2004; Campbell et al. 2010). However, recent studies have identified novel mechanisms of interaction between FHA and BRCT domains (Lloyd et al. 2009; Williams et al. 2009). Thus the concept that the FHA1 domain of Rad53 recognizes a single

pThr in the absence of any structural context may no longer be the paradigm that best describes FHA domain interactions.

Our results reveal that the structural integrity of the H-BRCT fold is more relevant than the presence of a phosphoepitope for the interaction between Dbf4 and Rad53. This finding was somewhat unexpected as we have previously seen that the inability of FHA1 to bind pThr reduces its affinity for Dbf4, leading to the hypothesis that Rad53 would recognize a phosphoepitope in Dbf4 (Duncker et al. 2002). Furthermore, previous structural work had shown that Rad53 recognizes phosphoepitopes in the absence of a structural context (Durocher et al. 2000). However, work with Rv1827 from *Mycobacterium tuberculosis* has shown that its FHA domain is able to recognize several binding partners in a phosphoindependent manner, while still using residues integral to the canonical pThr-binding surface (Nott et al. 2009). Therefore, it is conceivable that the FHA1 domain of Rad53 does not recognize a phosphoepitope in the H-BRCT domain of Dbf4, even though mutation of the conserved Arg70 in the FHA1 disrupts the interaction with Dbf4 (Duncker et al. 2002).The structurally unstable *dbf4Δ135-179*, *dbf4-GA159LL*, *dbf4-W202A* and *dbf4-T171R* variants have both a weakened interaction with Rad53 and an increased sensitivity to HU, MMS, and bleomycin (this study; Gabrielse et al. 2006). Interestingly, Gly159, Ala160, Thr163, Thr171 and Trp202 are all in close proximity to helix α0, potentially demarcating the surface of Dbf4 that interacts with Rad53.

The N-terminus of Dbf4 is known to mediate the interaction with Orc2 and origins of replication (Duncker et al. 2002; Hardy & Pautz 1996; Dowell et al. 1994), and mutation of the Leu158-Gly159 doublet or deletion of motif N (residues 126-160) has been observed to

abrogate the interaction between Dbf4 and origin DNA in a yeast one-hybrid assay (Ogino et al. 2001). We have observed that deletion of motif N (residues 135-179) delays cells entry to S-phase consistent with the reduced association with origins. Interestingly, mutations that disrupt the association of helix α0 with the BRCT fold disturb the interaction with Rad53 but do not cause a delay in entry to S-phase (**Appendix B Figure 6**) indicating that the association with origins of replication is intact. Thus the regions of Dbf4 that mediate the interaction between Rad53 and origins of replication overlap, but the mechanism of interaction does not appear to be the same.

It has been observed that the region containing the BRCT domain of Dbf4 can be replaced by the BRCT domain found in Rev1 with little loss of viability when challenged with genotoxic stress; several other BRCT domains were unable to complement in the same manner suggesting that the BRCT domains of Rev1 and Dbf4 might share a common interaction partner (Harkins et al. 2009). However, the ability of this Rev1-Dbf4 chimera to interact with Rad53 and suppress late origin firing was not examined in that study. Indeed another study by the same group has shown that in a *sld3-38A* background Dbf4 lacking of the first 109 residues, which would truncate helix α0 of the H-BRCT domain, is unable to suppress late origin firing in the presence of HU (Chen et al. 2013).

Collectively, our work indicates the presence of a phosphoindependent interaction between the FHA1 domain of Rad53 that relies on the unique H-BRCT domain found at the N-terminus of Dbf4. In a broader context, the identification of the H-BRCT domain suggests that other single BRCT domains may also require additional structural motifs for their function. The variable nature of these additional motifs would explain why the mechanisms

of interaction of single BRCT domains have remained elusive, while those of tandem BRCT domains have been characterized.

Chapter 5

A novel non-canonical FHA binding interface mediates the interaction between Rad53 and Dbf4

Portions of this chapter appear in the following journal article and are reproduced with permission.

This research was originally published in The Journal of Biological Chemistry. Matthews LA, Selvaratnam R*, Jones DR*, Akimoto M, McConkey BJ, Melacini G, Duncker BP & Guarné A. A novel, non-canonical FHA binding interface mediates the interaction between Rad53 and Dbf4. *J. Biol. Chem.* 2014; 289:2589-99. © the American Society for Biochemistry and Molecular Biology.

**these authors contributed equally to this work*

Figure 5.1; 5.2; 5.6A; 5.7 were contributed by L.A.M., R.S., M.A., G.M., and A.G.

Figure 5.3 was contributed by B.J.M.

5.1 Introduction

ForkHead Associated (FHA) domains are ubiquitous phosphoepitope-binding modules present in a number of proteins that play critical roles in the DNA damage and replication stress response (Durocher & Jackson 2002). The replication checkpoint preserves the genomic integrity of the cell by stabilizing stalled forks, boosting DNA repair enzyme levels and pausing the cell cycle (Labib & De Piccoli 2011). Rad53 (the budding yeast homolog of the tumor suppressor Chk2) is an effector kinase with integral roles in the replication checkpoint (Branzei & Foiani 2006). In contrast to other FHA-containing proteins, Rad53 has two FHA domains (FHA1 and FHA2) that mediate independent interactions of Rad53 with upstream and downstream branches of the checkpoint. One of the binding partners of FHA1 is Dbf4 (Duncker et al. 2002), the regulatory subunit of the initiator kinase Cdc7 (Kitada et al. 1992; Jackson et al. 1993). The association of Rad53 and Dbf4 mediates the Rad53-dependent phosphorylation of Dbf4 and consequent inhibition of Cdc7, thus preventing late origin firing (Kihara et al. 2000; Zegerman & Diffley 2010; Lopez-Mosqueda et al. 2010; Duch et al. 2011). This interaction involves the N-terminal region of Dbf4 that folds as a modified Breast cancer-1 C-Terminal (BRCT) domain (Duncker et al. 2002; Varrin et al. 2005; Gabrielse et al. 2006; Matthews et al. 2012).

BRCT domains are also commonly found in DNA damage and replication stress response proteins where they occur as single or multiple repeats (Leung & Glover 2011). Tandem BRCT repeats are phosphoepitope-binding modules with the phosphoepitope binding pocket residing at the interface between the two domains (Williams et al. 2004).

Conversely, single BRCT domains have diverse functions and their mechanisms cannot be extrapolated from one protein to another due to low sequence identity. Furthermore their specific functions remain elusive because many BRCT domains, like the one found in Dbf4, require additional structural elements to function (Matthews et al. 2012; Kobayashi et al. 2010; Li et al. 2012). The BRCT domain of Dbf4 is immediately preceded by an α-helix that is integral to stabilize the domain and this modified domain has been denoted HBRCT (Matthews et al. 2012; Matthews & Guarné 2013). The HBRCT domain of Dbf4 is necessary and sufficient for the interaction with Rad53, but curiously does not contain any threonine residue that could serve as the phosphorylation site recognized by Rad53 (Duch et al. 2011; Lopez-Mosqueda et al. 2010; Matthews et al. 2012; Chen et al. 2013). A phosphorylated peptide derived from the N-terminal sequence of the HBRCT domain of Dbf4 including the canonical pT-X-X-E FHA-binding motif can interact weakly with the FHA1 domain of Rad53 (Chen et al. 2013). However, mutation of this threonine in full-length Dbf4 does not disrupt the interaction with the FHA1 domain of Rad53 (Matthews et al. 2012; Chen et al. 2013).

Phospho-threonine (pThr) binding to FHA domains has been extensively studied using short phosphopeptides (Durocher et al. 2000). However, there is some evidence indicating that interactions with full-length partners may involve additional interfaces. The FHA domain of *Saccharomyces cerevisiae* Dun1 requires the presence of a second pThr for specific binding (Lee et al. 2008), prompting the comparison of FHA domains to logic gates (Zhang & Durocher 2008). *M. tuberculosis* Rv1827 uses the pThr-binding pocket of its FHA domain to mediate both phosphorylation-dependent and phosphorylation-independent

interactions (Nott et al. 2009). Dbf4 interacts preferentially with the FHA1 domain of Rad53 (Duncker et al. 2002) while Rad9 interacts with its FHA2 domain (Sun et al. 1998), indicating that defined features in each FHA domain determine their binding specificities. In the present study, we exploited this characteristic of Rad53 to analyze how FHA domains increase binding specificity for their targets. We have uncovered a novel interface defined by one of the lateral surfaces of the FHA1 domain and characterized its interaction with the HBRCT domain of Dbf4. We find that the FHA1 domain of Rad53 can bind simultaneously to the HBRCT domain of Dbf4 and a pThr-containing phosphoepitope, suggesting that a bipartite interaction may modulate the interaction between Rad53 and Dbf4 *in vivo.*

5.2 Results

5.2.1 Characterization of the Dbf4 region that interacts with Rad53

The minimal fragment of Dbf4 necessary and sufficient for the interaction with the FHA1 domain of Rad53 includes residues Thr105 to His220 (Matthews et al. 2012). Its crystal structure revealed that this fragment of Dbf4 folds as a modified BRCT domain that we named HBRCT domain because it includes an additional N-terminal helix (**Figure 5.1A**). In the crystal structure, this additional helix is stabilized by crystal contacts (Matthews et al. 2012). Secondary structure chemical shifts measured for ^{15N,13C}HBRCT indicated that residues 106-119 form a helix (**Figure 5.1B**). Furthermore, this helix exhibited HN-NOE values close to the theoretical maximum expected for a fully structured helix (**Figure 5.1C**), confirming that this region of the domain indeed forms a helix in solution.

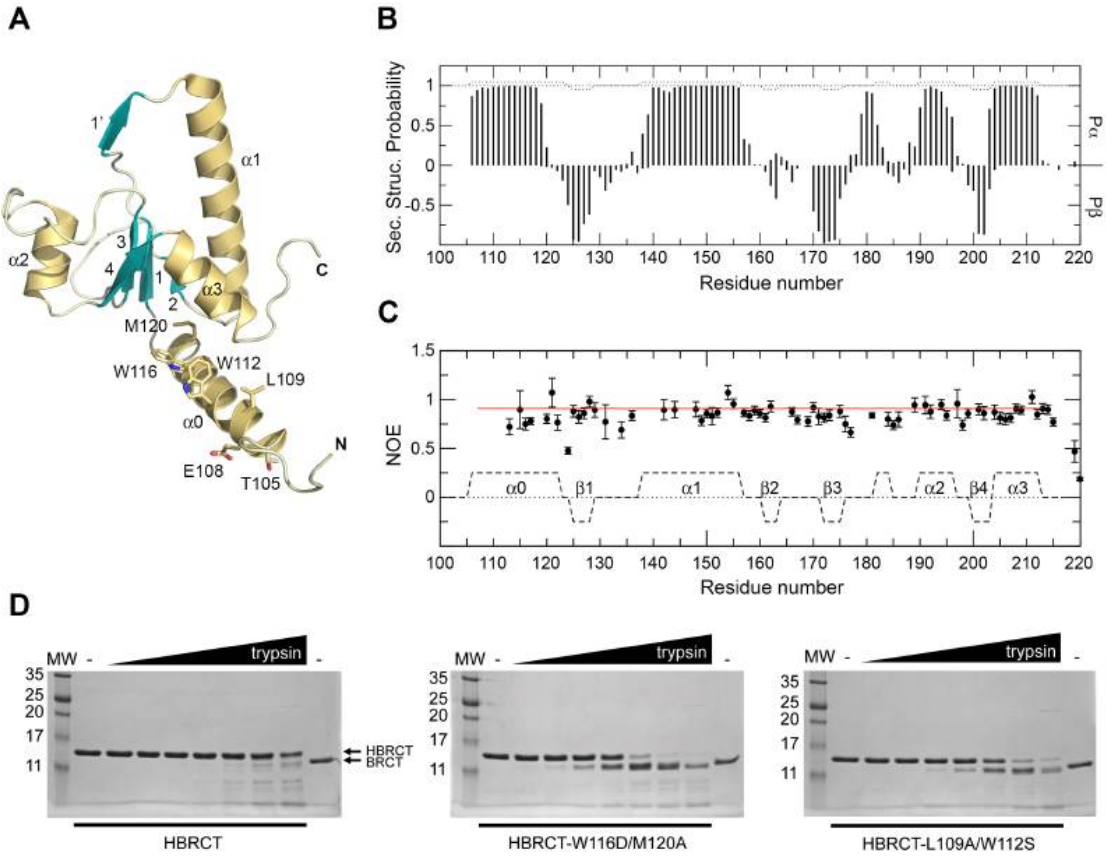

Figure 5.1: The N-terminal domain of Dbf4 folds as a stable HBRCT in solution.

(A) Ribbon diagram of the HBRCT domain of Dbf4 (PDB ID: 3QBZ) with α helices and β strands shown in yellow and teal, respectively. The side chains of the residues latching the α0 helix to the BRCT core, as well as residues in α3 deemed important for the interaction with Rad53, are shown as color-coded sticks and labeled. **(B)** Secondary structure probabilities (Pα and Pβ) of the HBRCT fragment of Dbf4 as a function of residue number. Positive values indicate α-helices and negative values indicate β-strands. **(C)** ^{1}H-^{15}N NOE values as a function of residue number. Closed circles represent the experimentally measured values at 306 K. The solid horizontal line close to 0.8 indicates the theoretical ^{1}H-^{15}N NOE values computed using HydroNMR based on the overall tumbling of HBRCT (PDB: 3QBZ) in the absence of internal ps-ns motions. The black dotted line represents the secondary structure of the crystal structure and is labeled as in (**A**). **(D)** Limited trypsin proteolysis of the HBRCT (left), the HBRCT-W116D/M120A (center), and the HBRCT-L109A/W112S (right) domains. From left to right each gel has molecular weight markers (MW, indicated in kDa), the HBRCT variant in the absence of trypsin, the HBRCT variant treated with increasing concentrations of trypsin (0.195 – 12.5 μg/mL) and the purified BRCT domain of Dbf4 in the absence of trypsin as a molecular weight reference.

We then checked whether the N-terminal helix is an integral part of the domain. Since the loop connecting this helix to the BRCT core includes several positively charged residues, its susceptibility to trypsin proteolysis should vary depending on whether α0 is anchored to the domain or free to move. Hence, we treated the HBRCT, HBRCT-W116D/M120A and HBRCT-L109A/W112S variants with increasing amounts of trypsin. We chose these variants because point mutations at these positions are known to disrupt the interaction with Rad53 presumably by destabilizing the interaction between α0 and the BRCT core (Matthews et al. 2012). We found that the HBRCT was degraded homogeneously, whereas the HBRCT-W116D/M120A and HBRCT-L109A/W112S variants were degraded stepwise (**Figure 5.1D**). The first step resulted in the formation of a fragment of similar size to a BRCT domain. The second step degraded the domain without the accumulation of any intermediate fragments, thereby confirming that the additional N-terminal helix is anchored to the BRCT core of the domain.

5.2.2 The HBRCT domain of Dbf4 and the FHA1 domain of Rad53 interact in vitro

The interaction between Rad53 and Dbf4 is transient, and it has only been studied *in vivo* by coimmunoprecipitation and two hybrid analysis (Duncker et al. 2002; Varrin et al. 2005; Matthews et al. 2012; Chen et al. 2013). However, these *in vivo* assays cannot discern whether or not the interaction between Rad53 and Dbf4 is direct or if their association is mediated by a cellular intermediary. To identify if the interaction between Rad53 and Dbf4 is direct, we sought to characterize the interaction *in vitro* using purified proteins.

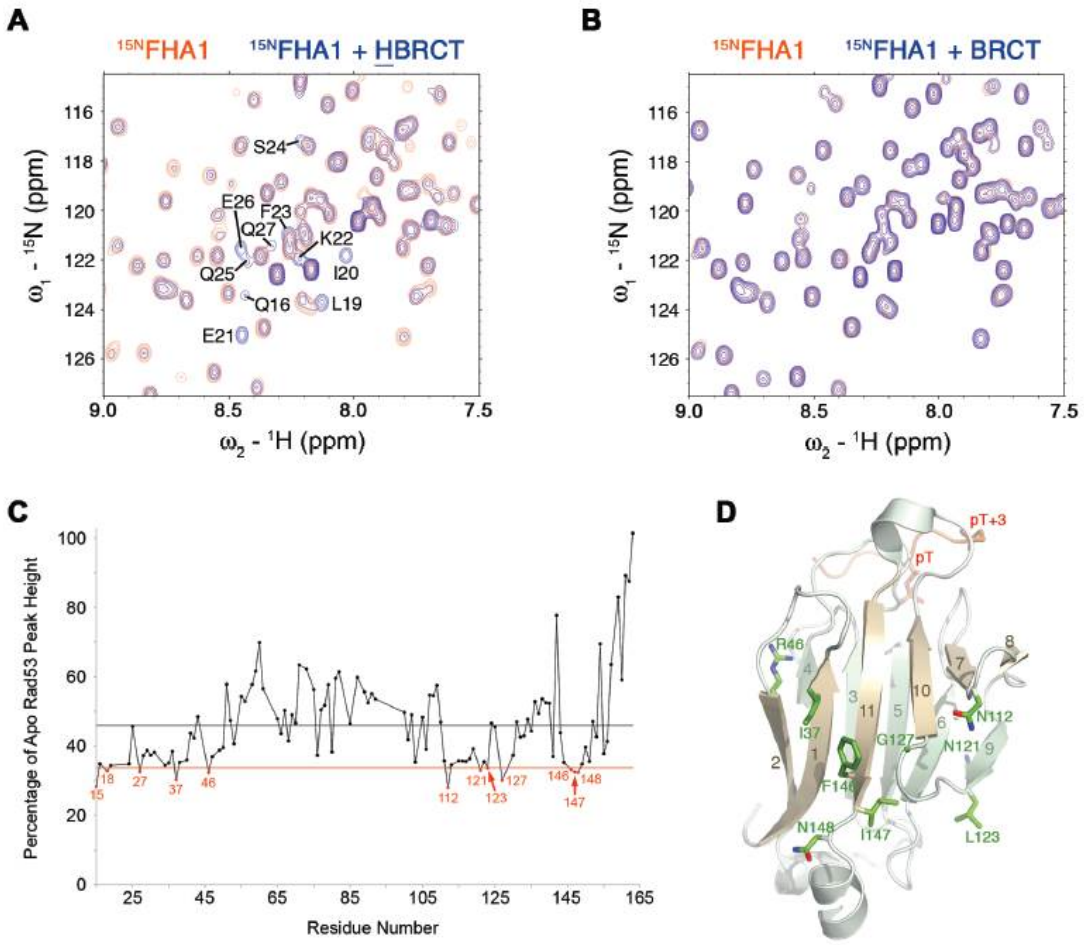

Figure 5.2: The FHA1 domain of Rad53 interacts with the HBRCT domain of Dbf4 *in vitro.*

(A) Detailed view of the HSQC spectra of ^{15N}FHA1 collected in the absence (orange) or presence (blue) of the HBRCT domain of Dbf4. The interaction is identified by residue-specific intensity losses, as well as by the appearance of ten new peaks (labeled in black) in the spectra. **(B)** Same as in **(A)** but with the HBRCT domain replaced by the BRCT domain of Dbf4. This control experiment confirms that the FHA1:HBRCT interaction detected by NMR specifically requires the N-terminal helix α0. **(C)** The peak height from the HSQC spectrum of ^{15N}FHA1 in the presence of the HBRCT domain measured as a percentage of the peak height of ^{15N}FHA1 alone. The black line marks the mean percentage (46.0%) and the red line marks one standard deviation below this value (33.8%). Peaks reduced beyond one standard deviation are labeled. **(D)** Ribbon diagram of the FHA1 domain of Rad53 (PDB ID: 1G6G), with the residues whose peak intensities were reduced beyond one standard deviation in the presence of the HBRCT domain shown as green sticks and labeled. The pThr-containing peptide shown as an orange ribbon with the side chains of pT and pT+3 labeled.

Once we determined that the HBRCT was a stable domain in solution, we over-expressed and purified the HBRCT (Dbf4 residues 105-220) and FHA1 (Rad53 residues 14-164) domains. We collected HSQC spectra of uniformly labeled ^{15N}FHA1 on its own or in the presence of equimolar amounts of unlabelled HBRCT domain. Since the HBRCT domain was not labeled and the experiments were collected in identical conditions, any differences in the HSQC spectrum are due to the direct interaction between the two domains. The main effect caused by the addition of the HBRCT domain was peak broadening for several ^{15N}FHA1 residues, which often is a reliable indicator of binding, as previously shown for other weakly interacting protein:protein complexes (Díaz-Moreno et al. 2005; Hagn et al. 2011; Gunasekara et al. 2012).

Additionally, ten new peaks appeared in the HSQC spectrum. To identify these residues, we assigned the HSQC spectrum of ^{15N,13C}FHA1:HBRCT and found that they corresponded to amino acids Gln16, Leu19, Ile20, Glu21, Lys22, Phe23, Ser24, Gln25, Glu26 and Gln27, which are all located at the N-terminus of the domain (**Figure 5.2A**). These peaks were absent in the HSQC spectrum of ^{15N}FHA1 collected in the presence of equimolar amounts of the BRCT fragment of Dbf4 (residues 120-220), which lacks the helix α0 and does not interact with Rad53 (**Figure 5.2B** and (Matthews et al. 2012)). Therefore, we conclude that the new peaks in the HSQC spectrum of ^{15N}FHA1:HBRCT are caused by the direct and specific interaction between the two proteins.

HSQC cross-peak intensity losses are useful to map the interface of protein:protein complexes (Matsuo et al. 1999; Walters et al. 2001). To determine whether the FHA1

residues involved in the interaction interface with Dbf4 could be identified this way, we compared the height of equivalent peaks in the ^{15N}FHA1 and ^{15N}FHA1:HBRCT HSQC spectra. We then integrated known peaks in the ^{15N}FHA1 and ^{15N}FHA1:HBRCT spectra and found that peak height was reduced to about 46% upon addition of the HBRCT domain, whereas it maintained 95% of the original height upon addition of the non-interacting BRCT domain, thereby confirming that peak broadening was caused by the interaction of the two domains.

We integrated known peaks in the ^{15N}FHA1 and ^{15N}FHA1:HBRCT spectra and calculated their intensity loss (**Figure 5.2C**). Perturbed residues were defined as those whose peak height was reduced by at least one standard deviation (S.D.) from the mean. Nine residues in the core of the FHA1 domain met this criterion and they were located on strands β1 (Ile37), β7 (Asn112), β9 (Asn121, Leu123), β10 (Gly127), and β11 (Phe146, Ile147, Asn148). With the exception of Asn121 and Leu123, all these residues reside on the same lateral surface of the FHA1 domain (**Figure 5.2D**). Residues Thr15, Phe18 and Gln27, located at the N-terminus of the FHA1 domain also met this criterion, but they were not present in the FHA1 fragment used for the crystallization studies (Durocher et al. 2000), and thus are not shown in **Figure 5.2D**. Therefore, the comparative HSQC analyses suggest that the FHA1:HBRCT interaction affects two main areas of the FHA1 domain, namely its N-terminus and one of the lateral surfaces.

5.2.3 The HBRCT domain of Dbf4 interacts with the lateral surface of the FHA1 domain

We decided to investigate whether either of these two surfaces defined the interface of the FHA1:HBRCT complex. If Rad53 interacts with Dbf4 through one of these surfaces, we would expect that surface to be conserved among Rad53 homologues. We have previously seen that Dbf4 binds preferentially to the FHA1 domain of Rad53 (Duncker et al. 2002), thus any conserved features required for the interaction with Dbf4 should be present in FHA1 but not FHA2 domains.

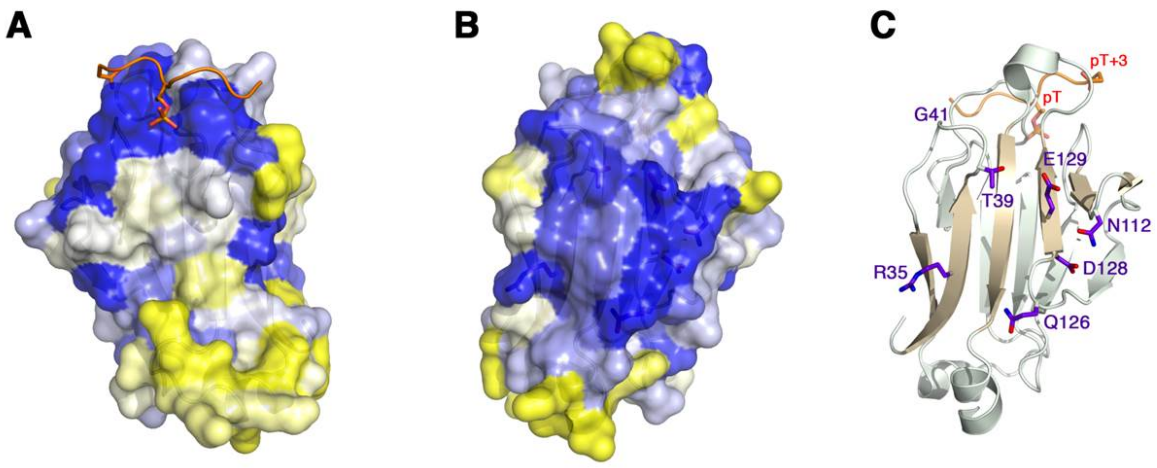

Figure 5.3: The FHA1 domain of Rad53 has a conserved lateral surface.

(A-B) Surface representation of the FHA1 domain of Rad53 (PDB ID: 1G6G) with residue conservation shown as standard deviations from the mean where blue indicates conserved and yellow indicates variable. The FHA1 domain has two highly conserved areas on opposite faces of the molecule: the phosphopeptide binding pocket (A) and the lateral β-sheet composed of strands β2-β1-β11-β10-β7-β8 (B). The view in (B) is a 180° rotation from panel (A). (C) Ribbon diagram of the FHA1 domain of Rad53 (PDB ID: 1G6G), shown in the same orientation as in (B) and colored as in Figure 5.2D. Residues defining the conserved lateral region of FHA1 domain are shown as purple sticks and labeled.

We retrieved representative protein sequences homologous to yeast Rad53 from the non-redundant UniRef90 database using PSI-BLAST (Altschul et al. 1997). Twenty-eight full-length Rad53 homologues containing both FHA1 and FHA2 domains were retained and used to compare the degree of conservation of residues in FHA1 and FHA2. In addition to residues associated with the phosphoepitope binding sites on FHA1 and FHA2, we found a second conserved surface patch on FHA1 that was not present on FHA2 **(Figure 5.3)**. This conserved patch includes residues on strands β1 (Arg35, Ile37, Thr39), β7 (Asn112, Gly113), β10 (Gln126, Asp128, Gln129), and β11 (Val144, Phe146), consistent with residues identified by NMR on the lateral surface of the domain. The lack of a corresponding conserved surface on FHA2 suggests that this conserved patch may mediate FHA1-specific interactions.

Given the agreement between the NMR and bioinformatics analyses, we probed the *in vivo* biological relevance of this surface via yeast two-hybrid. We conducted these analyses using a previously characterized Rad53 (residues 1-165) construct (Duncker et al. 2002) which includes the FHA1 domain, instead of the shorter fragment (residues 14-164) used for the NMR studies. Given the extent of the conserved lateral surface, we were concerned that the effect of single point mutations might result in changes too subtle to produce noticeable effects in our assay and thus we created variants of the FHA1 domain including both single and multiple mutations. Indeed, single point mutations on this surface had minimal effect (**Figure 5.4B**). Of the three mutation pairs (I37A/T39A, V144N/F146A, N112A/E129A) generated, only the N112A/E129A pair weakened the interaction with Dbf4

significantly (**Figure 5.4A**). However, combination of the N112A/E129A pair with any of the other two pairs completely abrogated the interaction (**Figure 5.4C**). Since all FHA1 variants had comparable expression levels (**Figure 5.4A-C**), we attributed the reduced β-galactosidase activity to a defect in the Rad53-Dbf4 interaction.

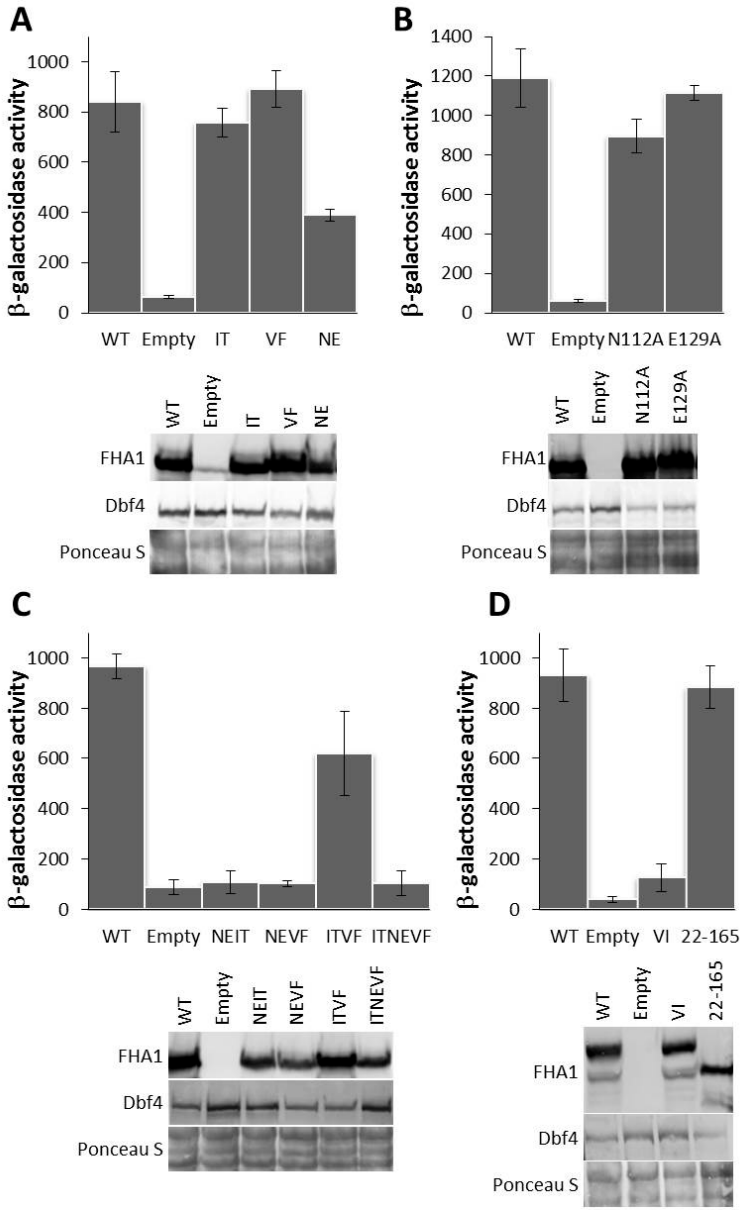

Figure 5.4: The lateral surface of the FHA1 domain of Rad53 is required for the interaction with the HBRCT domain of Dbf4.

(A-C) Yeast two-hybrid analysis using Dbf4 as bait and either the FHA1 domain (residues 1-165) of Rad53 (WT), empty vector (Empty) or variants of the FHA1 (residues 1-165) containing double **(A)**, single **(B)**, or multiple **(C)** mutations within the interaction surface predicted from NMR and bioinformatics analysis as preys. The double mutants and multiple mutants are labeled as: IT (I37A/T39A), VF (V144N/F146A), NE (N112A/E129A), NEIT (N112A/E129A/I37A/T39A), NEVF (N112A/E129A/V144N/F146A), ITVF (I37A/T39A/V144N/F146A), and ITNEVF (I37A/T39A/N112A/E129A/V144N/F146A). The interaction is shown as β-galactosidase activity units and in each case represents the mean of three independent measurements. Error bars represent standard deviation. **(D)** Yeast two-hybrid analysis using Dbf4 as bait and either the FHA1 domain (residues 1-165) of Rad53 (WT), empty vector (Empty), the FHA1-V134D/I140A variant containing a double mutant in the β10-β11 loop (VI), or the shortened FHA1 variant (residues 22-165). To control for the two-hybrid bait and prey expression levels in **A-C**, whole cell extracts were prepared from transformants following prey induction and analyzed by Western blot using rabbit anti-LexA antibody (bait) and a mouse monoclonal anti-HA antibody (prey), along with Alexa Fluor 647 goat anti-rabbit and 488 goat anti-mouse secondary antibodies, respectively. Prior to detection, the membrane was stained with Ponceau S to assess relative protein loading.

We then examined the ability of these Rad53 variants to complement the sensitivity seen in a Rad53 null strain upon exposure to replication stressors. In the presence of hydroxyurea (HU), a ribonucleotide reductase inhibitor that impairs DNA replication fork progression and induces the replication checkpoint, the *rad53Δ* strain had no detectable growth. However, the same strain when transformed with centromeric (CEN) plasmids encoding either *RAD53*, *rad53-V144N/F146A (rad53-VF,)* or *rad53-N112A/E129A (rad53-NE*), resulted in growth comparable to wild-type (*RAD53*) cells at 50 mM HU, and near wild-type growth at 150 mM HU (**Figure 5.5**). Conversely, cells expressing *rad53-N112A/E129A/V144N/F146A* (*rad53-NEVF*) displayed sensitivity to HU, growing poorly at 50 mM HU, and failing to grow at 150 mM HU. Similar results were obtained when we examined growth in the presence of methyl methanesulfonate (MMS), a DNA alkylating

agent known to cause fork stalling. The growth sensitivity observed in the presence of HU or MMS was not due to reduction in protein expression **(Figure 5.5)**, supporting the idea that the conserved lateral surface of the FHA1 domain is important for checkpoint function.

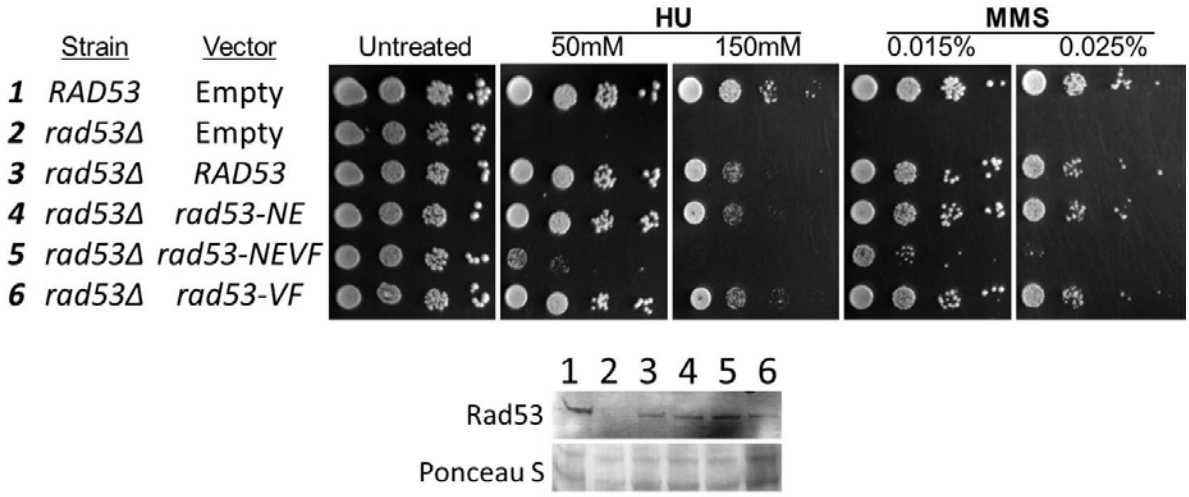

Figure 5.5: Lateral surface mutations on FHA1 that abrogate interaction with HBRCT results in sensitivity to genotoxic stress.

The ability of Rad53 variants to complement a Rad53 null strain was assessed, and the sensitivity of these Rad53 mutants to genotoxic stress was tested in the presence of hydroxyurea (HU) or methyl methanesulfonate (MMS). The growth of the *rad53Δ, sml1Δ* strain in the presence of CEN plasmids encoding *RAD53, rad53-NE, rad53-NEVF* and, *rad53-VF* was compared on SC-Leu plates containing increasing concentrations of HU or MMS by spotting 10-fold serial dilutions. The *RAD53*/*sml1Δ* and *rad53Δ/sml1Δ* strains transformed with empty vector were used as controls for normal sensitivity or hypersensitivity to genotoxic agents, respectively. Rad53 expression was assessed using a goat anti-Rad53 antibody (Santa Cruz Biotech) and Alexa Fluor 488 donkey anti-goat secondary antibody.

Additionally, we tested the effect of the loop connecting the β10 and β11 strands and found that mutation of V134D/I140A weakened the interaction with Dbf4 (**Figure 5.4D**). Interestingly, this loop is involved in a hydrogen bond network with the backbone of Arg70,

which is required for pThr binding. It also partially forms the pocket for the pThr+3 residue of a phosphorylated peptide, and this pocket is important for phosphoepitope specificity (Durocher et al. 2000). Thus, mutations in this loop may impair the ability of FHA1 to bind a phosphoepitope. The decrease in interaction with Dbf4 of this mutant indicates that the ability to bind to a phosphoepitope may still be required *in vivo*, consistent with our previous observations (Duncker et al. 2002).

Although mutations on the lateral surface of FHA1 abrogated the interaction with Dbf4 (**Figure 5.4**), we wanted to confirm that the N-terminal region of the domain (residues 15-29) were not necessary for the interaction with Dbf4. Therefore, we generated a variant of Rad53 corresponding to the minimum FHA1 fold (residues 22-165). This FHA1 variant interacted with the HBRCT domain of Dbf4 similarly to longer fragments of Rad53, confirming that the region immediately preceding the FHA1 domain is not necessary for the interaction between FHA1 and HBRCT (**Figure 5.4D**). Collectively, these results indicate that Rad53 likely interacts with Dbf4 through the lateral surface of the FHA1 domain defined by the β-sheet composed of strands β2-β1-β11-β10-β7-β8 (**Figure 5.2D, Figure 5.3C**).

5.2.4 The pThr-binding pocket of FHA1 is not required for the interaction with Dbf4

We have previously shown that a point mutation (Arg70Ala) in the phosphoepitope binding pocket of the FHA1 domain abrogates the interaction of this domain with Dbf4 through yeast two-hybrid analysis (Duncker et al. 2002). We confirmed this observation using full-length Rad53, and observed that the Arg70Ala mutation and not a neighboring residue significantly reduces the interaction with Dbf4 (**Figure 5.6B**). The phosphorylated

peptide consisting of residues 98-113 from Dbf4 (including a phosphorylated threonine, pThr105) interacts with the FHA1 domain weakly (Chen et al. 2013). However, mutation of Thr105, or any other threonine within the HBRCT domain, does not disrupt the interaction with Rad53 (Matthews et al. 2012), suggesting that the HBRCT domain does not contain a phosphoepitope targeted by Rad53. To elucidate how the Arg70Ala mutation affects the FHA1:HBRCT interaction *in vitro*, we collected HSQC spectra for ^{15N}FHA1 and ^{15N}FHA1-R70A to identify the residues that change their chemical environment due to the point mutation. Although a number of peaks exhibited chemical shift changes, addition of the HBRCT domain to the ^{15N}FHA1-R70A sample still caused an overall decrease in intensity and the appearance of the ten peaks indicative of complex formation (**Figure 5.6A**), thereby confirming that FHA1-R70A interacts with the HBRCT domain of Dbf4 *in vitro*. Taken together these observations suggest the possibility that Rad53 interacts with Dbf4 through a bipartite interface involving both the recognition of a phosphoepitope and the interaction of the HBRCT domain with the lateral surface of the FHA1 domain.

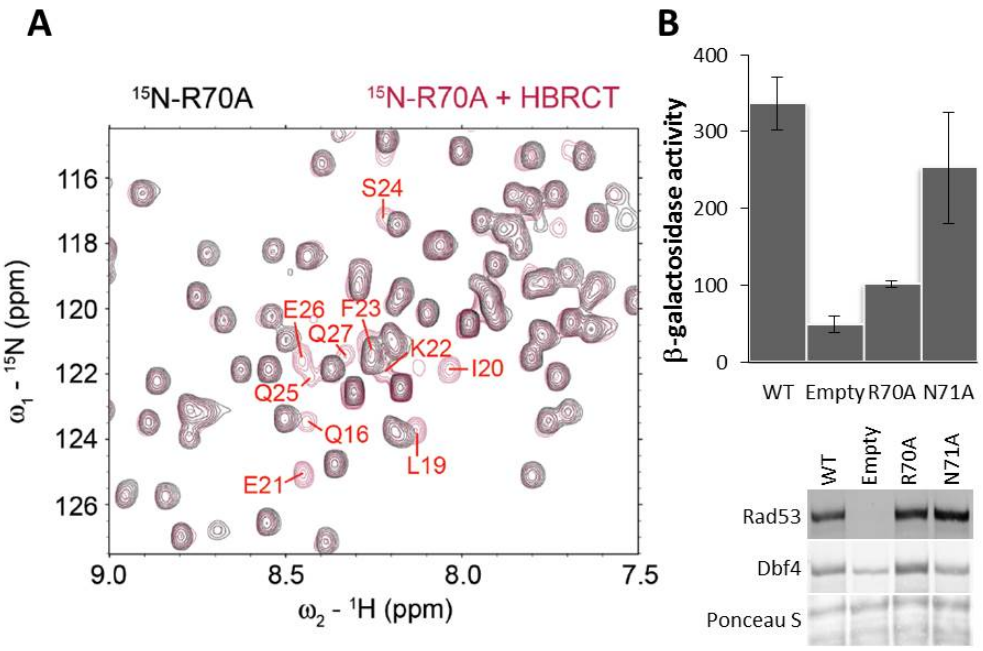

Figure 5.6: The ^{15N}FHA1-R70A variant interacts with the HBRCT domain.

(A) Overlay of the HSQC spectra of ^{15N}FHA1-R70A (black) and ^{15N}FHA1-R70A in the presence of unlabeled HBRCT (red). Peaks indicative of the FHA1:HBRCT interaction are labeled in red. **(B)** Two-hybrid analysis was carried out as in Figure 5.4, with full-length *DBF4* as bait and either *RAD53* (WT), empty vector (Empty), *rad53-R70A* (R70A), or *rad53-N71A* (N71A), as prey.

Among many other phosphorylated substrates, the FHA1 domain of Rad53 recognizes a phospoepitope within Cdc7 (Aucher et al. 2010). We reasoned that Cdc7 might modulate the interaction between Rad53 and Dbf4, and thus we tested whether a Cdc7-derived peptide (^{480}DGES**pT**DEDDVVS^{491}, herein referred to as pPEP) could outcompete the interaction of Rad53 with Dbf4. To this end, we incubated a mixture of ^{15N}FHA1 and HBRCT with increasing amounts of pPEP. HSQC spectra were collected at increasing concentrations of peptide corresponding to increasing ratios of pPEP:FHA1. We found that the presence of pPEP caused changes consistent with phosphopeptide binding, while the non-

phosphorylated version of the peptide (PEP) did not induce any changes in the ^{15N}FHA1 HSQC spectrum (**Figure 5.7**). Importantly, the peaks indicative of the interaction between FHA1 and HBRCT were present at all pPEP concentrations, although the peak corresponding to Gln16 could not be monitored in this experiment because it overlapped with the peak corresponding to Glu117 during the titration. Collectively, our data demonstrates that Rad53 is able to interact with a phosphoepitope and the HBRCT domain of Dbf4 through different surfaces of the FHA1 domain and that both these interactions can occur simultaneously.

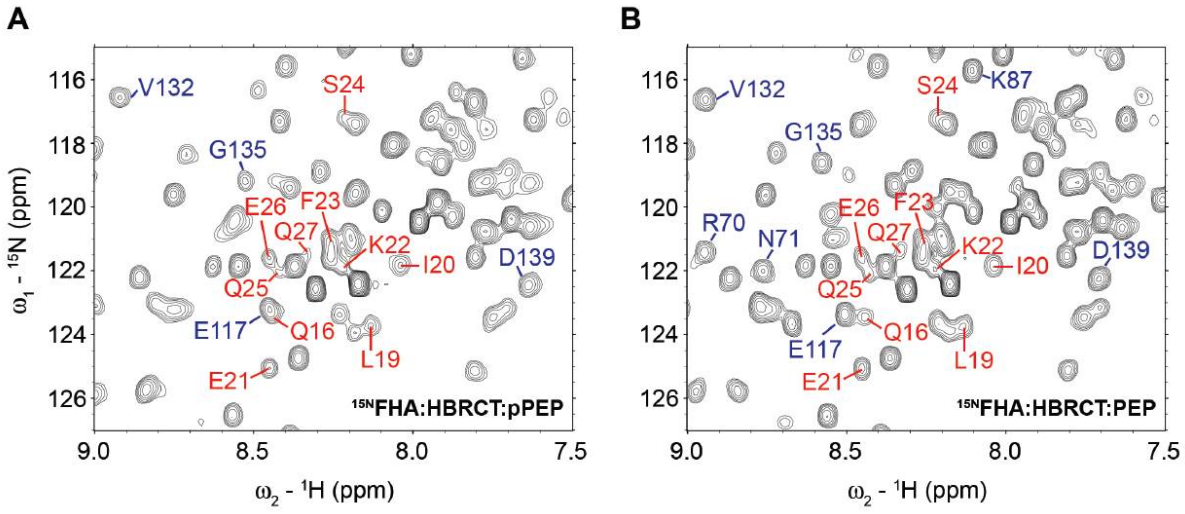

Figure 5.7: The HBRCT domain of Dbf4 does not bind to the phosphoepitope-binding pocket of the FHA1 domain.

HSQC spectra monitoring the formation of the complex between ^{15N}FHA1 and HBRCT at a 1:1 ratio in the presence of stoichiometric amounts of either DGES**pT**DEDDVVS **(A)** or DGESTDEDDVVS **(B)**. Some of the peaks corresponding to residues that undergo significant changes upon pPEP binding and the ten peaks signifying the interaction between with HBRCT are labeled in blue and red, respectively.

5.3 Discussion

We have shown that the HBRCT domain of Dbf4 interacts with the lateral surface of the Rad53 FHA1 domain, rather than its phosphoepitope-binding surface. This lateral surface is not conserved in the FHA2 domain of Rad53, indicating that the FHA1 domain of Rad53 gains specificity by engaging additional interaction surfaces. Additionally, FHA1 can simultaneously bind a phosphopeptide and the HBRCT domain. Therefore, the Rad53:Dbf4 interaction *in vivo* may occur through a bipartite interaction. The phosphorylated peptide consisting of 98-113 of Dbf4 includes a canonical pT_{105}-X-X-E_{108} FHA-binding motif and interacts with the FHA1 domain weakly (Chen et al. 2013). Mutation of Thr105 in the context of full-length Dbf4, however, does not disrupt the interaction between Dbf4 and Rad53 (Matthews et al. 2012). This same study has also shown that point mutations on the surface of the HBRCT domain defined by helices α0 and α3 abrogate the interaction with Rad53. This suggests that Thr105 may contribute to defining the interface between Rad53 and HBRCT rather than providing a pThr target site.

Several FHA domains have been shown to mediate bipartite interactions. For instance, the FHA domain of Dun1 requires the simultaneous interaction with two phosphorylated threonine residues (pThr) to recognize its target (Lee et al. 2008) and KIF13B interacts simultaneously with the ArfGAP and PH1 domains of CENTA1 (Tong et al. 2010). This has led to the analogy of FHA domains functioning as logic gates to integrate multiple inputs and generate a single output (Zhang & Durocher 2008). In the case of phosphopeptide binding, the FHA1 domain from Rad53 acts as an ‘OR’ logic gate as the domain can only bind to one pThr within a multiply phosphorylated peptide at a time. In

contrast, the FHA domain from Dun1 is considered an ‘AND’ logic gate because it must bind to two pThr simultaneously (Lee et al. 2008). If we extend the logic gate model to DDK targeting, the FHA1 domain of Rad53 also behaves as an ‘AND’ logic gate, requiring simultaneous binding of a phosphoepitope and engagement of the HBRCT domain of Dbf4 through its lateral interface for their normal physiological interaction. FHA1 interactions functioning as an ‘AND’ logic gate would also explain why disabling either contact point abrogates the Rad53:Dbf4 interaction in a yeast two-hybrid assay and would have important ramifications during the checkpoint response. DDK-mediated phosphorylation of Mcm2 has a role in the response to replicative stress, likely as a result of replication fork stabilization (Stead et al. 2012). Therefore, the lateral surface interaction may guarantee the specificity of Rad53 to target the HBRCT domain of Dbf4, while the phosphopeptide binding surface may ensure the stress-dependency of the interaction, recognizing a phosphoepitope generated by a stress-activated kinase. Thus these two surfaces allow FHA1 to integrate multiple inputs to bind Dbf4 *in vivo*, resulting in checkpoint dependent regulation of DDK activity.

Logic gates have emerged as critical components of biological signaling networks, and it is becoming increasingly clear that FHA domains function as highly specialized modules that integrate complex input signals (Zhang & Durocher 2008; Hasty et al. 2002; Lee et al. 2008; Li et al. 2002; this study). The Dbf4:Rad53 interface unveiled in this work is reminiscent of the BRCA1:Chk2 interaction, where the tandem BRCT repeat of BRCA-1 must recognize two distal surfaces in the FHA domain of Chk2 simultaneously (Li et al. 2002). In the BRCA1:Chk2 complex, the interaction involves the pThr-binding site and a conserved hydrophobic patch on one of the lateral surfaces of the FHA domain. Disruption of

either contact point prevents the interaction, and mutation of the hydrophobic patch has been linked to Li-Fraumeni syndrome, which predisposes patients to multi-organ cancers (Li et al. 2002). However, Dbf4 and BRCA-1 do not interact with the same lateral surface of the FHA domains of Rad53 and Chk2. Furthermore, the hydrophobic patch found in the FHA domain of Chk2 is not conserved in FHA1 from Rad53 revealing the extreme plasticity of FHA domains to enhance binding specificity. The interactions of Rad53 with Dbf4 or Chk2 with BRCA-1 lead to inhibition of late origin firing and double strand break repair, respectively. Given the importance of these associations it is not surprising that cells have developed strict selectivity mechanisms to modulate these two interactions. However, while the need for bipartite interactions increases Rad53 and Chk2 binding specificities, it also underlines the experimental difficulty in detecting dual input FHA domains as eliminating one binding site abrogates the interaction, effectively masking the presence of a second binding site.

Our work suggests that FHA domains may have a broader spectrum of interactions that have remained elusive due to the intrinsic limitations of studying ‘AND’ logic gates and it provides a novel approach to study functional interactions mediated by this highly prevalent signaling domain.

Chapter 6
General conclusions and future directions

6.1 The motif C zinc finger in Dbf4 is required for replication and response to genotoxic stress.

Here we find that mutation to conserved residues within Dbf4 motif C, but not deletions of this motif are able to complement the essential function of Dbf4. Mutation of conserved cysteine and histidine residues of motif C weaken interactions with origin DNA and the replicative helicase subunit Mcm2, while preserving interactions with the known Dbf4 binding partners Orc2, Rad53, and Cdc7. We see that this reduction in association with Mcm2 translates to reduced phosphorylation of recombinant Mcm2 by cellular extracts from cells containing mutations to motif C of Dbf4. Consistent with reduced association with origins of replication and decreased phosphorylation of Mcm2, cells harboring Dbf4 motif C mutations display slowed growth marked by delayed entry to and progression through S-phase. Additionally, motif C mediates resistance to genotoxic stress, as mutants are sensitive to long-term exposure to both MMS and HU, but not short-term exposure. These observations support the notion that Dbf4/Cdc7 plays a role in the stabilization or restart of replication forks (Duncker & Brown 2003).

To address the question of the involvement of DDK in replication fork stabilization, dense isotope substitution experiments could be used where motif C mutants are released into MMS or HU and replication progression can be monitored. Alternatively DNA combing experiments could be performed which would allow individual origins to be visualized, identifying fork collapse. An added benefit of this technique is that it would allow direct

observation of continued DNA replication from a stalled fork indicating restart. Furthermore, it would be possible to determine a relative rate of replication from track length.

Chromatin immunoprecipitation (ChIP) can be used to track replisome components, such as Cdc45 or PolƐ, to identify the cause of the S-phase defects seen in motif C mutants. If enrichment for replisome components is seen at early origins for the wild-type and not for mutants, then the S-phase defects seen are likely the result of reduced origin firing. Conversely, if equal levels of enrichment are seen this may indicate that a reduced rate of fork progression is the cause of the extended S-phase.

While the Mcm2-7 complex, Cdc45, and polymerase alpha all have potential as targets of DDK to promote fork stability or restart, and it is still unclear exactly what is targeted by DDK. To identify the role of motif C in fork stability or restart, motif C mutants can be crossed to mutants of these essential candidates, sporulated, and the resultant double mutants assessed for positive or negative genetic interactions. Alternatively, motif C mutants could be screened in a synthetic gene array, against both the essential temperature sensitive gene array, and the non-essential deletion collection (described in Tong et al. 2001; Baryshnikova et al. 2010).

Recent work from our lab has shown that Dbf4 and Cdc7 promote replication through association with distinct subunits of the Mcm2-7 complex, Dbf4 with Mcm2 and Cdc7 with Mcm4 (Ramer et al. 2013). Combination of the *mcm2ΔDDD* and *mcm4ΔDDD* mutants lacking their DDK docking domains (DDD) resulted in synthetic lethality (Ramer et al. 2013; Sheu & Stillman 2006). It would be interesting to combine a Dbf4 motif C mutant with the

mcm4ΔDDD allele to see if the same lethality is observed, confirming that motif C of Dbf4 promotes interaction with Mcm2.

Our results are consistent with a model whereby phosphorylation of the Mcm2-7 complex promotes fork stability. Interestingly, it appears DDK phosphorylation of Mcm2 imparts an inhibitory signal, slowing helicase activity by increasing the affinity with which it binds DNA (Stead et al. 2011). Inability of Dbf4/Cdc7 to phosphorylate Mcm2 has been shown to cause sensitivity to genotoxic stressors (Stead et al. 2011; Stead et al. 2012). In the context of checkpoint activity, the ability for DDK to slow the helicase might be important for replisome stability. As forks stall due to impediments to the polymerase, such as a lack of dNTPs, the helicase is still active and may uncouple from the rest of the replisome. This can result in large tracts of ssDNA, precarious sites, which have the potential to result in genomic instability. It is possible that during an invoked checkpoint, DDK phosphorylation of Mcm2 is required to inhibit DNA unwinding and prevent uncoupling of the helicase thus preserving fork stability.

6.2 Motif N of Dbf4 constitutes part of a larger modified BRCT domain required for interaction with Rad53.

In this study we have determined the crystal structure of a portion of the amino-terminus of Dbf4 and can verify that it folds as a *bona fide* BRCT domain. This domain on its own is not sufficient to mediate the interaction with Rad53. However, the restoration of fifteen amino acids preceding the BRCT domain reinstates the interaction with Rad53. Solving the crystal structure of a larger fragment of Dbf4 encompassing the BRCT domain shows that these extra amino acids form an additional α–helix which protrudes from the

BRCT domain, and we henceforth refer to this domain as HBRCT (Helix-BRCT). The additional helix forms an integral part of the domain, and mutations that destabilize association of the helix with the BRCT core abrogate the interaction with Rad53. We demonstrate that Dbf4 mutations previously observed to result in sensitivity to genotoxic agents show an abrogated interaction with Rad53 which is a result of destabilization of the HBRCT fold. Additionally, we find that conserved threonines within the HBRCT domain of Dbf4 do not serve as phosphoepitopes for recognition by Rad53, but act to stabilize the domain. Collectively these results indicate the potential for a phosphorylation independent interaction between Dbf4 and Rad53, which relies on the structural integrity of the HBRCT domain.

The amino terminus of Dbf4 is has been implicated in interactions with origins of replication and the origin recognition complex (Dowell et al. 1994; Hardy & Pautz 1996; Duncker et al. 2002). Mutations or deletions that completely disrupt the BRCT domain have been shown to abrogate the interaction with origin DNA in one-hybrid assays (Ogino et al. 2001). Curiously, cells harboring mutations to Dbf4 that disrupt the anchoring of helix α0 to the BRCT domain do not display the delayed entry to S-phase seen in cells where the BRCT core is disrupted (**Appendix B Figure 6**). We do not know the minimal sufficient region of Dbf4 to mediate interaction with origins and these observations indicate it is likely not the HBRCT domain. However, the BRCT domain does appear to be required for timely entry to S-phase and for the interaction of Dbf4 with origin DNA. We have proposed the BRCT domain is a modular core around which accessory structures can be assembled. The structure of a subunit of human replication factor C (RFC) bound to DNA has shown that this subunit

of RFC uses its BRCT domain and an additional amino-terminal α–helix to bind DNA (Kobayashi et al. 2010). It would be interesting to see if an alternate structural element interacts with the BRCT core in Dbf4 to promote origin association, and thus a single BRCT domain may be able to contribute to two distinct modes of interaction.

Dbf4 is a target of Rad53 in the block to late origin firing, and is removed from chromatin in a Rad53 dependent manner upon exposure to hydroxyurea (Zegerman & Diffley 2010; Lopez-Mosqueda et al. 2010; Duch et al. 2011; Pasero et al. 1999). We have shown that abrogation or significant reduction in the interaction between Rad53 and Dbf4 by destabilizing the HBRCT domain imparts sensitivity to cells when exposed to genotoxic stress. However, the ability to regulate late origin firing has not been assessed with HBRCT mutations that compromise the interaction with Rad53, nor has the chromatin status of Dbf4 in these mutants when exposed to HU.

6.3 FHA1 of Rad53 recognizes the HBRCT of Dbf4 in a novel non-canonical manner.

We have confirmed that a modified BRCT domain at the amino-terminus of Dbf4 includes an additional amino-terminal α-helix and that this helix is integral to the domain, which we refer to as HBRCT. Using NMR spectroscopy we are able to identify that FHA1 of Rad53 and HBRCT of Dbf4 interact directly *in vitro*, and thus this interaction does not rely on the presence of any cellular intermediary. Bioinformatic and NMR analysis have identified a conserved surface specific to FHA1 that could mediate the interaction between the FHA1 and HBRCT domains. Mutational analysis of this surface confirms that it is required to mediate the FH1:Dbf4 interaction *in vivo*, as disruption of this extensive interface abrogates the interaction. Additionally, disruption of the conserved lateral surface of FHA1

in vivo results in sensitivity when cells are grown in the presence of hydroxyurea or methyl methanesulfonate. We also show that the ability of full-length Rad53 to interact with Dbf4 *in vivo* requires the ability of FHA1 to bind phosphoepitope, while the direct *in vitro* interaction between FHA1 and HBRCT does not require this ability. Coalescing these two observations, NMR spectra indicate that FHA1 is able to simultaneously bind to both a phosphopeptide and HBRCT, using different surfaces of the FHA domain.

It is interesting to note that mutations to the lateral patch of FHA1 abrogating the interaction with Dbf4 do not appear equivalent to HBRCT mutations that abrogate this interaction. The *rad53-N112A/E129A/V144N/F146A* (NEVF) allele for which the lateral surface of FHA1 is mutated displays higher sensitivity when exposed to genotoxic agents than the *dbf4-ΔN* (deletion of residues 135-179), *dbf4-GA159LL* or *dbf4-W202E* HBRCT mutants (Varrin et al. 2005; Gabrielse et al. 2006). This indicates that the lateral surface of FHA1 may mediate other interactions aside from the HBRCT of Dbf4. Indeed, Rad53 is known to interact with several other proteins through its FHA1 domain including the RecQ like helicase Sgs1, and the essential replication fork component Cdc45 (Bjergbaek et al. 2005; Aucher et al. 2010). What is particularly interesting about these two proteins is that they have been implicated to interact with FHA1 in a phosphorylation dependent manner. Sgs1 contains an amino-terminal acidic region, phosphorylated by Mec1, required to interact with FHA1 and mutation of potential Mec1 target sites within this region reduces the interaction (Hegnauer et al. 2012). Similarly, Thr189 in Cdc45 has been shown to mediate the interaction with FHA1 of Rad53, and mutation of this residue reduces the interaction between the two (Aucher et al. 2010). While both Sgs1 and Cdc45 appear to interact with

FHA1 in a phosphorylation dependent manner, this does not preclude the possibility that their interaction with FHA1 is bipartite. As we have seen with the interaction between Dbf4 and Rad53, disruption of one surface in a bipartite interaction model is sufficient to disrupt interaction, thus mutations that implicate a phosphorylation dependent interaction may mask the presence of a second interaction with the lateral surface of FHA1.

It is of interest to take our understanding of how FHA1 mediates its interactions and extend that to other FHA domains. Our observations indicate that the lateral conserved patch of FHA1 is not found in FHA2, and may be poorly conserved in other yeast FHA domains. The presence of a second conserved patch in other FHA domains may indicate an ability to interact with partners in a bipartite manner and thus phosphorylation independent interactions could be a common feature of FHA domains. The presence of the same second patch in other FHA domains may be an indicator of commonly shared interaction partners. If the laterally conserved surface found on FHA1 is indeed unique to only FHA1 there may be other mechanisms by which FHA domains mediate phosphorylation independent and multipartite interactions. The FHA domain of Rv1827 from *Mycobacterium tuberculosis* mediates interactions with three related enzyme complexes independent of phosphorylation using residues integral to the canonical phosphoepitope binding domain (Nott et al. 2009). It has been seen with mammalian Chk2, and with Rad53 in this study, that intermolecular interactions are mediated by the canonical phosphoepitope binding site and an accessory lateral surface (Li et al. 2002). Thus FHA domains may mediate phosphorylation independent and dependent interactions in different ways, and perhaps there is not a universal mechanism for how FHA domains recognize their partners. It would be particularly

interesting to utilize the same bioinformatic approach used in this study to identify additional conserved surfaces in other FHA domains, and query the *in vivo* function of any such conserved region.

6.4 Role of Dbf4/Cdc7 in cancer

The body of this study deals with understanding the fundamental mechanisms by which Dbf4 interacts with DNA replication and checkpoint machinery. Failure to ensure true and faithful replication is a leading cause of genomic instability, a hallmark of cancers, and it is the purpose of cell cycle checkpoints to ensure the fidelity of the genome is maintained (discussed in Abbas et al. 2013; Negrini et al. 2010). While we do not directly examine these mechanisms in cancerous cells, or a mammalian system, the degree to which these processes are conserved, even in single celled eukaryotes, means that the underlying functions we uncover can apply to metazoan systems. Our discovery of how Dbf4 interacts with its cellular partners helps to understand the ways in which Dbf4/Cdc7 performs its roles during DNA replication and under checkpoint conditions. Understanding the ways normal cells function can provide a comparative basis to help explain errant cellular behavior. Thus, elucidating the role of Dbf4/Cdc7 can help to shed light on what may be occurring in abnormal or cancerous cells when the levels and molecular interactions of Dbf4/Cdc7 are perturbed.

Indeed the examination of several cancers and tumor derived cell lines has implicated up-regulation of Dbf4/Cdc7 (Nambiar et al. 2007; Bonte et al. 2008; Kulkarni et al. 2009; Cheng et al. 2013). In a study of patient derived dysplastic nevi, primary cutaneous melanomas, cutaneous melanoma metastases, and melanoma derived cell lines, over

expression of Dbf4 was documented compared to controls. Specifically, up-regulation was found in 66.7% of patients with primary cutaneous melanoma and 86.7% of those with cutaneous melanoma metastases, showing a median overexpression of 17.9 and 13.2 fold respectively (Nambiar et al. 2007). This study also revealed that Dbf4 overexpression in melanomas was associated with a higher percent (30.6%) of relapse at 186 weeks (Nambiar et al. 2007). In a study involving oral squamous cell carcinomas Cdc7 overexpression was found in 91.4% of primary tumors examined (Cheng et al. 2013). Similarly, in a study examining 62 tumor derived cell lines, representing lung, colon, brain, breast, prostate, and kidney cancers, approximately 50% were found to have increased Cdc7 levels and most of these cell lines were found to also have increased Dbf4 levels (Bonte et al. 2008). The same study also found up-regulation of Cdc7 expression in primary breast, colon, and lung tumors, where a high degree of p53 loss was seen in primary breast cancers expressing increased Dbf4/Cdc7 (Bonte et al. 2008).

Curiously, this brings about the question of whether Dbf4/Cdc7 overexpression is causative or merely correlative with cancers due to its required role in replication. Increased Cdc7 levels have been linked to advanced tumor stages which are associated with accelerated cell cycle rates and reduced length of G1 in primary ovarian tumors (Kulkarni et al. 2009; Williams & Stoeber 2007; Kulkarni et al. 2007). Alternatively increased expression of Dbf4 and Cdc7 in CHO cells has been seen to trigger cell cycle arrest (Guo et al. 2005).

While the jury still seems to be out on the causative or correlative nature of Dbf4/Cdc7 activity, their potential as prognostic biomarkers is clear. Early diagnosis and treatment are the current best methods to combat cancers and improve patient survival.

Cancerous cells are by nature fast growing and it can be expected that increased cellular expression of replication proteins or any others that promote proliferation would facilitate fast growth. Traditional biomarkers, such as PCNA or Ki67, have taken advantage of the concept of increased levels of factors associated with proliferation to identify cancers (discussed in Semple & Duncker 2004). Cdc7 kinase levels have been shown to be a strong predictor of survival in epithelial ovarian carcinoma, providing great potential as a prognostic biomarker (Kulkarni et al. 2009). In a cohort of 143 individuals with epithelial ovarian carcinoma, increased Cdc7 expression was associated with advanced clinical stage, genomic instability, aggressive tumors, and conventional indicators of poor clinical outcome such as tumor anaplasia (Kulkarni et al. 2009). Similarly, increased Cdc7 expression levels are associated with poor patient outcome in oral squamous cell carcinoma, but do not correlate with conventional indicators of poor clinical outcome (Cheng et al. 2013).

Interestingly, increased expression of Cdc7 in oral squamous cell carcinoma cell lines promotes increased cell survival from apoptosis in the presence of HU, the topoisomerase inhibitor Camptothecin, or UV radiation, by increasing the expression of anti-apoptotic proteins (Cheng et al. 2013). Conversely, siRNA knockdown of Cdc7 in HeLa cells has been shown to cause cell death by apoptosis or aberrant cell division (Montagnoli et al. 2004). However, normal fibroblasts do not undergo this cell death, instead activating a p53 dependent replication checkpoint preventing an abortive cell cycle, and maintaining viability under conditions of limiting Cdc7 (Montagnoli et al. 2004). This phenomenon has also been seen in the breast cancer derived BT549, MDAMB157, and MDAMB45 cell lines as well as the ovarian cancer derived SKOV3 and Caov-3 cell lines (Rodriguez-Acebes et al. 2010;

Kulkarni et al. 2009). The potential for a cancer therapeutic that specifically targets cancerous cells is of great interest and medical relevance. The loss of checkpoint function, specifically p53, seen in cancerous cells makes Cdc7 a very promising candidates for treatment (reviewed in Montagnoli et al. 2010; Swords et al. 2010).

Several Cdc7 inhibitors have been characterized and are in various stages of development (Natoni et al. 2013; Koltun et al. 2012; Montagnoli et al. 2008; Swords et al. 2010; Montagnoli et al. 2010). With the solved crystal structure now available for human Dbf4 bound to Cdc7 there is potential to develop new specific small molecule inhibitors of Cdc7. In the original study that solved the structure of Dbf4 bound to Cdc7, two ATP competitive small molecule inhibitors of Cdc7 (XL413 and PHA767491) were also co-crystallized with Dbf7/Cdc7, providing a mechanistic understanding of how these compounds are able to specifically inhibit Cdc7 (Hughes et al. 2012). The promise Cdc7 inhibitors hold as additions to the arsenal of treatments for cancers is high, and indeed several inhibitors are in pre-clinical and early stage clinical trials (Koltun et al. 2012; discussed in Swords et al. 2010; Montagnoli et al. 2010).

While cancer biology has not been the focus of this body of work, the fundamental mechanisms we explore are nonetheless conserved in mammals. The insight gained into the underlying mechanisms we study contributes to understanding how Dbf4 interacts with its cellular partners and these interactions have important consequences in the progression of cancers.

Bibliography

Abbas, T., Keaton, M.A. & Dutta, A., 2013. Genomic instability in cancer. *Cold Spring Harbor perspectives in biology*, 5(3), p.a012914.

Adams, P.D. et al., 2002. PHENIX: building new software for automated crystallographic structure determination. *Acta crystallographica. Section D, Biological crystallography*, 58(Pt 11), pp.1948–54.

Agarwal, R. et al., 2003. Two distinct pathways for inhibiting pds1 ubiquitination in response to DNA damage. *The Journal of biological chemistry*, 278(45), pp.45027–33.

Aguilera, A. & Gómez-González, B., 2008. Genome instability: a mechanistic view of its causes and consequences. *Nature reviews. Genetics*, 9(3), pp.204–17.

Alcasabas, a a et al., 2001. Mrc1 transduces signals of DNA replication stress to activate Rad53. *Nature cell biology*, 3(11), pp.958–65.

Allen, J.B. et al., 1994. The SAD1/RAD53 protein kinase controls multiple checkpoints and DNA damage-induced transcription in yeast. *Genes & development*, 8(20), pp.2401–15.

Altschul, S.F. et al., 1997. Gapped BLAST and PSI-BLAST: a new generation of protein database search programs. *Nucleic acids research*, 25(17), pp.3389–402.

Alvino, G.M. et al., 2007. Replication in hydroxyurea: it's a matter of time. *Molecular and cellular biology*, 27(18), pp.6396–406.

Aparicio, O.M., 2013. Location, location, location: it's all in the timing for replication origins. *Genes & development*, 27(2), pp.117–28.

Aparicio, O.M., Stout, a M. & Bell, S.P., 1999. Differential assembly of Cdc45p and DNA polymerases at early and late origins of DNA replication. *Proceedings of the National Academy of Sciences of the United States of America*, 96(16), pp.9130–5.

Aparicio, O.M., Weinstein, D.M. & Bell, S.P., 1997. Components and dynamics of DNA replication complexes in S. cerevisiae: redistribution of MCM proteins and Cdc45p during S phase. *Cell*, 91(1), pp.59–69.

Aparicio, T. et al., 2009. The human GINS complex associates with Cdc45 and MCM and is essential for DNA replication. *Nucleic acids research*, 37(7), pp.2087–95.

Araki, H., 2010. Regulatory mechanism of the initiation step of DNA replication by CDK in budding yeast. *Biochimica et biophysica acta*, 1804(3), pp.520–3.

Ares, M., Grate, L. & Pauling, M.H., 1999. A handful of intron-containing genes produces the lion's share of yeast mRNA. *RNA (New York, N.Y.)*, 5(9), pp.1138–9.

Ashkenazy, H. et al., 2010. ConSurf 2010: calculating evolutionary conservation in sequence and structure of proteins and nucleic acids. *Nucleic acids research*, 38(Web Server issue), pp.W529–33.

Aucher, W. et al., 2010. A strategy for interaction site prediction between phospho-binding modules and their partners identified from proteomic data. *Molecular & cellular proteomics : MCP*, 9(12), pp.2745–59.

Ayyagari, R. et al., 2003. Okazaki fragment maturation in yeast. I. Distribution of functions between FEN1 AND DNA2. *The Journal of biological chemistry*, 278(3), pp.1618–25.

Baker, S.P. et al., 2010. Histone H3 Thr 45 phosphorylation is a replication-associated post-translational modification in S. cerevisiae. *Nature cell biology*, 12(3), pp.294–8.

Barnett, J.A. & Robinow, C.F., 2002a. A history of research on yeasts 4: cytology part I, 1890-1950. *Yeast (Chichester, England)*, 19(2), pp.151–82.

Barnett, J.A. & Robinow, C.F., 2002b. A history of research on yeasts 4: cytology part II, 1950-1990. *Yeast (Chichester, England)*, 19(9), pp.745–72.

Baryshnikova, A. et al., 2010. *Synthetic genetic array (SGA) analysis in Saccharomyces cerevisiae and Schizosaccharomyces pombe.* 2nd ed., Elsevier Inc.

Bell, S. & Dutta, A., 2002. DNA replication in eukaryotic cells. *Annual review of biochemistry*, 71, pp.333–374.

Bell, S.P. & Dutta, A., 2002. DNA replication in eukaryotic cells. *Annual review of biochemistry*, 71, pp.333–74.

Bell, S.P. & Stillman, B., 1992. ATP-dependent recognition of eukaryotic origins of DNA replication by a multiprotein complex. *Nature*, 357(6374), pp.128–34.

Bertoli, C., Skotheim, J.M. & de Bruin, R.A.M., 2013. Control of cell cycle transcription during G1 and S phases. *Nature reviews. Molecular cell biology*, 14(8), pp.518–28.

Bjergbaek, L. et al., 2005. Mechanistically distinct roles for Sgs1p in checkpoint activation and replication fork maintenance. *The EMBO journal*, 24(2), pp.405–17.

Bloom, J. & Cross, F.R., 2007. Multiple levels of cyclin specificity in cell-cycle control. *Nature reviews. Molecular cell biology*, 8(2), pp.149–60.

Bonte, D. et al., 2008. Cdc7-Dbf4 kinase overexpression in multiple cancers and tumor cell lines is correlated with p53 inactivation. *Neoplasia (New York, N.Y.)*, 10(9), pp.920–31.

Bosl, W.J. & Li, R., 2005. Mitotic-exit control as an evolved complex system. *Cell*, 121(3), pp.325–33.

Botstein, D. & Fink, G.R., 2011. Yeast: an experimental organism for 21st Century biology. *Genetics*, 189(3), pp.695–704.

Botstein, D. & Fink, G.R., 1988. Yeast: an experimental organism for modern biology. *Science (New York, N.Y.)*, 240(4858), pp.1439–43.

Bousset, K. & Diffley, J.F., 1998. The Cdc7 protein kinase is required for origin firing during S phase. *Genes & development*, 12(4), pp.480–90.

Bowers, J.L. et al., 2004. ATP hydrolysis by ORC catalyzes reiterative Mcm2-7 assembly at a defined origin of replication. *Molecular cell*, 16(6), pp.967–78.

Branzei, D. & Foiani, M., 2010. Maintaining genome stability at the replication fork. *Nature reviews. Molecular cell biology*, 11(3), pp.208–19.

Branzei, D. & Foiani, M., 2009. The checkpoint response to replication stress. *DNA repair*, 8(9), pp.1038–1046.

Branzei, D. & Foiani, M., 2005. The DNA damage response during DNA replication. *Current opinion in cell biology*, 17(6), pp.568–75.

Branzei, D. & Foiani, M., 2006. The Rad53 signal transduction pathway: Replication fork stabilization, DNA repair, and adaptation. *Experimental cell research*, 312(14), pp.2654–9.

Brayer, K.J. & Segal, D.J., 2008. Keep your fingers off my DNA: protein-protein interactions mediated by C2H2 zinc finger domains. *Cell biochemistry and biophysics*, 50(3), pp.111–31.

Breslow, D.K. et al., 2008. A comprehensive strategy enabling high-resolution functional analysis of the yeast genome. *Nature methods*, 5(8), pp.711–8.

Brewer, B.J. & Fangman, W.L., 1987. The localization of replication origins on ARS plasmids in S. cerevisiae. *Cell*, 51(3), pp.463–471.

Burgers, P.M., 1991. Saccharomyces cerevisiae replication factor C. II. Formation and activity of complexes with the proliferating cell nuclear antigen and with DNA

polymerases delta and epsilon. *The Journal of biological chemistry*, 266(33), pp.22698–706.

Burgers, P.M.J., 2009. Polymerase dynamics at the eukaryotic DNA replication fork. *The Journal of biological chemistry*, 284(7), pp.4041–5.

Burgers, P.M.J., 1998. Structure and Processivity of Two Forms of Saccharomyces cerevisiae DNA Polymerase delta. *Journal of Biological Chemistry*, 273(31), pp.19756–19762.

Burke, D., Dawson, D. & Stearns, T., 2000. *Methods in Yeast Genetics: A Cold Spring Harbor Laboratory Course Manual*, CSHL Press.

Burke, T.W. et al., 2001. Replication factors MCM2 and ORC1 interact with the histone acetyltransferase HBO1. *The Journal of biological chemistry*, 276(18), pp.15397–408.

Byun, T.S. et al., 2005. Functional uncoupling of MCM helicase and DNA polymerase activities activates the ATR-dependent checkpoint. *Genes & development*, 19(9), pp.1040–52.

Calzada, A. et al., 2005. Molecular anatomy and regulation of a stable replisome at a paused eukaryotic DNA replication fork. *Genes & development*, 19(16), pp.1905–19.

Campbell, S.J., Edwards, R. a & Glover, J.N.M., 2010. Comparison of the structures and peptide binding specificities of the BRCT domains of MDC1 and BRCA1. *Structure (London, England : 1993)*, 18(2), pp.167–76.

Carr, A.M., 2002. DNA structure dependent checkpoints as regulators of DNA repair. *DNA repair*, 1(12), pp.983–994.

Cavalieri, D. et al., 2003. Evidence for S. cerevisiae fermentation in ancient wine. *Journal of molecular evolution*, 57 Suppl 1, pp.S226–32.

Chabes, A. et al., 2003. Survival of DNA damage in yeast directly depends on increased dNTP levels allowed by relaxed feedback inhibition of ribonucleotide reductase. *Cell*, 112(3), pp.391–401.

Chapman, J.W. & Johnston, L.H., 1989. The yeast gene, DBF4, essential for entry into S phase is cell cycle regulated. *Experimental cell research*, 180(2), pp.419–28.

Chen, S. & Bell, S.P., 2011. CDK prevents Mcm2-7 helicase loading by inhibiting Cdt1 interaction with Orc6. *Genes & development*, 25(4), pp.363–72.

Chen, S., de Vries, M. a & Bell, S.P., 2007. Orc6 is required for dynamic recruitment of Cdt1 during repeated Mcm2-7 loading. *Genes & development*, 21(22), pp.2897–907.

Chen, Y.-C. et al., 2013. DNA replication checkpoint signaling depends on a Rad53-Dbf4 N-terminal interaction in Saccharomyces cerevisiae. *Genetics*, 194(2), pp.389–401.

Chen, Y.-C. & Weinreich, M., 2010. Dbf4 regulates the Cdc5 Polo-like kinase through a distinct non-canonical binding interaction. *The Journal of biological chemistry*, 285(53), pp.41244–54.

Cheng, A.N. et al., 2013. Increased Cdc7 expression is a marker of oral squamous cell carcinoma and overexpression of Cdc7 contributes to the resistance to DNA-damaging agents. *Cancer letters*, 337(2), pp.218–25.

Cheng, Collyer & Hardy, 1999. Cell cycle regulation of DNA replication initiator factor Dbf4p. *Molecular and cellular biology*, 19(6), pp.4270–4278.

Cimprich, K. a & Cortez, D., 2008. ATR: an essential regulator of genome integrity. *Nature reviews. Molecular cell biology*, 9(8), pp.616–27.

Clémenson, C. & Marsolier-Kergoat, M.-C., 2009. DNA damage checkpoint inactivation: adaptation and recovery. *DNA repair*, 8(9), pp.1101–9.

Cobb, J. a et al., 2003. DNA polymerase stabilization at stalled replication forks requires Mec1 and the RecQ helicase Sgs1. *The EMBO journal*, 22(16), pp.4325–36.

Cohen-Fix, O. & Koshland, D., 1999. Pds1p of budding yeast has dual roles: inhibition of anaphase initiation and regulation of mitotic exit. *Genes & development*, 13(15), pp.1950–1959.

Collins, K.L. & Kelly, T.J., 1991. Effects of T antigen and replication protein A on the initiation of DNA synthesis by DNA polymerase alpha-primase. *Molecular and cellular biology*, 11(4), pp.2108–15.

Cortez, D., 2005. Unwind and slow down: checkpoint activation by helicase and polymerase uncoupling. *Genes & development*, 19(9), pp.1007–12.

Cotta-Ramusino, C. et al., 2005. Exo1 processes stalled replication forks and counteracts fork reversal in checkpoint-defective cells. *Molecular cell*, 17(1), pp.153–9.

Culotti, J. & Hartwell, L.H., 1971. Genetic control of the cell division cycle in yeast. 3. Seven genes controlling nuclear division. *Experimental cell research*, 67(2), pp.389–401.

Dahmann, C., Diffley, J.F. & Nasmyth, K.A., 1995. S-phase-promoting cyclin-dependent kinases prevent re-replication by inhibiting the transition of replication origins to a pre-replicative state. *Current biology*, 5(11), pp.1257–69.

Day, T. a et al., 2010. Phosphorylated Rad18 directs DNA polymerase η to sites of stalled replication. *The Journal of cell biology*, 191(5), pp.953–66.

Delaglio, F. et al., 1995. NMRPipe: a multidimensional spectral processing system based on UNIX pipes. *Journal of biomolecular NMR*, 6(3), pp.277–93.

Desany, B. a. et al., 1998. Recovery from DNA replicational stress is the essential function of the S-phase checkpoint pathway. *Genes & development*, 12(18), pp.2956–70.

Detweiler, C.S. & Li, J.J., 1998. Ectopic induction of Clb2 in early G1 phase is sufficient to block prereplicative complex formation in Saccharomyces cerevisiae. *Proceedings of the National Academy of Sciences of the United States of America*, 95(5), pp.2384–9.

Van Deursen, F. et al., 2012. Mcm10 associates with the loaded DNA helicase at replication origins and defines a novel step in its activation. *The EMBO journal*, 31(9), pp.2195–206.

Díaz-Moreno, I. et al., 2005. NMR analysis of the transient complex between membrane photosystem I and soluble cytochrome c6. *The Journal of biological chemistry*, 280(9), pp.7925–31.

Diffley, J.F.X., 2010. The many faces of redundancy in DNA replication control. *Cold Spring Harbor symposia on quantitative biology*, 75, pp.135–42.

Diffley, J.F.X. & Labib, K., 2002. The chromosome replication cycle. *Journal of cell science*, 115(Pt 5), pp.869–72.

Dolan, W.P. et al., 2010. Fission yeast Hsk1 (Cdc7) kinase is required after replication initiation for induced mutagenesis and proper response to DNA alkylation damage. *Genetics*, 185(1), pp.39–53.

Dolinski, K. & Botstein, D., 2007. Orthology and functional conservation in eukaryotes. *Annual review of genetics*, 41, pp.465–507.

Dowell, S.J., Romanowski, P. & Diffley, J.F., 1994. Interaction of Dbf4, the Cdc7 protein kinase regulatory subunit, with yeast replication origins in vivo. *Science (New York, N.Y.)*, 265(5176), pp.1243–6.

Downs, J. a et al., 2004. Binding of chromatin-modifying activities to phosphorylated histone H2A at DNA damage sites. *Molecular cell*, 16(6), pp.979–90.

Drury, L.S., Perkins, G. & Diffley, J.F., 2000. The cyclin-dependent kinase Cdc28p regulates distinct modes of Cdc6p proteolysis during the budding yeast cell cycle. *Current biology*, 10(5), pp.231–40.

Dua, R. et al., 2002. In vivo reconstitution of Saccharomyces cerevisiae DNA polymerase epsilon in insect cells. Purification and characterization. *The Journal of biological chemistry*, 277(10), pp.7889–96.

Duch, A. et al., 2011. A Dbf4 mutant contributes to bypassing the Rad53-mediated block of origins of replication in response to genotoxic stress. *The Journal of biological chemistry*, 286(4), pp.2486–91.

Duncker, B. & Brown, G.W., 2003. Cdc7 kinases (DDKs) and checkpoint responses: lessons from two yeasts. *Mutation Research*, 532(1-2), pp.21–27.

Duncker, B.P. et al., 2002. An N-terminal domain of Dbf4p mediates interaction with both origin recognition complex (ORC) and Rad53p and can deregulate late origin firing. *Proceedings of the National Academy of Sciences of the United States of America*, 99(25), pp.16087–92.

Duncker, B.P. et al., 1999. Cyclin B-cdk1 kinase stimulates ORC- and Cdc6-independent steps of semiconservative plasmid replication in yeast nuclear extracts. *Molecular and cellular biology*, 19(2), pp.1226–1241.

Durocher, D. et al., 1999. The FHA domain is a modular phosphopeptide recognition motif. *Molecular cell*, 4(3), pp.387–94.

Durocher, D. et al., 2000. The molecular basis of FHA domain:phosphopeptide binding specificity and implications for phospho-dependent signaling mechanisms. *Molecular cell*, 6(5), pp.1169–82.

Durocher, D. & Jackson, S.P., 2002. The FHA domain. *FEBS letters*, 513(1), pp.58–66.

Elledge, S.J. & Davis, R.W., 1990. Two genes differentially regulated in the cell cycle and by DNA-damaging agents encode alternative regulatory subunits of ribonucleotide reductase. *Genes & Development*, 4(5), pp.740–751.

Emsley, P. & Cowtan, K., 2004. Coot: model-building tools for molecular graphics. *Acta crystallographica. Section D, Biological crystallography*, 60(Pt 12 Pt 1), pp.2126–32.

Evrin, C. et al., 2009. A double-hexameric MCM2-7 complex is loaded onto origin DNA during licensing of eukaryotic DNA replication. *Proceedings of the National Academy of Sciences of the United States of America*, 106(48), pp.20240–5.

Farrow, N. a et al., 1994. Backbone dynamics of a free and phosphopeptide-complexed Src homology 2 domain studied by 15N NMR relaxation. *Biochemistry*, 33(19), pp.5984–6003.

Feng, W. et al., 2006. Genomic mapping of single-stranded DNA in hydroxyurea-challenged yeasts identifies origins of replication. *Nature cell biology*, 8(2), pp.148–55.

Fernández-Cid, A. et al., 2013. An ORC/Cdc6/MCM2-7 complex is formed in a multistep reaction to serve as a platform for MCM double-hexamer assembly. *Molecular cell*, 50(4), pp.577–88.

Ferreira, H. et al., 2007. Histone tails and the H3 alphaN helix regulate nucleosome mobility and stability. *Molecular and cellular biology*, 27(11), pp.4037–48.

Ferreira, M.F. et al., 2000. Dbf4p, an essential S phase-promoting factor, is targeted for degradation by the anaphase-promoting complex. *Molecular and cellular biology*, 20(1), pp.242–8.

Fields, S. & Johnston, M., 2005. Cell biology. Whither model organism research? *Science (New York, N.Y.)*, 307(5717), pp.1885–6.

Fillingham, J., Keogh, M. & Krogan, N.J., 2006. GammaH2AX and its role in DNA double-strand break repair. *Biochemistry and cell biology = Biochimie et biologie cellulaire*, 84(4), pp.568–77.

Fletcher, R.J. et al., 2003. The structure and function of MCM from archaeal M. Thermoautotrophicum. *Nature structural biology*, 10(3), pp.160–7.

Forsburg, S.L. & Nurse, P., 1991. Cell cycle regulation in the yeasts Saccharomyces cerevisiae and Schizosaccharomyces pombe. *Annual review of cell biology*, 7, pp.227–56.

Foury, F., 1997. Human genetic diseases: a cross-talk between man and yeast. *Gene*, 195(1), pp.1–10.

Francis, L.I. et al., 2009. Incorporation into the prereplicative complex activates the Mcm2-7 helicase for Cdc7-Dbf4 phosphorylation. *Genes & development*, 23(5), pp.643–54.

Friedel, A.M., Pike, B.L. & Gasser, S.M., 2009. ATR/Mec1: coordinating fork stability and repair. *Current opinion in cell biology*, 21(2), pp.237–44.

Frigola, J. et al., 2013. ATPase-dependent quality control of DNA replication origin licensing. *Nature*, 495(7441), pp.339–43.

Fry, R.C., Begley, T.J. & Samson, L.D., 2005. Genome-wide responses to DNA-damaging agents. *Annual review of microbiology*, 59, pp.357–77.

Fung, A.D. et al., 2002. A conserved domain of Schizosaccharomyces pombe dfp1(+) is uniquely required for chromosome stability following alkylation damage during S phase. *Molecular and cellular biology*, 22(13), pp.4477–90.

Futcher, A.B., 1988. The 2 micron circle plasmid of Saccharomyces cerevisiae. *Yeast (Chichester, England)*, 4(1), pp.27–40.

Gabrielse, C. et al., 2006. A Dbf4p BRCA1 C-terminal-like domain required for the response to replication fork arrest in budding yeast. *Genetics*, 173(2), pp.541–55.

Gambus, A. et al., 2009. A key role for Ctf4 in coupling the MCM2-7 helicase to DNA polymerase alpha within the eukaryotic replisome. *The EMBO journal*, 28(19), pp.2992–3004.

Gambus, A. et al., 2006. GINS maintains association of Cdc45 with MCM in replisome progression complexes at eukaryotic DNA replication forks. *Nature cell biology*, 8(4), pp.358–66.

Garg, P. & Burgers, P.M.J., 2005. DNA polymerases that propagate the eukaryotic DNA replication fork. *Critical reviews in biochemistry and molecular biology*, 40(2), pp.115–28.

Gasch, A.P. et al., 2001. Genomic expression responses to DNA-damaging agents and the regulatory role of the yeast ATR homolog Mec1p. *Molecular biology of the cell*, 12(10), pp.2987–3003.

Giaever, G. et al., 2002. Functional profiling of the Saccharomyces cerevisiae genome. *Nature*, 418(6896), pp.387–91.

Giaever, G. et al., 1999. Genomic profiling of drug sensitivities via induced haploinsufficiency. *Nature genetics*, 21(3), pp.278–83.

Gilbert, C.S., Green, C.M. & Lowndes, N.F., 2001. Budding yeast Rad9 is an ATP-dependent Rad53 activating machine. *Molecular cell*, 8(1), pp.129–36.

Glover, J.N.M., Williams, R.S. & Lee, M.S., 2004. Interactions between BRCT repeats and phosphoproteins: tangled up in two. *Trends in biochemical sciences*, 29(11), pp.579–85.

Gobbini, E. et al., 2013. Interplays between ATM/Tel1 and ATR/Mec1 in sensing and signaling DNA double-strand breaks. *DNA repair*, 12(10), pp.791–9.

Goffeau, A.A. et al., 1996. Life with 6000 genes. *Science (New York, N.Y.)*, 274(5287), pp.546, 563–7.

Gunasekara, N., Sykes, B. & Hugh, J., 2012. Characterization of a novel weak interaction between MUC1 and Src-SH3 using nuclear magnetic resonance spectroscopy. *Biochemical and biophysical research communications*, 421(4), pp.832–6.

Guo, B. et al., 2005. High levels of Cdc7 and Dbf4 proteins can arrest cell-cycle progression. *European journal of cell biology*, 84(12), pp.927–38.

Hagn, F. et al., 2011. Structural analysis of the interaction between Hsp90 and the tumor suppressor protein p53. *Nature structural & molecular biology*, 18(10), pp.1086–93.

Hamatake, R.K. et al., 1990. Purification and characterization of DNA polymerase II from the yeast Saccharomyces cerevisiae. Identification of the catalytic core and a possible holoenzyme form of the enzyme. *The Journal of biological chemistry*, 265(7), pp.4072–83.

Hardy, C.F. et al., 1997. mcm5/cdc46-bob1 bypasses the requirement for the S phase activator Cdc7p. *Proceedings of the National Academy of Sciences of the United States of America*, 94(7), pp.3151–5.

Hardy, C.F. & Pautz, A., 1996. A novel role for Cdc5p in DNA replication. *Molecular and cellular biology*, 16(12), pp.6775–82.

Harkins, V. et al., 2009. Budding yeast Dbf4 sequences required for Cdc7 kinase activation and identification of a functional relationship between the Dbf4 and Rev1 BRCT domains. *Genetics*, 183(4), pp.1269–82.

Harrison, J.C. & Haber, J.E., 2006. Surviving the breakup: the DNA damage checkpoint. *Annual review of genetics*, 40, pp.209–35.

Hartman, J.L. et al., 2001. Principles for the buffering of genetic variation. *Science (New York, N.Y.)*, 291(5506), pp.1001–4.

Hartwell, L.H., 1974. Saccharomyces cerevisiae cell cycle. *Bacteriological reviews*, 38(2), pp.164–98.

Hasty, J., McMillen, D. & Collins, J.J., 2002. Engineered gene circuits. *Nature*, 420(6912), pp.224–30.

Hegnauer, A.M. et al., 2012. An N-terminal acidic region of Sgs1 interacts with Rpa70 and recruits Rad53 kinase to stalled forks. *The EMBO journal*, 31(18), pp.3768–83.

Heller, R.C. et al., 2011. Eukaryotic origin-dependent DNA replication in vitro reveals sequential action of DDK and S-CDK kinases. *Cell*, 146(1), pp.80–91.

Hendrickson, W. a, Horton, J.R. & LeMaster, D.M., 1990. Selenomethionyl proteins produced for analysis by multiwavelength anomalous diffraction (MAD): a vehicle for direct determination of three-dimensional structure. *The EMBO journal*, 9(5), pp.1665–72.

Herskowitz, I., 1988. Life cycle of the budding yeast Saccharomyces cerevisiae. *Microbiological reviews*, 52(4), pp.536–53.

Hoang, M.L. et al., 2007. Structural changes in Mcm5 protein bypass Cdc7-Dbf4 function and reduce replication origin efficiency in Saccharomyces cerevisiae. *Molecular and cellular biology*, 27(21), pp.7594–602.

Hodgson, B., Calzada, A. & Labib, K., 2007. Mrc1 and Tof1 regulate DNA replication forks in different ways during normal S phase. *Molecular biology of the cell*, 18(10), pp.3894–902.

Homesley, L. et al., 2000. Mcm10 and the MCM2-7 complex interact to initiate DNA synthesis and to release replication factors from origins. *Genes & development*, 14(8), pp.913–26.

Huang, M., Zhou, Z. & Elledge, S.J., 1998. The DNA replication and damage checkpoint pathways induce transcription by inhibition of the Crt1 repressor. *Cell*, 94(5), pp.595–605.

Huertas, P., 2010. DNA resection in eukaryotes: deciding how to fix the break. *Nature structural & molecular biology*, 17(1), pp.11–6.

Hughes, S. et al., 2012. Crystal structure of human CDC7 kinase in complex with its activator DBF4. *Nature structural & molecular biology*, 19(11), pp.1101–7.

Ito, T., 2007. Role of histone modification in chromatin dynamics. *Journal of biochemistry*, 141(5), pp.609–14.

Jackson, A.L. et al., 1993. Cell cycle regulation of the yeast Cdc7 protein kinase by association with the Dbf4 protein. *Molecular and cellular biology*, 13(5), pp.2899–908.

Jelinsky, S. a & Samson, L.D., 1999. Global response of Saccharomyces cerevisiae to an alkylating agent. *Proceedings of the National Academy of Sciences of the United States of America*, 96(4), pp.1486–91.

Jenkinson, E.R. & Chong, J.P.J., 2003. Initiation of archaeal DNA replication. *Biochemical Society transactions*, 31(Pt 3), pp.669–73.

Jones, D.R. et al., 2010. The Dbf4 motif C zinc finger promotes DNA replication and mediates resistance to genotoxic stress. *Cell cycle*, 9(10), pp.2018–2026.

Kamimura, Y. et al., 2001. Sld3, which interacts with Cdc45 (Sld4), functions for chromosomal DNA replication in Saccharomyces cerevisiae. *The EMBO journal*, 20(8), pp.2097–107.

Kanke, M. et al., 2012. Mcm10 plays an essential role in origin DNA unwinding after loading of the CMG components. *The EMBO journal*, 31(9), pp.2182–94.

Katis, V.L. et al., 2010. Rec8 phosphorylation by casein kinase 1 and Cdc7-Dbf4 kinase regulates cohesin cleavage by separase during meiosis. *Developmental cell*, 18(3), pp.397–409.

Katou, Y. et al., 2003. S-phase checkpoint proteins Tof1 and Mrc1 form a stable replication-pausing complex. *Nature*, 424(6952), pp.1078–1083.

Kawasaki, Y. et al., 2006. Reconstitution of Saccharomyces cerevisiae prereplicative complex assembly in vitro. *Genes to cells : devoted to molecular & cellular mechanisms*, 11(7), pp.745–56.

Kelly, D.E., Lamb, D.C. & Kelly, S.L., 2001. Genome-wide generation of yeast gene deletion strains. *Comparative and functional genomics*, 2(4), pp.236–42.

Kihara, M. et al., 2000. Characterization of the yeast Cdc7p/Dbf4p complex purified from insect cells. Its protein kinase activity is regulated by Rad53p. *The Journal of biological chemistry*, 275(45), pp.35051–62.

Kim, J.M., Yamada, M. & Masai, H., 2003. Functions of mammalian Cdc7 kinase in initiation/monitoring of DNA replication and development. *Mutation research*, 532(1-2), pp.29–40.

Kitada, K. et al., 1992. Temperature-sensitive cdc7 mutations of Saccharomyces cerevisiae are suppressed by the DBF4 gene, which is required for the G1/S cell cycle transition. *Genetics*, 131(1), pp.21–9.

Kobayashi, M. et al., 2010. Structure of the DNA-bound BRCA1 C-terminal region from human replication factor C p140 and model of the protein-DNA complex. *The Journal of biological chemistry*, 285(13), pp.10087–97.

Koltun, E.S. et al., 2012. Discovery of XL413, a potent and selective CDC7 inhibitor. *Bioorganic & medicinal chemistry letters*, 22(11), pp.3727–31.

Kulkarni, A. a et al., 2009. Cdc7 kinase is a predictor of survival and a novel therapeutic target in epithelial ovarian carcinoma. *Clinical cancer research : an official journal of the American Association for Cancer Research*, 15(7), pp.2417–25.

Kulkarni, A. a et al., 2007. DNA replication licensing factors and aurora kinases are linked to aneuploidy and clinical outcome in epithelial ovarian carcinoma. *Clinical cancer research : an official journal of the American Association for Cancer Research*, 13(20), pp.6153–61.

De la Torre Ruiz, M.A. & Lowndes, N.F., 2000. DUN1 defines one branch downstream of RAD53 for transcription and DNA damage repair in Saccharomyces cerevisiae. *FEBS letters*, 485(2-3), pp.205–6.

Labib, K., 2010. How do Cdc7 and cyclin-dependent kinases trigger the initiation of chromosome replication in eukaryotic cells? *Genes & development*, 24(12), pp.1208–19.

Labib, K. & Gambus, A., 2007. A key role for the GINS complex at DNA replication forks. *Trends in cell biology*, 17(6), pp.271–8.

Labib, K. & Hodgson, B., 2007. Replication fork barriers: pausing for a break or stalling for time? *EMBO reports*, 8(4), pp.346–53.

Labib, K. & De Piccoli, G., 2011. Surviving chromosome replication: the many roles of the S-phase checkpoint pathway. *Philosophical transactions of the Royal Society of London. Series B, Biological sciences*, 366(1584), pp.3554–61.

Labib, K., Tercero, J.A. & Diffley, J.F., 2000. Uninterrupted MCM2-7 function required for DNA replication fork progression. *Science (New York, N.Y.)*, 288(5471), pp.1643–7.

Lambert, S. & Carr, A.M., 2013. Impediments to replication fork movement: stabilisation, reactivation and genome instability. *Chromosoma*, 122(1-2), pp.33–45.

Lambert, S., Froget, B. & Carr, A.M., 2007. Arrested replication fork processing: interplay between checkpoints and recombination. *DNA repair*, 6(7), pp.1042–61.

Landry, C.R. et al., 2006. Ecological and evolutionary genomics of Saccharomyces cerevisiae. *Molecular ecology*, 15(3), pp.575–91.

Le, A.-H., Mastro, T.L. & Forsburg, S.L., 2013. The C-terminus of S. pombe DDK subunit Dfp1 is required for meiosis-specific transcription and cohesin cleavage. *Biology open*, 2(7), pp.728–38.

Lee, A.Y.-L. et al., 2012. Dbf4 is direct downstream target of ataxia telangiectasia mutated (ATM) and ataxia telangiectasia and Rad3-related (ATR) protein to regulate intra-S-phase checkpoint. *The Journal of biological chemistry*, 287(4), pp.2531–43.

Lee, H. et al., 2008. Diphosphothreonine-specific interaction between an SQ/TQ cluster and an FHA domain in the Rad53-Dun1 kinase cascade. *Molecular cell*, 30(6), pp.767–78.

Lee, S., Duong, J.K. & Stern, D.F., 2004. A Ddc2-Rad53 fusion protein can bypass the requirements for RAD9 and MRC1 in Rad53 activation. *Molecular biology of the cell*, 15(12), pp.5443–55.

Lei, M. et al., 1997. Mcm2 is a target of regulation by Cdc7-Dbf4 during the initiation of DNA synthesis. *Genes & Development*, 11(24), pp.3365–3374.

Leung, C.C.Y. & Glover, J.N.M., 2011. BRCT domains: easy as one, two, three. *Cell cycle (Georgetown, Tex.)*, 10(15), pp.2461–70.

Li, J. et al., 2002. Structural and functional versatility of the FHA domain in DNA-damage signaling by the tumor suppressor kinase Chk2. *Molecular cell*, 9(5), pp.1045–54.

Li, X. et al., 2012. Structure of C-terminal tandem BRCT repeats of Rtt107 protein reveals critical role in interaction with phosphorylated histone H2A during DNA damage repair. *The Journal of biological chemistry*, 287(12), pp.9137–46.

Li, X. & Heyer, W.-D., 2008. Homologous recombination in DNA repair and DNA damage tolerance. *Cell research*, 18(1), pp.99–113.

Liang, F. & Wang, Y., 2007. DNA damage checkpoints inhibit mitotic exit by two different mechanisms. *Molecular and cellular biology*, 27(14), pp.5067–78.

Lloyd, J. et al., 2009. A supramodular FHA/BRCT-repeat architecture mediates Nbs1 adaptor function in response to DNA damage. *Cell*, 139(1), pp.100–11.

Longtine, M.S. et al., 1998. Additional modules for versatile and economical PCR-based gene deletion and modification in Saccharomyces cerevisiae. *Yeast (Chichester, England)*, 14(10), pp.953–961.

Lopes, M. et al., 2001. The DNA replication checkpoint response stabilizes stalled replication forks. *Nature*, 412(6846), pp.557–61.

Lopez-Mosqueda, J. et al., 2010. Damage-induced phosphorylation of Sld3 is important to block late origin firing. *Nature*, 467(7314), pp.479–83.

Lucca, C. et al., 2004. Checkpoint-mediated control of replisome-fork association and signalling in response to replication pausing. *Oncogene*, 23(6), pp.1206–13.

Lum, P.Y. et al., 2004. Discovering modes of action for therapeutic compounds using a genome-wide screen of yeast heterozygotes. *Cell*, 116(1), pp.121–37.

Ma, J.-L. et al., 2006. Activation of the checkpoint kinase Rad53 by the phosphatidyl inositol kinase-like kinase Mec1. *The Journal of biological chemistry*, 281(7), pp.3954–63.

MacDougall, C. a et al., 2007. The structural determinants of checkpoint activation. *Genes & development*, 21(8), pp.898–903.

Majka, J., Binz, S.K., et al., 2006. Replication protein A directs loading of the DNA damage checkpoint clamp to 5'-DNA junctions. *The Journal of biological chemistry*, 281(38), pp.27855–61.

Majka, J., Niedziela-Majka, A. & Burgers, P.M.J., 2006. The checkpoint clamp activates Mec1 kinase during initiation of the DNA damage checkpoint. *Molecular cell*, 24(6), pp.891–901.

Mantiero, D. et al., 2011. Limiting replication initiation factors execute the temporal programme of origin firing in budding yeast. *The EMBO journal*, 30(23), pp.4805–14.

Martín-García, R. et al., 2011. The FN3 and BRCT motifs in the exomer component Chs5p define a conserved module that is necessary and sufficient for its function. *Cellular and molecular life sciences : CMLS*, 68(17), pp.2907–17.

Masai, H. et al., 2006. Phosphorylation of MCM4 by Cdc7 kinase facilitates its interaction with Cdc45 on the chromatin. *The Journal of biological chemistry*, 281(51), pp.39249–61.

Masai, H. & Arai, K., 2000. Dbf4 motifs: conserved motifs in activation subunits for Cdc7 kinases essential for S-phase. *Biochemical and biophysical research communications*, 275(1), pp.228–32.

Masumoto, H. et al., 2005. A role for cell-cycle-regulated histone H3 lysine 56 acetylation in the DNA damage response. *Nature*, 436(7048), pp.294–8.

Matos, J. et al., 2008. Dbf4-dependent CDC7 kinase links DNA replication to the segregation of homologous chromosomes in meiosis I. *Cell*, 135(4), pp.662–78.

Matsuo, H. et al., 1999. Identification by NMR Spectroscopy of Residues at Contact Surfaces in Large , Slowly Exchanging Macromolecular Complexes. *Journal of the American Chemical Society*, 121(42), pp.9903–9904.

Matthews, L. a & Guarné, A., 2013. Dbf4: The whole is greater than the sum of its parts. *Cell cycle (Georgetown, Tex.)*, 12(8), pp.1–9.

Matthews, L.A. et al., 2009. Crystallization and preliminary X-ray diffraction analysis of motif N from Saccharomyces cerevisiae Dbf4. *Acta crystallographica. Section F, Structural biology and crystallization communications*, 65(Pt 9), pp.890–4.

Matthews, L.A. et al., 2012. Saccharomyces cerevisiae Dbf4 has unique fold necessary for interaction with Rad53 kinase. *The Journal of biological chemistry*, 287(4), pp.2378–87.

McCoy, A.J. et al., 2007. Phaser crystallographic software. *Journal of applied crystallography*, 40(Pt 4), pp.658–674.

McGovern, P.E. et al., 2004. Fermented beverages of pre- and proto-historic China. *Proceedings of the National Academy of Sciences of the United States of America*, 101(51), pp.17593–8.

Melendy, T. & Stillman, B., 1993. An interaction between replication protein A and SV40 T antigen appears essential for primosome assembly during SV40 DNA replication. *The Journal of biological chemistry*, 268(5), pp.3389–95.

Merchant, A.M. et al., 1997. A lesion in the DNA replication initiation factor Mcm10 induces pausing of elongation forks through chromosomal replication origins in Saccharomyces cerevisiae. *Molecular and cellular biology*, 17(6), pp.3261–71.

Miller, C.T. et al., 2009. Cdc7p-Dbf4p regulates mitotic exit by inhibiting Polo kinase. *PLoS genetics*, 5(5), p.e1000498.

Mimitou, E.P. & Symington, L.S., 2009. DNA end resection: many nucleases make light work. *DNA repair*, 8(9), pp.983–95.

Mohammad, D.H. & Yaffe, M.B., 2009. 14-3-3 proteins, FHA domains and BRCT domains in the DNA damage response. *DNA repair*, 8(9), pp.1009–1017.

Moldovan, G.-L., Pfander, B. & Jentsch, S., 2007. PCNA, the maestro of the replication fork. *Cell*, 129(4), pp.665–79.

Montagnoli, A. et al., 2008. A Cdc7 kinase inhibitor restricts initiation of DNA replication and has antitumor activity. *Nature chemical biology*, 4(6), pp.357–65.

Montagnoli, A. et al., 2004. Cdc7 inhibition reveals a p53-dependent replication checkpoint that is defective in cancer cells. *Cancer research*, 64(19), pp.7110–6.

Montagnoli, A. et al., 2006. Identification of Mcm2 phosphorylation sites by S-phase-regulating kinases. *The Journal of biological chemistry*, 281(15), pp.10281–90.

Montagnoli, A., Moll, J. & Colotta, F., 2010. Targeting cell division cycle 7 kinase: a new approach for cancer therapy. *Clinical cancer research : an official journal of the American Association for Cancer Research*, 16(18), pp.4503–8.

Mordes, D.A., Nam, E.A. & Cortez, D., 2008. Dpb11 activates the Mec1-Ddc2 complex. *Proceedings of the National Academy of Sciences of the United States of America*, 105(48), pp.18730–4.

Mortimer, R.K. & Johnston, J.R., 1986. Genealogy of principal strains of the yeast genetic stock center. *Genetics*, 113(1), pp.35–43.

Moyer, S.E., Lewis, P.W. & Botchan, M.R., 2006. a candidate for the eukaryotic DNA replication fork helicase.

Muramatsu, S. et al., 2010. CDK-dependent complex formation between replication proteins Dpb11, Sld2, Pol (epsilon}, and GINS in budding yeast. *Genes & development*, 24(6), pp.602–12.

Nambiar, S. et al., 2007. Identification and functional characterization of ASK/Dbf4, a novel cell survival gene in cutaneous melanoma with prognostic relevance. *Carcinogenesis*, 28(12), pp.2501–10.

Nasmyth, K., 1996. At the heart of the budding yeast cell cycle. *Trends in Genetics*, 10(October), pp.405–412.

Nasmyth, K., 2005. How do so few control so many? *Cell*, 120(6), pp.739–46.

Natoni, A. et al., 2013. Characterization of a Dual CDC7/CDK9 Inhibitor in Multiple Myeloma Cellular Models. *Cancers*, 5(3), pp.901–18.

Navadgi-Patil, V.M. & Burgers, P.M., 2011. Cell-cycle-specific activators of the Mec1/ATR checkpoint kinase. *Biochemical Society transactions*, 39(2), pp.600–5.

Navadgi-Patil, V.M. & Burgers, P.M., 2009. The unstructured C-terminal tail of the 9-1-1 clamp subunit Ddc1 activates Mec1/ATR via two distinct mechanisms. *Molecular cell*, 36(5), pp.743–53.

Navadgi-Patil, V.M. & Burgers, P.M., 2008. Yeast DNA replication protein Dpb11 activates the Mec1/ATR checkpoint kinase. *The Journal of biological chemistry*, 283(51), pp.35853–9.

Negrini, S., Gorgoulis, V.G. & Halazonetis, T.D., 2010. Genomic instability--an evolving hallmark of cancer. *Nature reviews. Molecular cell biology*, 11(3), pp.220–8.

Neiman, A.M., 2011. Sporulation in the budding yeast Saccharomyces cerevisiae. *Genetics*, 189(3), pp.737–65.

Nott, T.J. et al., 2009. An intramolecular switch regulates phosphoindependent FHA domain interactions in Mycobacterium tuberculosis. *Science signaling*, 2(63), p.ra12.

Nougarède, R. et al., 2000. Hierarchy of S-phase-promoting factors: yeast Dbf4-Cdc7 kinase requires prior S-phase cyclin-dependent kinase activation. *Molecular and cellular biology*, 20(11), pp.3795–806.

Nurse, P., 1985. Cell cycle control genes in yeast. *Trends in Genetics*, (1), pp.51–55.

Nyberg, K. a et al., 2002. Toward maintaining the genome: DNA damage and replication checkpoints. *Annual review of genetics*, 36, pp.617–56.

Ockey, C.H. & Saffhill, R., 1976. The comparative effects of short-term DNA Inhibition on replicon synthesis in mammalian cells. *Experimental cell research*, 103(2), pp.361–73.

Ogi, H. et al., 2008. The role of the Saccharomyces cerevisiae Cdc7-Dbf4 complex in the replication checkpoint. *Gene*, 414(1-2), pp.32–40.

Ogino, K. et al., 2001. Bipartite binding of a kinase activator activates Cdc7-related kinase essential for S phase. *The Journal of biological chemistry*, 276(33), pp.31376–87.

Osborn, A.J. & Elledge, S.J., 2003. Mrc1 is a replication fork component whose phosphorylation in response to DNA replication stress activates Rad53. *Genes & development*, 17(14), pp.1755–67.

Otwinowski, Z. & Minor, W., 1997. Macromolecular Crystallography Part A. *Methods in enzymology*, 276, pp.307–326.

Paciotti, V. et al., 2001. Characterization of mec1 kinase-deficient mutants and of new hypomorphic mec1 alleles impairing subsets of the DNA damage response pathway. *Molecular and cellular biology*, 21(12), pp.3913–25.

Pasero, P. et al., 1999. A role for the Cdc7 kinase regulatory subunit Dbf4p in the formation of initiation-competent origins of replication. *Genes & development*, 13(16), pp.2159–2176.

Pasero, P. & Schwob, E., 2000. Think global, act local--how to regulate S phase from individual replication origins. *Current opinion in genetics & development*, 10(2), pp.178–86.

Pellicioli, a et al., 1999. Activation of Rad53 kinase in response to DNA damage and its effect in modulating phosphorylation of the lagging strand DNA polymerase. *The EMBO journal*, 18(22), pp.6561–72.

Pessoa-Brandão, L. & Sclafani, R. a, 2004. CDC7/DBF4 functions in the translesion synthesis branch of the RAD6 epistasis group in Saccharomyces cerevisiae. *Genetics*, 167(4), pp.1597–610.

Pfander, B. & Diffley, J.F.X., 2011. Dpb11 coordinates Mec1 kinase activation with cell cycle-regulated Rad9 recruitment. *The EMBO journal*, 30(24), pp.4897–907.

Pike, B.L. et al., 2004. Mdt1, a novel Rad53 FHA1 domain-interacting protein, modulates DNA damage tolerance and G(2)/M cell cycle progression in Saccharomyces cerevisiae. *Molecular and cellular biology*, 24(7), pp.2779–88.

Puddu, F. et al., 2008. Phosphorylation of the budding yeast 9-1-1 complex is required for Dpb11 function in the full activation of the UV-induced DNA damage checkpoint. *Molecular and cellular biology*, 28(15), pp.4782–93.

Raghuraman, M.K. et al., 2001. Replication dynamics of the yeast genome. *Science (New York, N.Y.)*, 294(5540), pp.115–21.

Ralser, Markus et al., 2012. The Saccharomyces cerevisiae W303-K6001 cross-platform genome sequence: insights into ancestry and physiology of a laboratory mutt. *Open biology*, 2(8), p.120093.

Ramer, M.D. et al., 2013. Dbf4 and Cdc7 proteins promote DNA replication through interactions with distinct Mcm2-7 protein subunits. *The Journal of biological chemistry*, 288(21), pp.14926–35.

Randell, J.C.W. et al., 2006. Sequential ATP hydrolysis by Cdc6 and ORC directs loading of the Mcm2-7 helicase. *Molecular cell*, 21(1), pp.29–39.

Rao, H. & Stillman, B., 1995. The origin recognition complex interacts with a bipartite DNA binding site within yeast replicators. *Proceedings of the National Academy of Sciences of the United States of America*, 92(6), pp.2224–8.

Remus, D. et al., 2009. Concerted loading of Mcm2-7 double hexamers around DNA during DNA replication origin licensing. *Cell*, 139(4), pp.719–30.

Ricke, R.M. & Bielinsky, A.-K., 2004. Mcm10 regulates the stability and chromatin association of DNA polymerase-alpha. *Molecular cell*, 16(2), pp.173–85.

Riera, A., Fernández-Cid, A. & Speck, C., 2013. The ORC/Cdc6/MCM2–7 complex, a new power player for regulated helicase loading. *Cell cycle (Georgetown, Tex.)*, 12(14), pp.2155–6.

Rodriguez-Acebes, S. et al., 2010. Targeting DNA replication before it starts: Cdc7 as a therapeutic target in p53-mutant breast cancers. *The American journal of pathology*, 177(4), pp.2034–45.

Rupnik, A., Lowndes, N.F. & Grenon, M., 2010. MRN and the race to the break. *Chromosoma*, 119(2), pp.115–35.

Sancar, A. et al., 2004. Molecular mechanisms of mammalian DNA repair and the DNA damage checkpoints. *Annual review of biochemistry*, 73, pp.39–85.

Sanchez, Y. et al., 1999. Control of the DNA damage checkpoint by chk1 and rad53 protein kinases through distinct mechanisms. *Science (New York, N.Y.)*, 286(5442), pp.1166–71.

Santocanale, C. & Diffley, J.F., 1998. A Mec1- and Rad53-dependent checkpoint controls late-firing origins of DNA replication. *Nature*, 395(6702), pp.615–8.

Santocanale, C., Sharma, K. & Diffley, J.F., 1999. Activation of dormant origins of DNA replication in budding yeast. *Genes & development*, 13(18), pp.2360–4.

Sasanuma, H. et al., 2008. Cdc7-dependent phosphorylation of Mer2 facilitates initiation of yeast meiotic recombination. *Genes & development*, 22(3), pp.398–410.

Sato, N. et al., 2003. Cell cycle regulation of chromatin binding and nuclear localization of human Cdc7-ASK kinase complex. *Genes to cells : devoted to molecular & cellular mechanisms*, 8(5), pp.451–63.

Schleker, T., Nagai, S. & Gasser, S.M., 2009. Posttranslational modifications of repair factors and histones in the cellular response to stalled replication forks. *DNA repair*, 8(9), pp.1089–100.

Schvartzman, J.B. et al., 2013. The benefit of DNA supercoiling during replication. *Biochemical Society transactions*, 41(2), pp.646–51.

Schwartz, M.F. et al., 2002. Rad9 phosphorylation sites couple Rad53 to the Saccharomyces cerevisiae DNA damage checkpoint. *Molecular cell*, 9(5), pp.1055–65.

Sclafani, R.A. & Holzen, T.M., 2007. Cell cycle regulation of DNA replication. *Annual review of genetics*, 41, pp.237–80.

Segurado, M. & Diffley, J.F.X., 2008. Separate roles for the DNA damage checkpoint protein kinases in stabilizing DNA replication forks. *Genes & development*, 22(13), pp.1816–27.

Selvaratnam, R. et al., 2012. The auto-inhibitory role of the EPAC hinge helix as mapped by NMR. *PloS one*, 7(11), p.e48707.

Semple, J.W. & Duncker, B.P., 2004. ORC-associated replication factors as biomarkers for cancer. *Biotechnology advances*, 22(8), pp.621–31.

Sherman, F., 2002. Getting started with yeast. *Methods in enzymology*, 350(2002), pp.3–41.

Sheu, Y. & Stillman, B., 2006. Cdc7-Dbf4 phosphorylates MCM proteins via a docking site-mediated mechanism to promote S phase progression. *Molecular cell*, 24(1), pp.101–13.

Sheu, Y. & Stillman, B., 2010. The Dbf4-Cdc7 kinase promotes S phase by alleviating an inhibitory activity in Mcm4. *Nature*, 463(7277), pp.113–7.

Shima, N. et al., 2007. A viable allele of Mcm4 causes chromosome instability and mammary adenocarcinomas in mice. *Nature genetics*, 39(1), pp.93–8.

Shirahige, K. et al., 1998. Regulation of DNA-replication origins during cell-cycle progression. *Nature*, 395(6702), pp.618–21.

Sidorova, J.M. & Breeden, L.L., 1997. Rad53-dependent phosphorylation of Swi6 and down-regulation of CLN1 and CLN2 transcription occur in response to DNA damage in Saccharomyces cerevisiae. *Genes & Development*, 11(22), pp.3032–3045.

Sikorski, R.S. & Hieter, P., 1989. A system of shuttle vectors and yeast host strains designed for efficient manipulation of DNA in Saccharomyces cerevisiae. *Genetics*, 122(1), pp.19–27.

Snaith, H.A., Brown, G.W. & Forsburg, S.L., 2000. Schizosaccharomyces pombe Hsk1p is a potential cds1p target required for genome integrity. *Molecular and cellular biology*, 20(21), pp.7922–32.

Sogo, J.M., Lopes, M. & Foiani, M., 2002. Fork reversal and ssDNA accumulation at stalled replication forks owing to checkpoint defects. *Science (New York, N.Y.)*, 297(5581), pp.599–602.

Solomon, N. a et al., 1992. Genetic and molecular analysis of DNA43 and DNA52: two new cell-cycle genes in Saccharomyces cerevisiae. *Yeast (Chichester, England)*, 8(4), pp.273–89.

Speck, C. et al., 2005. ATPase-dependent cooperative binding of ORC and Cdc6 to origin DNA. *Nature structural & molecular biology*, 12(11), pp.965–71.

Stead, B.E. et al., 2012. Mcm2 phosphorylation and the response to replicative stress. *BMC genetics*, 13, p.36.

Stead, B.E., Brandl, C.J. & Davey, M.J., 2011. Phosphorylation of Mcm2 modulates Mcm2-7 activity and affects the cell's response to DNA damage. *Nucleic acids research*, 39(16), pp.6998–7008.

Steinmetz, L.M. et al., 2002. Systematic screen for human disease genes in yeast. *Nature genetics*, 31(4), pp.400–4.

Stillman, B., 2005. Origin recognition and the chromosome cycle. *FEBS letters*, 579(4), pp.877–84.

Sun, Z. et al., 1998. Rad53 FHA domain associated with phosphorylated Rad9 in the DNA damage checkpoint. *Science (New York, N.Y.)*, 281(5374), pp.272–4.

Sweeney, F.D. et al., 2005. Saccharomyces cerevisiae Rad9 acts as a Mec1 adaptor to allow Rad53 activation. *Current biology : CB*, 15(15), pp.1364–75.

Swords, R. et al., 2010. Cdc7 kinase – A new target for drug development. *European Journal of Cancer*, 46(1), pp.33–40.

Szyjka, S.J. et al., 2008. Rad53 regulates replication fork restart after DNA damage in Saccharomyces cerevisiae. *Genes & development*, 22(14), pp.1906–20.

Szyjka, S.J., Viggiani, C.J. & Aparicio, O.M., 2005. Mrc1 is required for normal progression of replication forks throughout chromatin in S. cerevisiae. *Molecular cell*, 19(5), pp.691–7.

Tak, Y.-S. et al., 2006. A CDK-catalysed regulatory phosphorylation for formation of the DNA replication complex Sld2-Dpb11. *The EMBO journal*, 25(9), pp.1987–96.

Takayama, Y. et al., 2003. GINS, a novel multiprotein complex required for chromosomal DNA replication in budding yeast. *Genes & development*, 17(9), pp.1153–65.

Takeda, T. et al., 1999. A fission yeast gene, him1(+)/dfp1(+), encoding a regulatory subunit for Hsk1 kinase, plays essential roles in S-phase initiation as well as in S-phase

checkpoint control and recovery from DNA damage. *Molecular and cellular biology*, 19(8), pp.5535–47.

Tam, A.T.Y., Pike, B.L. & Heierhorst, J., 2008. Location-specific functions of the two forkhead-associated domains in Rad53 checkpoint kinase signaling. *Biochemistry*, 47(12), pp.3912–6.

Tanaka, S. et al., 2007. CDK-dependent phosphorylation of Sld2 and Sld3 initiates DNA replication in budding yeast. *Nature*, 445(7125), pp.328–32.

Tanaka, S. et al., 2011. Origin association of Sld3, Sld7, and Cdc45 proteins is a key step for determination of origin-firing timing. *Current biology : CB*, 21(24), pp.2055–63.

Tanaka, S. & Araki, H., 2011. Multiple regulatory mechanisms to inhibit untimely initiation of DNA replication are important for stable genome maintenance. *PLoS genetics*, 7(6), p.e1002136.

Tanaka, S. & Araki, H., 2010. Regulation of the initiation step of DNA replication by cyclin-dependent kinases. *Chromosoma*, 119(6), pp.565–74.

Tanaka, S. & Diffley, J.F.X., 2002. Interdependent nuclear accumulation of budding yeast Cdt1 and Mcm2-7 during G1 phase. *Nature cell biology*, 4(3), pp.198–207.

Tanaka, T., Knapp, D. & Nasmyth, K., 1997. Loading of an Mcm protein onto DNA replication origins is regulated by Cdc6p and CDKs. *Cell*, 90(4), pp.649–60.

Tanaka, T.U., 2008. Bi-orienting chromosomes: acrobatics on the mitotic spindle. *Chromosoma*, 117(6), pp.521–33.

Taylor, J.H., 1977. Increase in DNA replication sites in cells held at the beginning of S phase. *Chromosoma*, 62(4), pp.291–300.

Tercero, J.A. & Diffley, J.F., 2001. Regulation of DNA replication fork progression through damaged DNA by the Mec1/Rad53 checkpoint. *Nature*, 412(6846), pp.553–7.

Tercero, J.A., Longhese, M.P. & Diffley, J.F.X., 2003. A central role for DNA replication forks in checkpoint activation and response. *Molecular cell*, 11(5), pp.1323–36.

Thu, Y.M. & Bielinsky, A.-K., 2013. Enigmatic roles of Mcm10 in DNA replication. *Trends in biochemical sciences*, 38(4), pp.184–94.

Tinker-Kulberg, R.L. & Morgan, D.O., 1999. Pds1 and Esp1 control both anaphase and mitotic exit in normal cells and after DNA damage. *Genes & development*, 13(15), pp.1936–49.

Tong, A.H. et al., 2001. Systematic genetic analysis with ordered arrays of yeast deletion mutants. *Science (New York, N.Y.)*, 294(5550), pp.2364–8.

Tong, Y. et al., 2010. Phosphorylation-independent dual-site binding of the FHA domain of KIF13 mediates phosphoinositide transport via centaurin alpha1. *Proceedings of the National Academy of Sciences of the United States of America*, 107(47), pp.20346–51.

Tourrière, H. et al., 2005. Mrc1 and Tof1 promote replication fork progression and recovery independently of Rad53. *Molecular cell*, 19(5), pp.699–706.

Tsuji, T. et al., 2008. The role of Dbf4/Drf1-dependent kinase Cdc7 in DNA-damage checkpoint control. *Molecular cell*, 32(6), pp.862–9.

Varrin, A.E. et al., 2005. A mutation in Dbf4 motif M impairs interactions with DNA replication factors and confers increased resistance to genotoxic agents. *Molecular and cellular biology*, 25(17), pp.7494–504.

Walker, G.M., 1998. *Yeast Physiology and Biotechnology*, John Wiley & Sons.

Walters, K.J. et al., 2001. Characterizing protein-protein complexes and oligomers by nuclear magnetic resonance spectroscopy. *Methods in enzymology*, 339, pp.238–58.

Wan, L. et al., 2008. Cdc28-Clb5 (CDK-S) and Cdc7-Dbf4 (DDK) collaborate to initiate meiotic recombination in yeast. *Genes & development*, 22(3), pp.386–397.

Watase, G., Takisawa, H. & Kanemaki, M.T., 2012. Mcm10 plays a role in functioning of the eukaryotic replicative DNA helicase, Cdc45-Mcm-GINS. *Current biology : CB*, 22(4), pp.343–9.

Weinert, T. & Hartwell, L., 1988. The RAD9 gene controls the cell cycle response to DNA damage in Saccharomyces cerevisiae. *Science*, 241(4863), pp.317–322.

Weinreich, M. & Stillman, B., 1999. Cdc7p–Dbf4p kinase binds to chromatin during S phase and is regulated by both the APC and the RAD53 checkpoint pathway. *The EMBO journal*, 18(19), pp.5334–5346.

Weiss, E.L., 2012. Mitotic exit and separation of mother and daughter cells. *Genetics*, 192(4), pp.1165–202.

Williams, G.H. & Stoeber, K., 2007. Cell cycle markers in clinical oncology. *Current opinion in cell biology*, 19(6), pp.672–9.

Williams, G.J., Lees-Miller, S.P. & Tainer, J. a, 2010. Mre11-Rad50-Nbs1 conformations and the control of sensing, signaling, and effector responses at DNA double-strand breaks. *DNA repair*, 9(12), pp.1299–306.

Williams, R.S. et al., 2009. Nbs1 flexibly tethers Ctp1 and Mre11-Rad50 to coordinate DNA double-strand break processing and repair. *Cell*, 139(1), pp.87–99.

Williams, R.S. et al., 2004. Structural basis of phosphopeptide recognition by the BRCT domain of BRCA1. *Nature structural & molecular biology*, 11(6), pp.519–25.

Williams, R.S., Green, R. & Glover, J.N., 2001. Crystal structure of the BRCT repeat region from the breast cancer-associated protein BRCA1. *Nature structural biology*, 8(10), pp.838–42.

Winey, M. & O'Toole, E.T., 2001. The spindle cycle in budding yeast. *Nature cell biology*, 3(1), pp.E23–7.

Winzeler, E.A. et al., 1999. Functional characterization of the S. cerevisiae genome by gene deletion and parallel analysis. *Science (New York, N.Y.)*, 285(5429), pp.901–6.

Wyman, C., Ristic, D. & Kanaar, R., 2004. Homologous recombination-mediated double-strand break repair. *DNA repair*, 3(8-9), pp.827–33.

Yamada, M. et al., 2013. ATR-Chk1-APC/CCdh1-dependent stabilization of Cdc7-ASK (Dbf4) kinase is required for DNA lesion bypass under replication stress. *Genes & Development*, 27(22), pp.2459–2472.

Yamashita, N. et al., 2005. Functional analyses of mouse ASK, an activation subunit for Cdc7 kinase, using conditional ASK knockout ES cells. *Genes to cells : devoted to molecular & cellular mechanisms*, 10(6), pp.551–63.

Yan, Z. et al., 2008. Yeast Barcoders: a chemogenomic application of a universal donor-strain collection carrying bar-code identifiers. *Nature methods*, 5(8), pp.719–25.

Yongkiettrakul, S., Byeon, I.-J.L. & Tsai, M.-D., 2004. The ligand specificity of yeast Rad53 FHA domains at the +3 position is determined by nonconserved residues. *Biochemistry*, 43(13), pp.3862–9.

You, Z. et al., 2002. Roles of Mcm7 and Mcm4 subunits in the DNA helicase activity of the mouse Mcm4/6/7 complex. *The Journal of biological chemistry*, 277(45), pp.42471–9.

Yuen, K.W.Y. et al., 2007. Systematic genome instability screens in yeast and their potential relevance to cancer. *Proceedings of the National Academy of Sciences of the United States of America*, 104(10), pp.3925–30.

Zegerman, P. & Diffley, J.F.X., 2010. Checkpoint-dependent inhibition of DNA replication initiation by Sld3 and Dbf4 phosphorylation. *Nature*, 467(7314), pp.474–8.

Zegerman, P. & Diffley, J.F.X., 2009. DNA replication as a target of the DNA damage checkpoint. *DNA repair*, 8(9), pp.1077–88.

Zegerman, P. & Diffley, J.F.X., 2007. Phosphorylation of Sld2 and Sld3 by cyclin-dependent kinases promotes DNA replication in budding yeast. *Nature*, 445(7125), pp.281–5.

Zhang, D. & Oliferenko, S., 2013. Remodeling the nuclear membrane during closed mitosis. *Current opinion in cell biology*, 25(1), pp.142–8.

Zhang, W. & Durocher, D., 2008. Dun1 counts on rad53 to be turned on. *Molecular cell*, 31(1), pp.1–2.

Zhao, X. et al., 2001. The ribonucleotide reductase inhibitor Sml1 is a new target of the Mec1/Rad53 kinase cascade during growth and in response to DNA damage. *The EMBO journal*, 20(13), pp.3544–53.

Zhao, X., Muller, E.G. & Rothstein, R., 1998. A suppressor of two essential checkpoint genes identifies a novel protein that negatively affects dNTP pools. *Molecular cell*, 2(3), pp.329–40.

Zhao, X. & Rothstein, R., 2002. The Dun1 checkpoint kinase phosphorylates and regulates the ribonucleotide reductase inhibitor Sml1. *Proceedings of the National Academy of Sciences of the United States of America*, 99(6), pp.3746–51.

Zhou, Z. & Elledge, S.J., 1993. DUN1 encodes a protein kinase that controls the DNA damage response in yeast. *Cell*, 75(6), pp.1119–27.

Zou, L. & Elledge, S.J., 2003. Sensing DNA damage through ATRIP recognition of RPA-ssDNA complexes. *Science (New York, N.Y.)*, 300(5625), pp.1542–8.

Zou, L. & Stillman, B., 2000. Assembly of a complex containing Cdc45p, replication protein A, and Mcm2p at replication origins controlled by S-phase cyclin-dependent kinases and Cdc7p-Dbf4p kinase. *Molecular and cellular biology*, 20(9), pp.3086–96.

Appendix A

Chapter 3 supplementary material

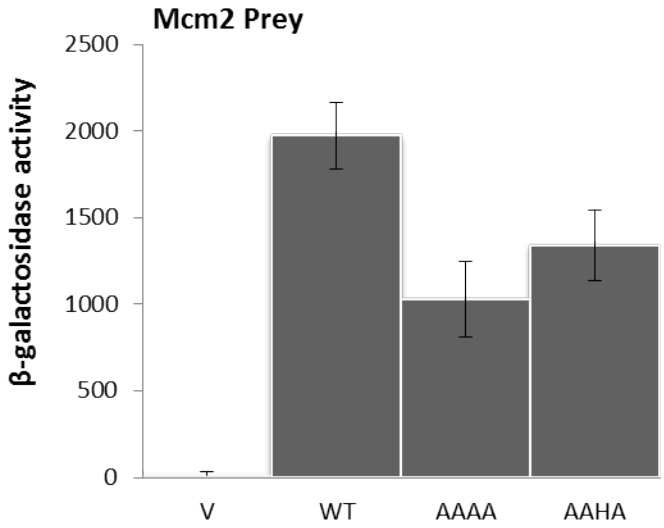

Appendix A Figure 1: Dbf4-AAHA and AAAA mutants are no further impaired for interaction with Mcm2 than other motif C mutants

Two-hybrid analysis of Dbf4 motif C AAAA and AAHA mutants. Indicated Dbf4 mutants, along with wild-type Dbf4 (WT) and empty pEG202 vector (V) were used as baits with Mcm2 as prey in two-hybrid assays as described in materials and methods. β-galactosidase activity values represent the averages of three independent experiments, and the error bars indicate standard deviation.

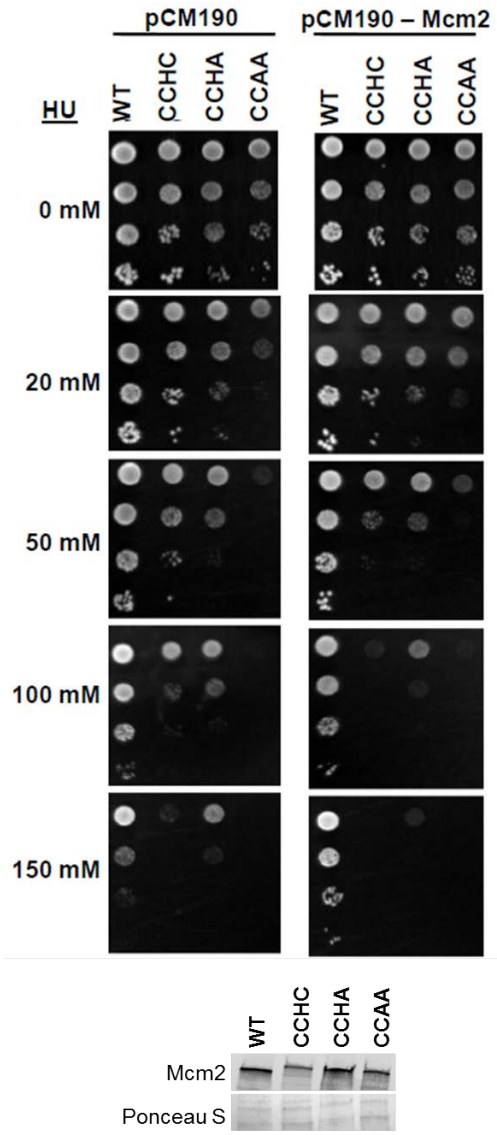

Appendix A Figure 2: Mcm2 overexpression in motif C mutant strains increases sensitivity to hydroxyurea.

Isogenic wild-type and motif C mutant strains transformed with either empty vector (pCM190) or a Mcm2 expression construct (pCM190-Mcm2), were spotted in 10-fold dilution series onto selective medium plates containing the indicated concentrations of HU. Each plate was incubated at 30°C for three days. Levels of Mcm2 expression in the pCM190-Mcm2 transformants was confirmed by Western blot, using a mouse monoclonal anti-Myc antibody (Sigma) and Alexa Fluor 488 goat anti-mouse IgG polyclonal secondary antibody (Invitrogen).

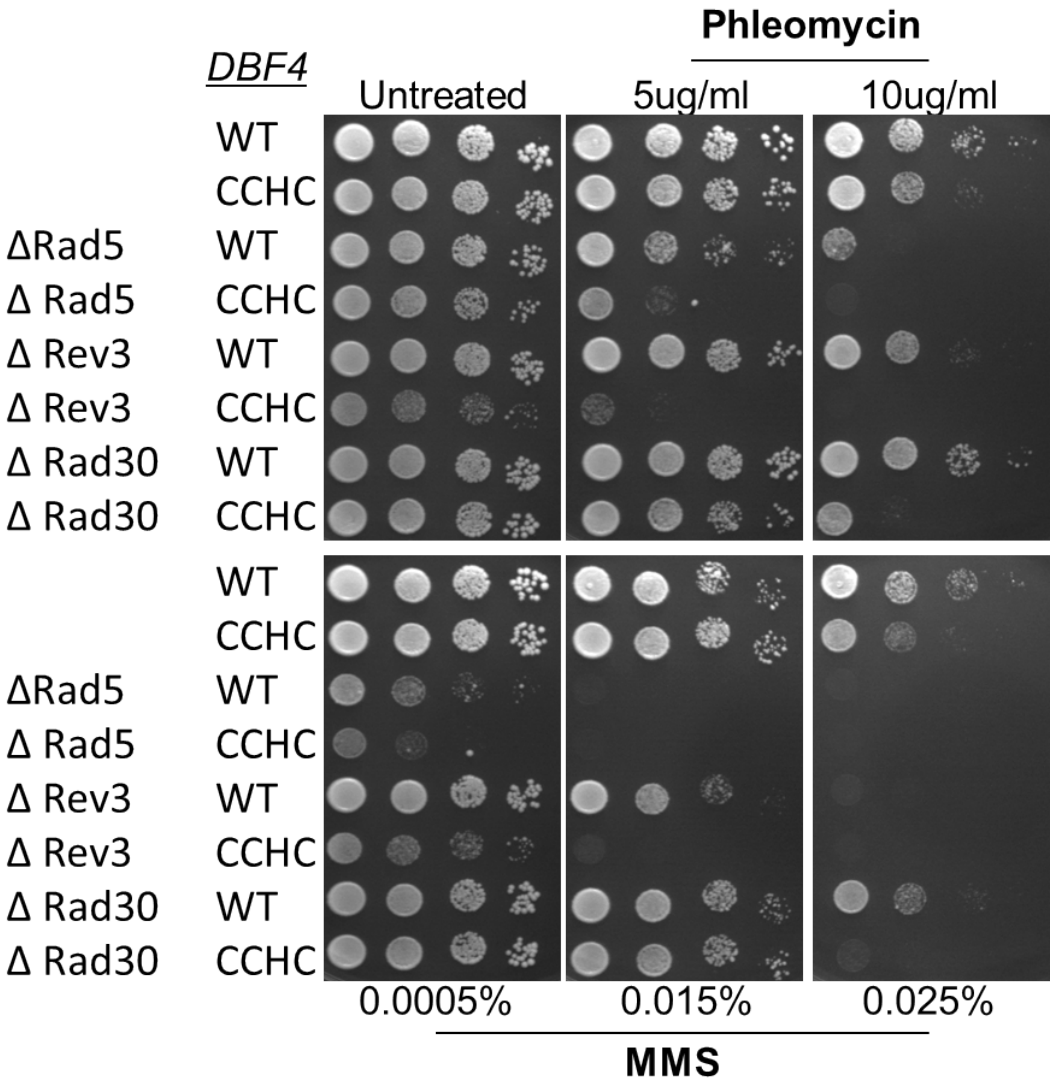

Appendix A Figure 3: Dbf4 motif C mutation when combined with deletion of components of the translesion synthesis pathway results in synergistic sensitivity to genotoxic stress.

A mating type alpha *dbf4-CCHC* mutant was mated to strains lacking Rad5, Rev3, or Rad30 (Polη), the resulting diploids were then sporulated and screened to isolate haploid double mutants. Wild-type, CCHC, ΔRad5, ΔRev3, ΔRad30, and double mutant strains ΔRad5/CCHC, ΔRev3/CCHC, ΔRad30/CCHC were spotted in 10-fold dilution series onto YPD plates containing the indicated concentrations of phleomycin or MMS. Each plate was incubated at 30°C for three days.

Appendix B

Chapter 4 supplementary material

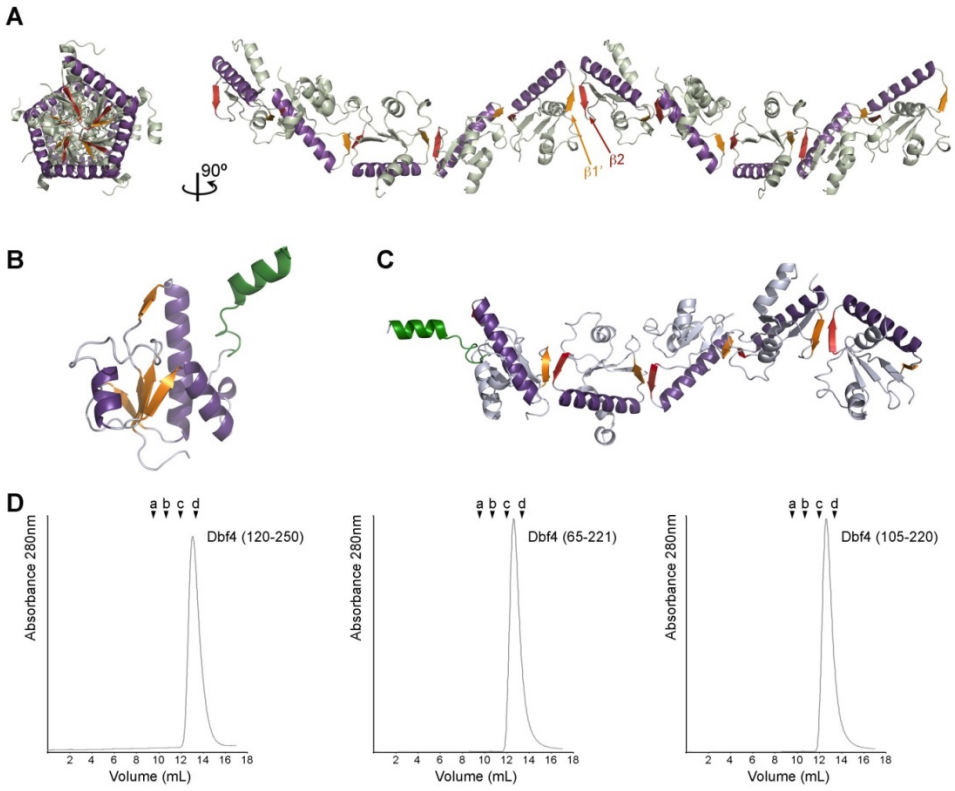

Appendix B Figure 1: Oligomerization of the BRCT domain of Dbf4.

(A) Orthogonal views of the 5-fold helical filament defined by the 10 molecules found in the asymmetric unit of the (6xHis)BRCT crystals. Strands β1' and β2 are labeled and colored orange and red, respectively. (B) Ribbon diagram of the BRCT domain crystallized in the absence of the hexa-histidine tag colored as in Figure 4.2. The C-terminal region of the domain (residues 225-242, colored in green) was ordered in one of the molecules of the asymmetric unit due to crystal contacts with a symmetry mate. (C) Organization of the asymmetric unit of the BRCT crystals. The five molecules form a 5-five helical filament very similar to the one seen in the structure of with tag. (D) Size exclusion chromatography profiles of three variants of Dbf4 over a Superdex-75 column (GE Healthcare). From left to right: Dbf4 (residues 120-250), Dbf4 (residues 65-221) and the sufficient domain of Dbf4 for the interaction with Rad53 (residues 105-220). The three samples elute as apparent monomers. The molecular markers used to calibrate the column are: a) albumin (67 kDa); b) ovoalbumin (43 kDa), c) chymotrypsinogen A (25 kDa) and d) ribonuclease A (13.7 kDa).

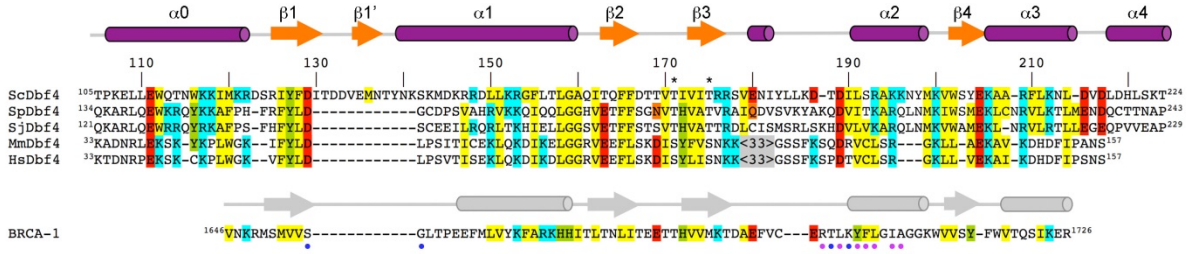

Appendix B Figure 2: Sequence alignment of the region of Dbf4 that mediates the interaction with Rad53.

Structure-based sequence alignment of the H-BRCT domains found in Dbf4 homologues from *S. cerevisiae* (Sc), *S. pombe* (Sp), *S. japonicus* (Sj), *M. musculus* (Mm), *H. sapiens* (Hs), as well as the first BRCT domain found in human BRCA-1 (32). Secondary structure elements of ScDbf4 and BRCA-1 are shown as arrows (strands) and cylinders (helices) and colored as in Figure 1A. Conserved hydrophobic (yellow), positive-charged (blue) and negative-charged (red) residues are highlighted. The positions of the conserved Thr171 and Thr175 are marked with an asterisk. Residues of BRCA1 necessary for the recognition of a pSer residue are marked with a blue dot and those involved in stabilizing the BRCT repeat with a purple dot.

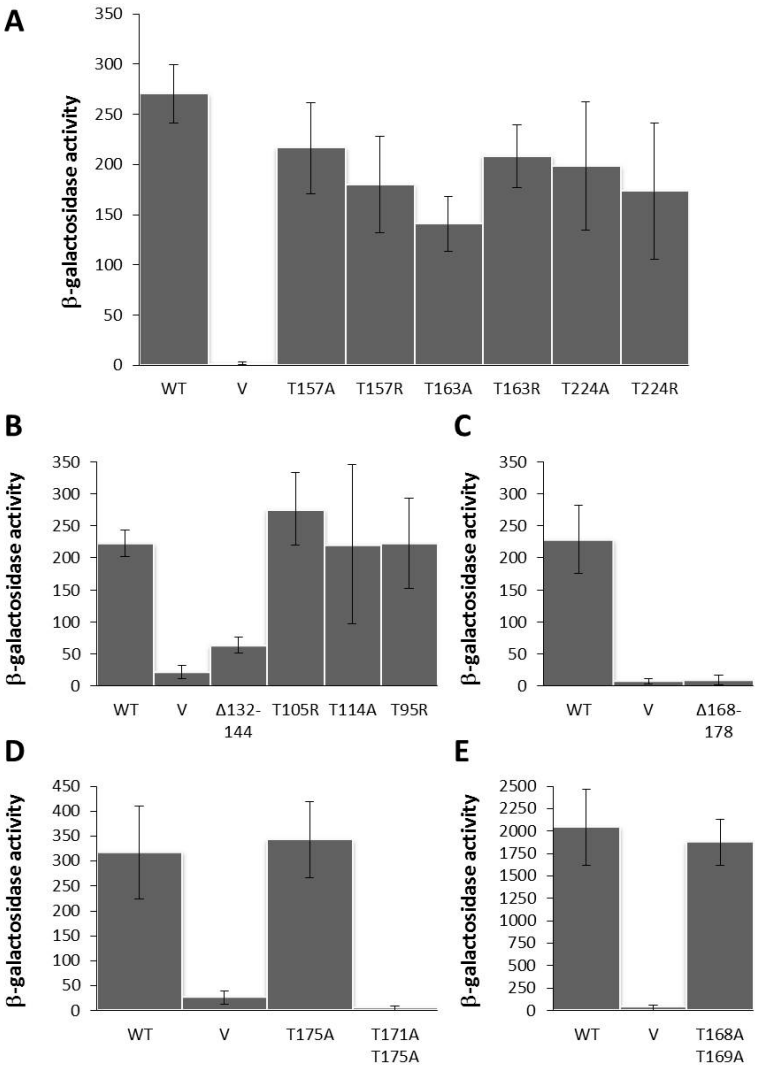

Appendix B Figure 3: Effect of point mutation or deletion to Dbf4 on the interaction with Rad53.

(A-D) Two-hybrid analysis was carried out using full-length Rad53 as prey and either (A) wild-type *DBF4* (WT), empty vector (V), *dbf4-T157A* (T157A), *dbf4-T157R* (T157R), *dbf4-T163A* (T163A), *dbf4-T163R* (T163R), *dbf4-T224A* (T224A), or *dbf4-T224R* (T224R) (B) wild-type *DBF4* (WT), empty vector (V), *dbf4Δ135-179* (Δ135-179), *dbf4-T105R* (T105R), *dbf4-T114A* (T114A), or *dbf4-T95R* (T95R) (C) wild-type *DBF4* (WT), empty vector (V), or *dbf4Δ168-178* (Δ168-178), (D) *DBF4* (WT), empty vector (V), *dbf4-T175A* (T175A), or *dbf4-T171A-T175A* (T171A T175A), as bait. (E) FHA1 (residues 4-165) was used as prey and either *DBF4* (WT), empty vector (V), or *dbf4-T168A-T169A* (T168A T169A), as bait. The interaction strength is shown as β-galactosidase activity units, and each graph represents the average of three independent trials with error bars representing standard deviation.

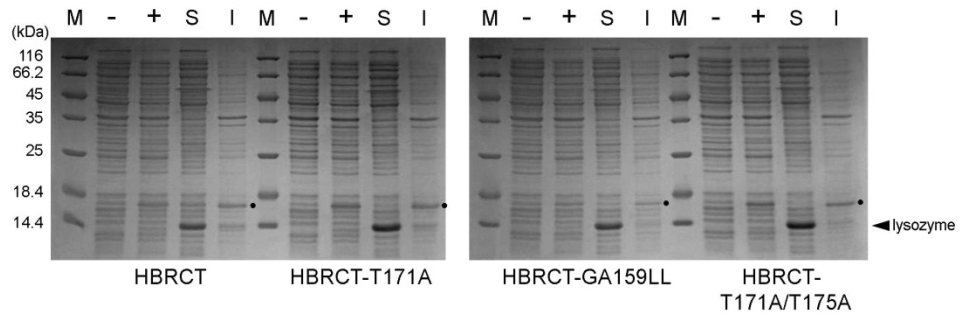

Appendix B Figure 4: Solubility assays of Dbf4 variants encompassing H-BRCT-destabilizing point mutations.

15% SDS-polyacrylamide gels showing the levels of expression of H-BRCT (residues 105-220) variants as indicated. From left to right, molecular weight markers (M), uninduced cell lysate (-), induced cell lysate (+), soluble fraction of the cell lysate (S) and insoluble fraction of the cell lysate (I) is shown for every Dbf4 variant. The band corresponding to Dbf4 is marked with a black dot and that corresponding to lysozyme is marked with an arrowhead.

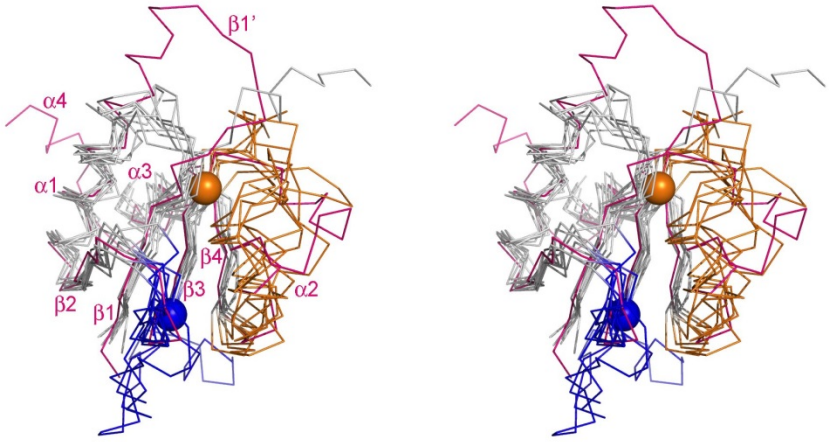

Appendix B Figure 5: Superimposition of multiple *bona fide* BRCT domains onto the structure of Dbf4.

Stereo view of the BRCT domain of Dbf4 shown as a pink Cα-tracing with the Cα atoms of Thr171 and Thr175 shown as spheres (blue and orange, respectively) and secondary structure motifs labeled. BRCT domains from proteins containing single or multiple BRCT repeats (PDB IDs: 1JNX, 1CDZ, 1GZH, 2NTE, 3L3E and 3L46) reveals that the β2-β3 (shown in blue) and β3-α2 (shown in orange) loops are the most variable regions of the domain.

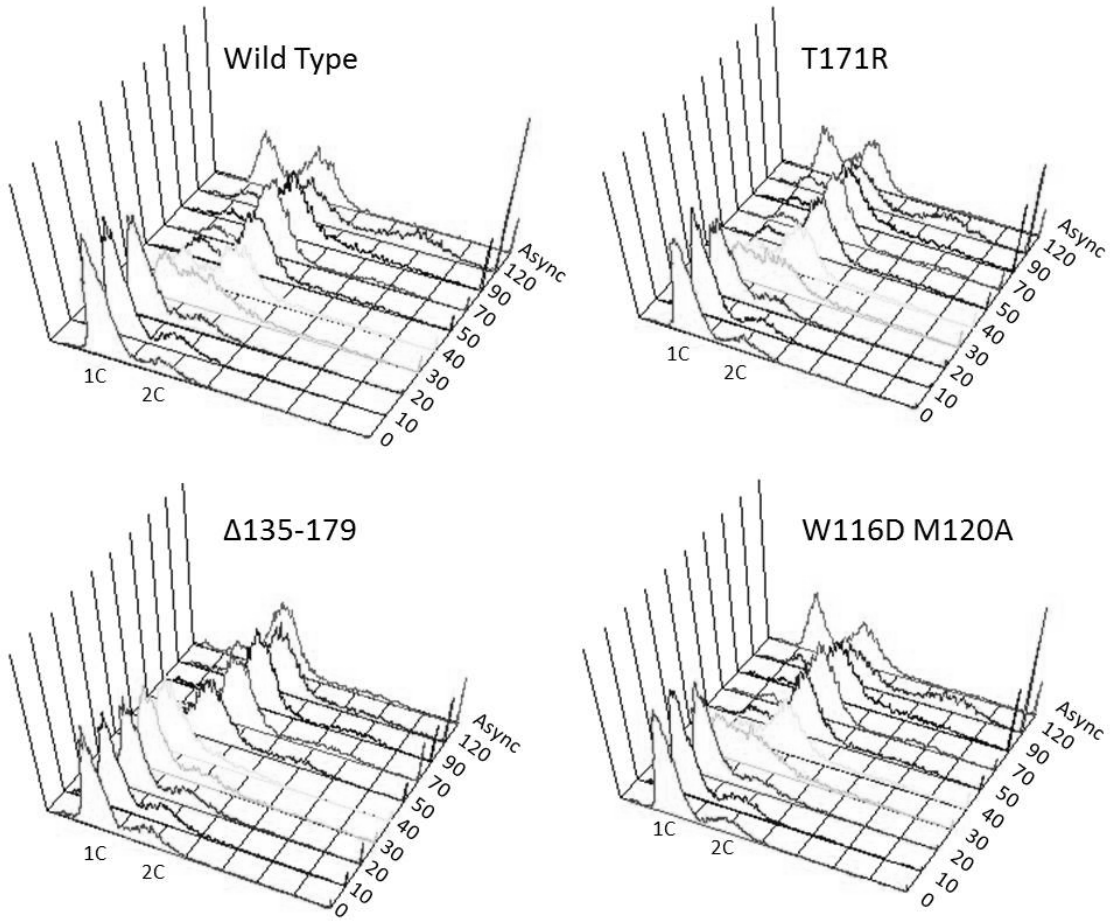

Appendix B Figure 6: Mutations that disrupt the anchoring of helix α0 to the BRCT fold in Dbf4 do not impair S-phase progression.

Dbf4 null cells were transformed with the pRS315 CEN vector expressing, either wild-type *DBF4* (WT), *dbf4Δ135-179* (deletion of motif N), *dbf4-W116D-M120A* (W116D-M120A), or *dbf4-T171R* (T171R). Cultures were grown to a concentration of 5 x 10^6 cells/ ml, arrested in late G1 phase for 3 h with 5 µg/ml α-factor, washed once in sterile dH_2O, then resuspended in fresh medium without α-factor to release them from the block. Shown is FACS analysis of culture aliquots taken at the indicated time points following release from the a-factor block as well as from the original asynchronous cultures (Async). The positions of 1C and 2C DNA peaks are indicated.